Suicide Enzymes: Purification, Characterization and Encapsulation for Therapeutic Implications

A Thesis Submitted in Partial Fulfilment of the

Requirements for the Degree of

Doctor of Philosophy

by

VINOD KUMAR YATA

Department of Biotechnology

Indian Institute of Technology Guwahati

Assam, India

December, 2011

My unconditional love and

dedication to

my mother

DECLARATION

I do hereby declare that the matter embodied in this thesis is the result of investigations carried out by me in the Department of Biotechnology, Indian Institute of Technology Guwahati, India, under the guidance of Dr. Siddhartha Sankar Ghosh. This thesis has not been previously submitted for the award of any degree, diploma, associate-ship, fellowship or its equivalent to any other University or Institution.

December, 2011. **Vinod Kumar Yata**

Indian Institute of Technology Guwahati

Guwahati-781039

Assam, India

Dr Siddhartha Sankar Ghosh, PhD
Head, Centre for Nanotechnology &
Associate Professor
Tel# +91-361-258-2206
Fax# +91-361-258-2249
Email# sghosh@iitg.ernet.in

Department of Biotechnology

CERTIFICATE

This is to certify that the thesis entitled "Suicide Enzymes: Purification, Characterization and Encapsulation for Therapeutic Implications", that is being submitted by Mr. Vinod Kumar Yata for the award of degree of Doctor of Philosophy is an authentic record of the results obtained from the research work carried out under my supervision in the Department of Biotechnology, Indian Institute of Technology Guwahati, India.

The results embodied in this thesis have not been submitted to any other University or Institute for the award of any degree.

December, 2011.

Dr. Siddhartha Sankar Ghosh

(Thesis Supervisor)

Acknowledgements

I would like to express my gratitude to **Dr. Siddhartha Sankar Ghosh** for his supervision, advice, and guidance from the very early stage of this research as well as giving me extraordinary experiences through out the work. Above all and the most needed, he provided me unflinching encouragement and support in various ways.

I gratefully acknowledge doctoral committee (Chairman: Dr. A. Ramesh, Members: Dr.B.Bose and Dr.L.Sahoo) for their advice, and willingness to share their bright thoughts with me, which were very fruitful for shaping up my ideas and research.

I thank Dr. MVV Satish, Mr. Kausik Sen, Mr. Vijay Kumar Ravi and Mr. Subhamoy Banerjee for their invaluable help in my thesis work.

I also wish to thank Dr. A. Kiran and Dr.P.Gopinath who have taught me the techniques of protein purification and cell culture.

Collective and individual acknowledgments are also owed to my friends at IITG (Asim, Urmila, Shadab, Sukhwinder, Pojul, Ashok, Souvika, Sagarika, kohila, Chockalingam, Nidhi**,** Manab, Vijay and Rachana) whose presence somehow perpetually refreshed, helpful, and memorable.

Words alone cannot express the thanks I owe to Dr. Smitha, my wife, for her encouragement and assistance. I also extend thanks to my father, Mr.Sathyanarayana and all other family members.

Finally, I would like to thank everybody who was important to the successful realization of thesis, as well as expressing my apology that I could not mention personally one by one.

ABSTRACT

Suicide gene therapy has been extensively investigated as an alternative approach to increase selectivity in cancer treatment. The strategy involves transfer of suicide gene to tumor cells followed by administration of prodrug, in which the transgene encodes enzyme that activates the prodrug to create toxic products and there by kill cancer cells. In addition, direct delivery of encapsulated suicide enzyme to cancer cells is another recent approach to activate prodrug. Two main themes of my thesis focus on purification, characterization of the suicide enzymes and development of nanocarriers encapsulating suicide enzyme.

Non-mammalian cytosine deaminase (CD) catalyzes conversion of nontoxic prodrug, 5-fluorocytosine (5-FC) into the anticancer drug, 5-fluorouracil (5-FU). Therefore, 5-FC/CD mediated suicide gene therapy has strong potential in clinical application. In my thesis work, I have purified the suicide enzyme, cytosine deaminase to homogeneity from *E. coli* K-12 MTCC 1302 by fast performance liquid chromatography (FPLC) using DEAE-cellulose anion exchange column. I have characterized the enzyme and interestingly found that the enzyme was thermostabile at high temperatures. The enzyme was also active at a wide range of pH (7 to 10).

Furthermore, *E. coli* uracil phosphoribosyltransferase (UPRT) enzyme is known to convert 5FU into active metabolite, 5-fluorouracil monophospahte (5FUMP) which kill the cells by inhibiting DNA and RNA synthesis. Therefore, the combine use of CD and UPRT generates very efficient gene therapy system. I purified UPRT from the same *E. coli* K-12 MTCC 1302 strain and studied inhibition kinetics to determine enzyme

inhibition constant (K_i) of 5FU. I also persuaded *in silico* molecular dynamics stimulation to confer interactions of uracil and its selective inhibitor 5FU with UPRT enzyme. The computational results revealed key residues of UPRT involved in ligand binding interactions.

In this part of my thesis, I have developed a biodegradable chitosan based nanocarrier (NC) for protein encapsulation using a completely green method. It is a novel strategy for protein therapeutics, as cancer gene therapy is limited by the level of gene transduction. Green fluorescence protein (GFP) was used as a model protein to develop encapsulated NC. Fluorescence measurements and secondary structure analysis of GFP by circular dichoism, revealed that both fluorescence and intrinsic conformation were retained during entrapment and after release from NC. Further, I developed a chitosan based cytosine deaminase nanocarrier with an average size of 80 nm diameter. Long term release of active cytosine deaminase from the NC was monitored up to one week.

Targeted drug delivery is known to be effective in enhancing tissue-specificity with low systemic toxicity. One such preferred target is folate receptor (FR), which is overexpressed in several types of cancer cells, and has high affinity for folic acid (FA). Therefore, I have developed a folic acid (FA) conjugated NC for targeted delivery of suicide enzyme to cancer cells, and finally demonstrated the functional efficacy of CD. I synthesized FA functionalized chitosan/poly-n-isopropyl acrylamide nanocarrier (FANCs) for delivery of CD to the FR positive cancer cell lines. Interestingly, FA conjugated NC showed increased thermal stability as compared to the unconjugated NC. The FA conjugated NC loaded with purified *E.coli* cytosine deaminase showed cytotoxicity on HT-29 cells after 5FC treatment.

In brief, purification and characterization of two important suicide enzymes, cytosine deaminase and urail phosphoribosyltransferase concurred development of enzyme encapsulated nanocarriers. Experimental results presented in this thesis implicated that functional delivery of encapsulated suicide enzyme could be a viable approach of protein therapeutics for cancer therapy.

CONTENTS

ACKNOWLEDGEMENTS i

ABSTRACT ii

CONTENTS v

ABBREVIATIONS ix

Chapter 1 Introduction and Literature Review

1. Overview..... 1

2. Review of Literature 2

2.1. Suicide enzymes 2

2.1.1. Cytosine deaminase..... 3

2.1.2. Uracil phosphoribosyltransferase..... 15

2.2. Targeted delivery of therapeutic enzymes by nanocarrires..... 16

3. Significance of the work 19

4. Specific objectives.....20

Chapter 2 Purification and characterization of *E.coli* cytosine deaminase

2.1 Overview..... 21

2.2. Experimental Approaches 22

2.2.1. Materials 22

2.2.2.Bacterial strain, culture conditions 22

2.2.3. Purification of cytosine deaminase..... 22

2.2.4. Enzyme assay..... 23

2.2.5. Determination of K_m and V_{max}..... 23

2.2.6. Determination of pH and temperature optima and stability of cytosine deaminase……..... 24

2.3 Results and Discussion ……..... 24

2.3.1 Purification of cytosine deaminase …… 24

2.3.2 Effect of pH and Temperature…… 26

2.3.3. Kinetic analysis and substrate specificity…….. 28

2.4 Summary …….. 28

Chapter 3 Purification and *in silico* characterization of *E. coli* uracil Phosphoribosyltransferase

3.1. Overview……. 29

3.2. Experimental Approaches ……..... 31

3.2.1 Materials……..... 31

3.2.2.Purification of UPRT……... 31

3.2.3.Enzyme assay and Determination of K_i……..... 32

3.2.4. MD simulation ……. 32

3.2.5 Ligand preparation…… 33

3.2.6. Protein preparation…… 33

3.2.7. Docking procedure ……. 34

3.3. Results and discussion…… 34

3.4. Summary ……..... 43

Chapter 4 Development of chitosan nanocarrier using green fluorescent protein (GFP) as a model protein

4.1. Overview…… 44

4.2. Experimental Approaches …… 45

4.2.1. Materials …… 45

4.2.2. Purification of GFP…… 45

4.2.3. Synthesis of chitosan nanocarriers …… 46

4.2.4. Loading of GFP in chitosan nanocarriers……... 46

4.2.5. *In vitro* release of GFP from chitosan nanocarriers……. 47

4.3. Results and discussions……. 47

4.4. Summary …… 54

Chapter 5 Development of cytosine deaminase- chitosan nanocarrier

5.1. Overview…… 55

5.2. Experimental Approaches …… 56

5.2.1. Synthesis of CSCD nanocarrier …….. 56

5.2.2. Characterization of CSCD nanocarrier…….. 56

5.2.3. *In vitro* release studies of cytosine deaminase from CSCD nanocarrier…… 58

5.3. Results…… 58

5.3.1. Characterization of CSCD nanocomposite…… 58

5.3.2. *In vitro* release of cytosine deaminase…… 62

5.4. Discussion…… 62

5.5. Summary ……. 63

Chapter 6 Development of folic acid conjugated targeted delivery system

6.1 Overview …… 64

6.2. Experimental Approaches…… 66

6.2.1. Materials …… 66

6.2.2. Synthesis of CS/PNIPAM nanocarriers…….. 66

6.2.3. Folic acid conjugation of CS/PNIPAM nanocarriers…….. 67

6.2.4. FTIR spectroscopy…….. 67

6.2.5. Simultaneous TG-DSC analysis…… 68

6.2.6. Loading of CD in FANCs and *in vitro* release……. 68

6.2.7. Cell culture..... 69

6.2.8. Semi-quantitative reverse transcriptase-polymerase chain reaction (RT-PCR)..... 69

6.2.9. Cell viability studies……... 70

6.2.9.1. XTT assay…… 70

6.2.9.2. Acridine orange (AO)/ ethidium bromide (EB) staining…….. 70

6.3. Results and discussion…….. 71

6.4. Summary……... 78

Chapter 7 Conclusions and scope for future work…… 79

BIBLIOGRAPHY 81

LIST OF PUBLICATIONS 100

ABBREVIATIONS

5FC…….....	5-Fluorocytosine
5FU……..	5-Fluorouracil
5FUMP….....	5-Fluorouracil Monophospahte
AFM ……	Atomic Force Microscopy
AO……	Acridine Orange
APS……..	Ammonium Persulfate
CD…….....	Cytosine deaminase
CFU	Colony -Forming Units
CS …….....	Chitosan
CSCD……	Chitosan-Cytosinedemainse
CSNCs …….....	Chitosan Nanocarriers
DEAE……...	Diethylaminoethyl
DMEM ……. ……..	Dulbecco's Modified Eagle's Medium
DMSO……. …….	Dimethyl Sulfoxide
DNA…. …….	Deoxyribonucleic acid
DSC …….....	Differential Scanning Calorimetry
EB…..……. ……..	Ethidium Bromide
EDC……..	1 -(3-dimethylaminopropyl)-3-Ethylcarbodiimide hydrochloride
FA …….	Folicacid
FANCs ……..	FA-Conjugated CS/PNIPAM Nanocarriers
FBS……	Fetal Bovine Serum
FdUDP……..	Fluorodeoxyuridine Diphosphate
FdUMP …….	Fluorodeoxyuridine Monophosphate

FdUTP ……..	Fluorodeoxyuridine Triphosphate
FEB ……	Free Energy of Binding
FPLC ……..	Fast Performance Liquid Chromatography
FTIR ……...	Fourier Transform Infrared Spectroscopy
FUDP……..	Fluorouridine Diphosphate
FUMP…….	Fluorouridine Monophosphate
FUTP……	Fluorouridine Triphosphate
GDEPT ……	Gene-Directed Enzyme-Prodrug therapy
GFP ……	Green Fluorescent Protein
GTP ……	Guanosine Triphosphate
HSV-tk ……	Herpes Simplex Virus Thymidine kinase
K_i ……	Inhibition Constant
K_m……...	Michaelis-Menten constant
MBA……	N,N-methylene-bisacrylamide
MD ……	Molecular dynamics
NCs……	Nanocarriers
NIPAM ……	N-isopropylacrylamide,
OPRT……	Orotate Phosphoribosyltransferase
PBS ……..	Phosphate Buffer Saline
PDB……...	Protein Data Bank
PNIPAM ……..	Poly (N-isopropylacrylamide)
PRPP ……	α-D-5-Phosphoribosyl-1-R-diphosphate
Ps……	Pico seconds
RMSD……	Root Mean Square Deviations
RNA….....	Ribonucleic acid

RR ……	Ribonucleotide Reductase
RT- PCR.....	Reverse Transcriptase Polymerase Chain Reaction
SDS-PAGE …….....	Sodium Dodecyl Sulfate-Polyacrylamide Gel Electrophoresis
TEM ……	Transmission Electron Microscopy
TG……	Thermogravimetry
TK……	Thymidine Kinase
TP ……	Thymidine Phosphorylase
TS…….	Thymidine Synthase
UCSF……	University of California, San Francisco
UMP …….	Uridine Monophosphate
UPRT……	Uracil Phosphoribosyltransferase
V_{max}……	Maximum Velocity
XRD ……..	X-ray Diffraction Measurements
XTT ……..	2,3-bis[2- Methoxy-4-Nitro-5-Sulfophenyl]- 2H-Tetrazolium-5-Carboxyanilide Inner salt

Chapter 1

Introduction and literature review

1. Overview

Chemotherapy has been established as the most common approach for cancer treatment (Chabner and Roberts 2005). Currently available drugs are quite effective in treating certain type of cancers, but these drugs lack the specificity and selectivity against tumours, which lead to the destructions of non-target tissues. Attempts to target therapy to tumours have been directed toward the discovery of pharmacologically inactive anticancer drug precursors (prodrugs) that can be activated by selective enzymes in cancer cells. Gene therapy development aimed at enhancing the selectivity of cancer chemotherapy by intra-tumoural delivery and expression of the 'suicide genes', which encode proteins that converts the less toxic or non toxic prodrug to highly toxic metabolites. The gene therapy approach using suicide gene and prodrug combinations for improving the selectivity of cancer chemotherapy is called gene directed enzyme prodrug therapy (GDEPT) and also known as suicide gene therapy (Marais et al. 1996). The advantage of gene therapy in cancer treatment depends on the bystander effect, which facilitates transfer of gene product or active metabolite to neighbour cells by non- faciltated diffusion or via functional gap junctions (Dilber et al. 1997), but the success of GDEPDT is limited due to inefficient gene delivery (Yazawa et al. 2002). The main difficulties associated with viral gene delivery are immunogenicity, proinflamtory effects, integration in human genome and lack of stable integration. Viral

vector mediated gene therapy commonly associated with the respiratory failure, fever and hypotension (Marshall 1999, Anderson 2002). Poor delivery efficiency is associated with nonviral systems, like bacteria, anti sense RNA, ribozyme and lipofection (Gottesman 2003). To overcome the above problems, protein therapy may offer many potential opportunities against cancer. Therefore, it is a necessary to develop the efficient nonviral delivery systems for protein delivery. Hence, "suicide enzyme" delivery needs to be established. Future success of tumour specific treatment will build new technologies, such as nanocarrier mediated delivery of therapeutic agents. So, I am focusing on nanocarrier mediated delivery of suicide enzymes and conjugation of nanocarriers with targeting agents for improved tumor selectivity.

2. Review of Literature

A literature review of "suicide" enzymes and nanocarriers for its encapsulation ha been conducted. The review aims to provide the details of the "suicide" enzymes with promising therapeutic appeals and also suitable nanocarriers for efficient delivery of the suicide genes and enzymes. Enzyme prodrug therapy has numerous applications for the targeted delivery in cancer treatment.

2.1. Suicide enzymes

Numerous suicide enzymes have been used to activate prodrugs of antitumor agents. Examples include viral thymidine kinase (TK), bacterial cytosine deaminase (CD),bacterial Uracil phosphoribosyl transferase (UPRT), bacterial carboxypeptidase G2, cytochrome P450 enzymes, purine nucleotide phosphorylase, thymidine phosphorylase, nitroreductase , Carboxypeptidase G2, D-amino-acid oxidase, xanthine–guanine phosphoribosyl transferase (Portsmouth et al. 2007, Niculescu-Duvaz and

Springer 2005). Although several strategies using so-called suicide genes for the treatment of cancer have been explored, one in particular, a strategy relying on converting the nontoxic prodrug 5-fluorocytosine (5FC) into the anticancer drug 5-fluorouracil (5FU) by non mammaian cytosine deaminses may be especially suited for the treatment of a variety of different kinds of cancer (Gopinath and Ghosh 2007, 2008a). In contrast to other suicide genes, CD mediated conversion of prodrug had shown strong bystander effect. In addition, this strategy can be combined with bacterial UPRT which can potentiate therapeutic effuicacy by metabolizing the 5FU to its toxicmetabolites (Gopinath and Ghosh 2008b, 2009).CD-UPRT mediated intracellular conversion of prodrug 5FC is illustrated in Figure.1.1. These enzymes are not present in human and are likely to be non-immunogenic. The other suicide enzymes of human origin and their presence in normal tissues limit their use in prodrug/enzyme therapy (Niculescu-Duvaz and Springer 2005). Non mammalian CDs and UPRTs were reviewed for their potential implications in cancer treatment.

2.1.2. Cytosine deaminase (CD): Cytosine deaminase (CD) is an important member of the pyrimidine salvage pathway and catalyzes the deamination of cytosine, producing uracil. This enzyme is present in prokaryotes and fungi but not multicellular eukaryotes. In the past decade, it has been well appreciated that non mammalian cytosine deaminase enzyme emerged as a suicide enzyme as a result of significant conversion of prodrug, 5FC to anticancer drug 5fluorouracil (5FU) in mammalian cancer cells both *in vitro* and *in vivo* (Portsmouth et al. 2007).

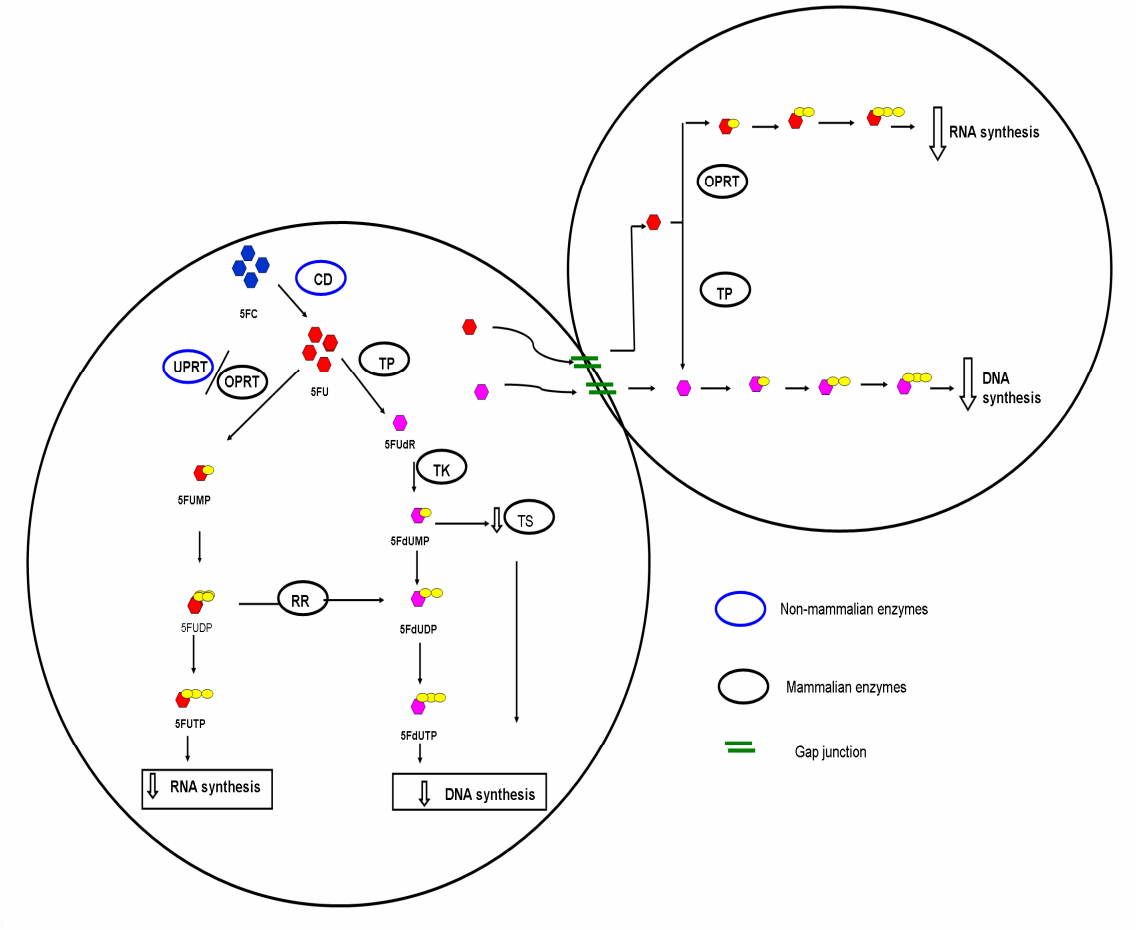

Figure.1.1. Schematic representation of CD-UPRT mediated intracellular conversion of prodrug 5FC. The toxic metabolites released from the CD/5FC treated cells can kill the adjacent untransfected cancer cells through gap junctions i.e. bystander effect ***Abbreviations*** : CD-cytosine deaminase, UPRT-Uracil phosphoribosyl transferase, FUMP-fluorouridine monophosphate, FUDP-fluorouridine diphosphate, FUTP-fluorouridine triphosphate, FdUMP-fluorodeoxyuridine monophosphate, FdUDP-fluorodeoxyuridine diphosphate, FdUTP -fluorodeoxyuridine triphosphate, OPRT-orotate phosphoribosyltransferase, TP - thymidine phosphorylase, TK-thymidine kinase, TS-thymidine synthase, RR-ribonucleotide reductase

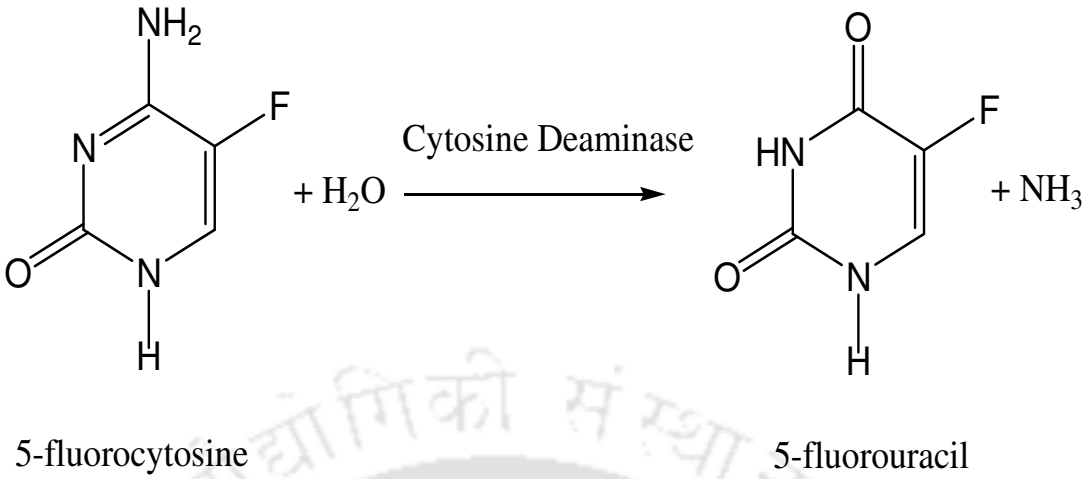

Figure.1.2. Cytosine deaminase catalysed deamination of 5FC

Historical background

Early studies confirmed that, 5FC is an antifungal drug used to treat the fungal infections in humans. This is because, the susceptible fungi could convert the prodrug, 5FC to cytotoxic 5FU (Waldorf and Polak 1983, Polak and Scholer 1975). Later studies employing the rat models demonstrated the partial conversion of 5FC to 5FU by the action of the intestinal microbial flora upon oral administration of 5FC, where as parenteral administration of 5FC was not metabolized (Koechlin et al. 1966). Based on these data, Harris et al. (1986) proposed that, the human intestinal micro flora consists of some micro organisms that express cytosine deaminase can convert the 5FC to 5FU (Fig.1.2). However, some microorganisms present in normal intestinal microflora may not have cytosine deaminase, whereas, *Escherichia coli* have been shown to possess high cytosine deaminase activity. Based on this fact, Sakai et al. (1985) isolated *E.coli* cytosine deaminase and combined the use of this enzyme with 5FC in experimental brain tumors. Subsequent studies showed significant levels of 5FU in rats bearing subcutaneous tumors, when administered with capsules containing 5FC and *E.coli*

cytosine deaminase (Nishiyama et al. 1985). A real break through occurred when Mullen et al. (1992) showed the conversion of the prodrug 5FC to the active metabolite 5FU by CD in GDEPT of mammalian cells. In summary, several lines of evidence strongly suggest that cytosine deaminase is a successful suicide enzyme in prodrug mediated cancer therapy.

Structure, stability and activity of non-mammalian CDs

The enzyme has been purified from several organisms and exhibits different structural, kinetic and regulatory properties depending on the source of origin (Table.1). The enzyme from *E. coli* is highly thermostable and purified enzyme has shown significant conversion of 5FC to 5FU. Moreover, *E.coli* CD is stable and active for the conversion of 5FC at physiological conditions like 37°C and pH 7.3 (Katsuragi et al. 1986). These properties make *E.coli* CD functionally distinct from other CDs making it an ideal candidate for therapeutic applications. Several crystal structures of CDs have been determined and Protein Data Bank currently lists 15 crystal structures of CDs (Table 2). CD has been isolated from variety of organisms, but structures of CDs isolated form *E.coli* and *S. cerevisiae* have been solved. CD structure of *E.coli* is divergent from that of *S. cerevisiae*, even though both act on cytosine for conversion to uracil by deamination. The 426-residue *E.coli* CD forms an $(\alpha\beta)_8$ barrel structure and packed into a hexameric assembly is formed through the association of three strand-swapped dimmers, which is homologous to mammalian adenosine deaminase (Ireton et al. 2002). The *S. cerevisiae* CD structure composed of a central five-stranded sheet is sandwiched between two helices in one side, and three helices on the other side forming a tightly packed dimer in the crystallographic asymmetric unit, which is homologous to the bacterial cytidine deaminase (Ireton et al. 2003).

Even though there is structural dissimilarity, cytosine deaminases of *S. cerevisiae* shares similar active site architecture with bacterial CDs. In *S. cerevisiae* CD, Glu 64 and Phe 114 residues play key role in the substrate interaction, where as in *E.coli* CD, key residues are Asp134 and Glu217 (Ko et al. 2003, Ireton et al. 2003). These findings support the experimental data provided by kievit et al. (1999). In their experiments, *S. cerevisiae* CD showed lower k_m value than *E.coli* CD for the 5FC. Investigation of structure activity relationship between mutant CDs and prodrug 5FC is important for development of high efficient prodrug/enzyme cancer therapy.

Table .1. Characteristics of CDs isolated from various organisms

Source organism	Molecular weight (kDa)	Km value (mM) for 5FC	Stability	References
E. coli	200	1.8	Optimum temperature was 50°Cand optimum activity was pH9. stable between pH 7 to 10 and stable upto 55°C over 72 hrs	Yata and Ghosh 2011 a; Katsuragi et al.1986
S. cerevisiae	34	0.16	Activity optimum is found near pH 7. The enzyme is stable at 4 C in the pH range 5-9 for at least 48 hr	Ipata et al. 1971 ; Yao et al. 2005
A. fumigatus	32	6.5	Optimum at around pH 7 and temperature optimum at 35°C	Yu TS et al. 1991
C. violaceum YK 391	126	0.38	The enzyme was stable at pH 6.0 to 8.0, and at 30°C for a week	Jung and Yu 2004
S.typhimurium	230	-	pH optimum of 7.30 to 7.50 and a temperature optimum of 45 to 50°C	West et al. 1982

Therapeutic implications

Suicide gene therapy

Suicide gene therapy represents another modality for the treatment of cancer, which uses the prodrug activating transgene and systemic or local administration of prodrug to kill the tumours. Suicide gene mediated prodrug activations have definite antitumor activity in both *in vitro* and *in vivo* experimental systems (Niculescu-Duvaz and Springer 2005). Numerous scientific studies have characterized CD in GDEPT on variety of cancer cell lines and various vectors, including retroviruses, and adenoviruses, have been used to transfer these suicide genes to cancer cells (Table.3). *E. coli* CD is the best characterized suicide gene that kills the tumor cells by intratumoral conversion of 5FC (Mullen et al. 1992). The *E.coli* CD received its immense focus on suicide gene therapy in cancer for two reasons, primarily due to the apoptosis mediated cell death of the cancer cells and secondarily due to the bystander effect where toxic metabolites of prodrug are transferred via intracellular gap junctions to the non- CD transfected neighbouring cells (Gopinath and Ghosh 2009). Previous studies have shown that combination of CD/5FC suicide gene therapy with *E. coli* Uracil phosphoribosyltransferase (UPRT) gene is therapeutically more efficient than single unit of suicide gene alone (Kanai et al. 1998,Gopinath and Ghosh 2009). Moreover, combination of herpes simplex virus thymidine kinase (HSV-tk)/ ganciclovir and 5-fluorocytosine/ CD prodrug gene therapies have shown synergistic effect in an experimental brain tumor model (Aghi et al. 1998). After *E.coli* CD, *S. cerevisiae* CD received attention among other CDs due to its improved therapeutic efficacy than *E.coli* CD for intratumoral conversion of 5FC (Erbs et al. 2000). This is due to the high affinity of *S. cerevisiae* CD towards 5FC than *E.coli* CD

(Kievit et al. 1999). Though, *S. cerevisiae* CD/5FC system exhibited superior effects over *E. coli* CD/5FC system, the molecular mechanism of *S. cerevisiae* CD/5FC has yet to be established. Therefore, it is worthwhile to further investigate molecular mechanisms to evaluate both the strategies.

Table.2. Description of the crystal structures of cytosine deaminase and its mutants in the Protein Databank

PDB ID	Organism	Description	References
1K6W	*E. coli*	Wild type	Ireton et al. 2002
1K70	*E. coli*	Bound to 4-Hydroxy-3,4-Dihydro-1H-Pyrimidin-2-one	Ireton et al. 2002
1UAQ	*S. cerevisiae*	Complex with the inhibitor 2-hydroxypyrimidine	Ko et al. 2003
1OX7	*S. cerevisiae*	Apo-enzyme: inorganic zinc bound	Ireton et al. 2003
1P6O	*S. cerevisiae*	Bound to 4(R)-hydroxyl-3,4-dihydropyrimidine	Ireton et al. 2003
1RB7	*S. cerevisiae*	Crystal form p212121 with sodium acetate	Ireton et al. 2004
1R9X	*E. coli*	D314G mutant	Mahan et al. 2004
1R9Y	*E. coli*	D314A mutant	Mahan et al.2004
1R9Z	*E. coli*	D314S mutant	Mahan et al.2004
1RA0	*E. coli*	D314G mutant bound to 5-fluoro-4-(S)-hydroxy-3,4-dihydropyrimidine	Mahan et al. 2004
1RA5	*E. coli*	D314A mutant bound to 5-fluoro-4-(S)-hydroxyl-3,4-dihydropyrimidine	Mahan et al. 2004
1RAK	*E. coli*	D314S mutant bound to 5-fluoro-4-(S)-hydroxyl-3,4-dihydropyrimidine	Mahan et al. 2004
1YSB	*S. cerevisiae*	Triple Mutant	Korkegian et al. 2005
1YSD	*S. cerevisiae*	Double Mutant	Korkegian et al. 2005
3G77	*E. coli*	V152A/F316C/D317G mutant	Fuchita et al. 2009

Table.3. Selected examples of CD/5FC mediated suicide gene therapy

Genes transferred	Gene transfer method	Therapy route	Model system	References
E. coli CD	Adenovirus vector	*In vitro*	14 human cell lines derived from both GI (colon, pancreas) and non-GI (prostate, glioma) tumors	Miller et al. 2002
E. coli CD-UPRT	Electroporation method	*In vitro*	Human colon adenocarcinoma cells	Gopinath and Ghosh 2008 a
E. coli CD	Retroviral vector	*In vitro*	Murine fibroblast lines	Mullen et al. 1992
S. cerevisiae CD	Hemagglutinating Virus of Japan-Liposome Method	*In vitro*	Human pancreatic cancer cell line BXPC3	Kanyama et al. 2001
		In vivo	Mice	Kanyama et al. 2001
S. cerevisiae CD-UPRT	Adenoviruses	*In vivo*	Mice	Erbs et al. 2000
		In vitro	Colon cancer breast cancer pancreas cancer cell lines	Erbs et al. 2000

Enzyme therapy

The success of GDEPT is limited due to inefficient gene delivery to the cancer cells (Yazawa et al. 2002). The main difficulties associated with viral gene therapy are respiratory failure, fever and hypotension, proinflammatory effects, integration in human genome and lack of stable integration and induced immunological response, which led to the death of patients (Marshall 1999, Thomas et al. 2003). Poor gene delivery efficiency is associated with nonviral systems, like bacteria, ribozyme and lipofection (Gottesman 2003). To overcome the above problems and minimize the systemic toxicity, direct delivery of enzyme in prodrug mediated cancer therapy is becoming promising solution for cancer treatment. A number of different cancer protein

therapy protocols are currently underway, including those using CD enzymes. In the Li et al. (2008b) study, *E.coli* CD was conjugated with biodegradable poly-l-lysine carrier which demonstrated the high therapeutic efficacy by accelerating the intra cellular uptake of the enzyme in breast cancer cells *in vitro*. The same group showed *in vivo* and *ex vivo* data by dynamically monitoring the enzyme levels in tumors and also showed the efficient conversion of 5FC to 5FU by using fluorine magnetic resonance spectroscopy (Li et al. 2006, 2008a). Previous studies have shown that antibody conjugation of CD improving the therapeutic efficiency of 5FC mediated cancer therapy. Wallace et al. (1994) demonstrated improved systemic levels of 5FU by chemically conjugated the CD-L6 monoclonal antibody in combination with an anticancer prodrug 5FC compared to the non-conjugated CD. In another study, the combination of L6- *S. cerevisiae* CD and 5FC was equivalent in cytotoxic activity to 5FU when tested against the H2981 human lung adenocarcinoma cell lines (Senter et al. 1991)

Bystander Effects of CD/5FC:

Suicide genes with strong bystander effect could overcome the major limitations in cancer gene therapy, such as ineffective gene delivery and expression. Bystander effect is the extension of cell killing effects of the active drug to kill the non-transfected adjacent cells in the local microenvironment (Moolten 1986). This bystander effect is due to the transport of the toxic metabolites from suicide gene transfected cells to adjacent non-transfected cells through gap junctions; (Dilber et al. 1997), apoptotic vesicles (Colombo et al. 1995) or by passive diffusion Stribbling et al. 2000). The major advantage in the bystander effect of CD/5FC is independent of gap junctions (Lawrence et al. 1998) and it has very high bystander effect when compared to the HSV-1

TK/GCV combination (Trinh et al. 1995). The strong bystander effect of CD/5FC could be due to the non-facilitated diffusion of small size uncharged 5FU molecule, diffused through cellular membranes (Corban-Wilhelm et al. 2002).

Mechanism of CD/5FC mediated Cell death:

Recent reports indicated that CD mediated conversion of 5FC could induce apoptosis in various human tumor cell lines (Kurozumi et al. 2004, Lv et al. 2009). CD/5FC induced apoptosis was established by characteristic biochemical and cytological signatures, including nuclear condensation, membrane blebbing and DNA fragmentation (Gopinath and Ghosh 2007,2008a) . On the other hand, the up-regulation of apoptotic genes such as caspase- 3, c-myc, bad, bax and bak and down-regulation of anti-apoptotic genes such as bcl-2 and bclXL were observed by semi-quantitative RT-PCR analysis.Furthermore, up-regulation of p53 gene in the treated cells clearly revealed that suicide gene therapy follow the p53 mediated apoptotic pathway, through which most of the anticancer drugs trigger apoptosis (Gopinath and Ghosh 2009,2008b)

Combination therapy:

The rationale for the use of combination therapy was the prospect of synergistic cancer cell death. CD/5FC strategies have been studied in combination with radiation therapy and other anticancer drugs to use specifically in combination therapy. The use of combination of gene therapy is supported by previous reports for its superiority over mono therapy. The major advantage of combination therapy is the simultaneous use of drugs with different or same mechanisms of action is considered to be more effective than monotherapy to overcome the drug resistance problem. Such combination therapy has opened up new avenues in suicide gene therapy for cancer.

Radiation therapy:

Previous studies demonstrated that, 5FU is a promising radio sensitizer, which enhances the radio sensitivity of tumor cells (Mierzwa et al. 2010). Early studies of 5 FU in combination with radiation therapy suggested an additive effect in anti cancer activity (Lawrence et al. 1994). Based on these data, numerous reports have shown the benefit of additional radiation therapy in combination with CD/5FC mediated suicide gene therapy *in vitro* and *in vivo* (Table. 4). In this combination therapy, 5FU and its metabolites could inhibit the repair of radiation induced DNA damage which leads to the enhanced therapeutic efficacy (Kambara et al. 2002). Radiation dose and area plays important role in reducing the toxicity to the normal cells. Furthermore combination of radiation therapy could alter the signalling pathways (Mierzwa et al. 2010). Therefore, it is worthwhile to further investigate the CD/5FC plus radiation therapy in cancer treatment.

Combinations with other anti cancer drugs

Despite enormous progress in understanding CD/5FC strategies, advanced forms of cancer remain unmanageable to treatment. To overcome this problem, little work has taken place by combining the CD/5FC gene therapy with conventional anti cancer agent curcumin (Kievit et al. 2000 Gopinath and Ghosh 2008a). This combination showed synergistic apoptosis, where the individual components (5FC and curcumin) were used at much lower concentration than their IC_{50} values. The results suggest that combination therapy of CD/5FC strategies with other anti-cancer drugs may be of value in the treatment of cancer.

Table.4. Selected examples of CD/5FC mediated suicide gene therapy in combination with radiation therapy

Genes transferred	**Therapy route**	**Model system**	**References**
E.coli CD-UPRT	*In vitro*	Glioma cells	Kambara et al. 2002
	In vivo	Rat brain tumor	Kambara et al. 2002
HSV-tk / *E. coil* cytosine deaminase (CD)	*In vivo*	Nude mice	Rogulski et al. 1997
E. *coil* cytosine deaminase	*In vitro*	Human colorectal carcinoma cells	Khil et al. 1996
	In vivo	Human Cholanglocarcinoma Tumor Therapy Model in Nude Mice	Pederson et al. 1997
S. cerevisiae Cytosine Deaminase	*In vitro*	Human Colorectal Cancer	Kievit et al. 2000

Suicide gene therapy and Nanotechnology:

Most of the conventional anticancer drugs are not successful due to the multi-drug resistance of cancer, which can be overcome by the application of silver nanoparticles in combination with suicide gene therapy. Gopinath et al. (2008 c) were the first to report that nanoparticles could be used to synergize the therapeutic effect of suicide gene mediated cancer therapy. The same group have established the synergistic effect of silver nanoparticles on suicide gene therapy.

2.1.2. Uracil-phosphoribosyl transferase (UPRT): Uracil phosphoribosyl transferase (UPRT, EC 2.4.2.9), is a key enzyme involved in the pyrimidine salvage pathway for nucleotide biosynthesis, which catalyzes the conversion of uracil and 5-phosphoribosyl-1-R-diphosphate to uridine monophosphate (UMP) (Neuhard 1983). UPRTs have been identified in lower eukaryotes and most microorganisms and this enzyme is homologs to human orotate phosphoribosyl transferase (OPRT). UPRT is also able to mediate the conversion of 5-FU into 5FUMP (Fig.1.3) The enzyme has been purified from several different organisms such as, *E.coli* (Jenson and Mygard 1996, Anderson et al. 1992), *T gonidi* (Carter et al. 1997) and *Sacharomces seveciae* (Perez-Zuniga et al.2008). In addition to this UPRT have been identified from variety of other organisms, like *Sulfolobus shibatae* (Linde and Jensen 1996), *Acholeplasma laidlawii* (McIvor et al. 1983), *Candida albicans* (Alloush and Kerridge 1994), *Crithidia luciliae* (Asai et al. 1990), *Bacillus subtilis* (Martinussen et al. 1995), *Giardia intestinalis* (Dai et al. 1995), *Lactococcus lactis* (Martinussen and Hammer 1994), *Streptococcus salivarius* (Giffard et al. 1993), *Saccharomyces cerevisiae* (Kern et al. 1990) *Arabidopsis thaliana*(Islam et al. 2006). Kinetic studies have shown that *E. coli* UPRT is inhibited by 5FU with a k_m value lower than *T. gonidi* (Carter et al. 1997, Rasmussen et al.1986). .UPRT, isolated from *E.coli* (Jenson and Mygard 1996), *G. intestinalis* (Martinussen and Hammer 1994), *T. gondi*i (Schumacher et al. 2002), *S. shibatae* (Linde and Jensen 1996), and *S. solfataricus* (Jensen et al. 2005) are activated by GTP. Expression of *E.coli* UPRT gene in cancer cells found to sensitize cells to lower concentrations of 5FU (Kanai et al. 1998; Kawamura et al. 2000). Combined effect of *E. coli* CD and UPRT genes expression resulted increased 5FC toxicity both *in vitro* and *in vivo* (Koyama et al. 2000; Adachi et al. 2000)

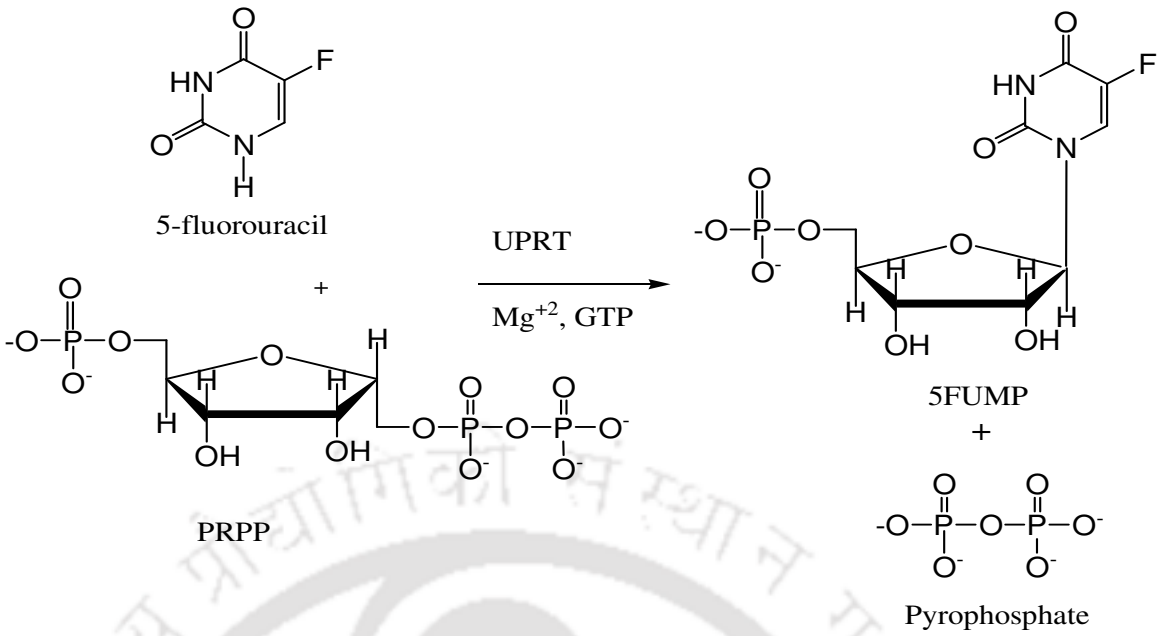

Fig.1.3. UPRT catalyzed reaction of 5FU

2.2. Targeted delivery of therapeutic enzymes by nanocarrires

The ability to selectively target tumors and the capability to deliver molecules and activate them responsively at specific locations in the body also has potential applications in cancer therapy. Tumor-specific targeting has the likely to reduce adverse effects and increase the efficacy of highly toxic chemotherapeutic drugs (Jaracz et al. 2005). The tumor vasculature manifested itself as a dense network located mainly at the periphery of tumor cell in order to continue an adequate supply by nutrients and oxygen for rapid tumour growth. In comparison with normal cells, tumor cells have hyper vascular permeability and leaky vasculature, which is highly permeable to nanoparticles and macromolecules. The cut-off pore size of solid tumor tissue has been reported ranging from 380 to 780 nm (Yuan et al. 1995). Hence, nanoparticle-based protein delivery systems have considerable potential for targeted delivery of therapeutic protein

and suicide gene for the treatment of cancer. Furthermore, functionalization of nanoparticles with tumour targeting agents such as folic acid and chemokine increase the selectivity for tumor cells (Chatterjee and Zhang 2007).Folic acid plays crucial role in cell growth and development by involving in the nucleic and amino acid synthesis. The human body does not produce it and it has to be consumed externally through supplements and natural food and diet. It has been found that cancer cells have more number of FR in it than normal cells and density of FR increases with the increasing the age of tumour (Antony 1996). From the previous reports, it is evident that FR internalizes the FA (Kamen and Capdevila 1986), FA-drug conjugates (Low and Antony 2004) and FA functionalized nanoparticles (Chatterjee and Zhang 2007) in to the cancer cells via receptor mediated endocytosis.

Polymeric-materials for the development of nanocarrier mediated-enzyme delivery

The most promising systems for the sustained release of enzymes involve encapsulation or entrapment of enzymes in biocompatible polymeric devices. In recent years, significant effort has been devoted to the development of biocompatible polymeric materials for delivery of therapeutic agents. Among the various biocompatible polymers used for the development of sustained-release formulations, chitosan and Poly n-isopropylacrylamide (PNIPAM) have been reported to be advantageous since these are nontoxic, biocompatible products with the potential for biodegradability.

Chitosan

Chitosan is a promising natural polymer that shows good biodegradability, non-toxicity, controlled release as well as bioadhesive Properties (Hejazi et al. 2003). The molecule is highly hydrophilic in solution due to the presence of amine groups and it exhibits much

greater potential for use in different applications. Chitosan hydrogels undergo abrupt changes in response to external stimuli such as changes in pH and temperature. Hydrophilic chitosan nanoparticles showed prolonged circulating time in blood, and therefore, are important for delivering of bioactive molecules such as therapeutic proteins and genes (Janes et al.2001). Early reports clearly emphasized that chitosan based nanoparticles can be prepared according to required compositions and particle size for protein, gene and drug delivery (Ieva et al. 2009, Katherine and Kam 2006).

Poly n-isopropylacrylamide (PNIPAM)

PNIPAM is one of the extensively studied thermoresponsive polymer actively investigated for sustained delivery of therapeutic agents. This polymer exhibits the lower critical solution temperature (LCST) in an aqueous solution at and around 32ºC, which is in the vicinity of the body's physiological temperature (Dhara et al. 2000). The PNIPAM gel will collapse and shrinks at temperatures above the LCST and it swells when cooled below the LCST (Khan 2007). The LCST of PNIPAM can be easily be manipulated by changing the polymer compositions by copolymerization with hydrophilic or hydrophobic monomers and by addition of salts or surfactants to the polymer compositions (Lee et al. 2001). Since the LCST of PNIPAM in aqueous solution is slightly below body's physiological temperature and can be changed to above the physiological temperature, PNIPAM has become a potential candidate for pharmaceutical use and is widely used for designing temperature sensitive controlled delivery of therapeutic agents (Ganta et al. 2008).

A promising approach for designing novel enzyme delivery systems is based on combining the merits of the above two polymeric systems, which are both biodegradable and responsive to physiological stimuli.

3. Significance of the work

The rationale of the present research work is described based on the recent knowledge and its lacunae on *E. coli* cytosine deaminase. Pioneering studies have established intra-tumoral conversion of prodrug 5FC to its active metabolites by suicide enzymes. In our laboratory suicide gene therapy system was demonstrated using *E. coli* cytosine deaminase and hybrid *E. coli* cytosine deaminase- uracil phosphoribosyltransferase (CD-UPRT) genes which can convert pro drug 5FC to anti cancer drug 5FU and its metabolites in mammalian cells (Gopinath and Ghosh 2007,2008a,2008b). The primary goal of this strategy is to selectively increase tumor cell exposure to cytotoxic drug metabolites generated locally by a prodrug-activating cytosine deaminse enzyme. Previous work from our group established the suicide enzyme mediated apoptotic cell death involving apoptotic signalling path way (Gopinath and Ghosh 2009). Furthermore, cytosine deaminase gene therapy is accompanied by substantial bystander cytotoxicity which greatly enhances the therapeutic effect by extending it to nearby tumor cells not transduced with the therapeutic cytosine deaminse gene. This formed a strong basis of the present research work. However, the basic studies on suicide enzymes for their potential applications are not adequately addressed so far. Literature reports suggest that complete characterization of the suicide enzyme and its broad substrate specificity is required to enumerate wide applications- such as, its possible role in enzyme based therapy. Thus the major endeavour of the research project is to isolate suicide enzymes from non mammalian sources. I tried to reveal the molecular interactions of 5FU with molecular dynamics snapshots of UPRT. Dynamic nature of the protein is very important biological phenomenon by which a protein attains the several conformations in picoseconds to nanoseconds time period.

After thorough literature review, we have observed the paucity of gene delivery systems could be overcome by direct delivery of 'suicide' enzymes to the cancer cells. To overcome the existing problems in suicide gene therapy, it is imperative to develop biodegradable, polymeric nanoparticle based delivery systems for the targeted delivery of suicide genes and enzymes.

My investigations would enhance the present knowledge on suicide enzyme characteristics for engineering the recombinant enzymes with superior therapeutic efficacy. Present study would also consecutively facilitate the development of a nanocarrier for the targeted delivery of the suicide enzymes.

3. Specific objectives

Three specific objectives of present work are as follows:

Purification and detailed characterization of "suicide" enzymes: cytosine deaminase and uracil-phosphoribosyltranferase from *E. coli*

Development of nanocarriers for encapsulation of "suicide" enzymes using biocompatible materials such as, chitosan and poly (n-isopropylacrylamide)

Functionalization of the nanocarriers for targeted delivery

Chapter 2

Purification and characterization of E.coli cytosine deaminase

2.1. Overview

In the recent past, advances in suicide gene therapy have enormous impact on eradication of various types of malignant tumors, which is mainly due to widespread therapeutic efficacy of suicide genes (Portsmouth et al. 2007). Cytosine deaminase (CD), a microbial pyrimidine salvage pathway enzyme, catalyzes hydrolytic deamination of cytosine to uracil and liberates ammonia, was reported to be quite efficient as a prodrug gene therapy system. CD converts prodrug 5FC to toxic 5FU, which inhibits DNA synthesis, was found quite useful in cancer therapy (Springer and Niculescu 1996). Our laboratory has developed a novel suicide gene therapy systems based on cytosine deaminase (CD) and its hybrid form with the uracil-phosphoribosyltransferase gene (UPRT)- both of them found to induce apoptotic cell death over a wide range of cells treated with 5-FC (Gopinath and Ghosh 2007; 2008a). Additional work delineated the molecular mechanism of cell death using suicide gene therapy vectors in cancer cells (Gopinath and Ghosh 2008b, 2009). CD enzyme has been purified from different organisms like, *E.coli* (Katsuragi et al. 1986), *Saccharomyces Cervisiae* (Ipata et al. 1971), *Salmonella Typhirium* (West et al. 1982), *Aspargillus Fiumigatus* (Yu et al. 1991) and *Chromobacterium Violaceum* (Kim et al. 2004). However, complete characterization of the enzyme and its broad substrate

specificity is needed to enumerate its wide applications- such as, development of antibody and its possible use in enzyme based therapy. Reports on protein purification using FPLC (fast performance liquid chromatography) were shown to be time saving, low cost, reproducible and efficient (Quan et al. 2009; Tangvarasittichai et al. 2009; Plank et al. 2008). Therefore, in the present work, CD has been purified using DEAE-cellulose ion exchange chromatography by FPLC.

2.2. Experimental Approaches

2.2.1. Materials

DEAE-cellulose, chitosan, 5-fluorocytosine were obtained from Sigma-Aldrich, USA. Luria–Bertani (LB) medium was purchased from HiMedia, India for bacterial growth. All other materials and reagents were of the highest purity commercially available

2.2.2. Bacterial strain, culture conditions

Escherichia coli K-12 MTCC 1302 was from the Institute of Microbial Technology Chandigarh, India. It was cultivated using 1% (v/v) inoculum in 500 ml Erlenmeyer flasks containing 100 ml LB media for 12 h at 37°C with shaking at 180 rpm.

2.2.3. Purification of cytosine deaminase

Cells (5 x 10^8 CFU/ml) were centrifuged at 4000 x g for 10 min, the pellet was suspended in 15 ml 50 mM phosphate buffer, pH 6.3, and disrupted in a Constant Cell Disrupter at 103 MPa. The disrupted cell suspension was centrifuged at 16000 x g for 15 min. The supernatant was fractionated with 35% $(NH_4)_2SO_4$ and the precipitated protein was collected by centrifugation (19000 x g for 20 min). The protein was resuspended in 6 ml 50 mM phosphate buffer and dialyzed against same buffer for 6 h

at 4°C. The sample was filtered through 0.45 µm filter and applied on to a pre-equilibrated DEAE-cellulose fast-flow column (1.9 x 15 cm) connected to a FPLC system at 0.5 ml/min. The bound protein was eluted with 50 mM phosphate buffer with a linear gradient of 0–1 M NaCl at 1 ml/min. One (01) ml protein fractionswere collected and analyzed by SDS-PAGE. Enzymatically-active fractions were pooled, lyophilized, resuspended in 1 ml PBS buffer and stored at 4°C

2.2.4. Enzyme assay

Enzyme activity was measured with slight modifications to the method of Hayden et al. 1998. One ml reaction mixture, containing 3 mM 5FC in phosphate buffered saline, pH 7.3 (PBS), plus enzyme, was held at 37°C for 2 h. The reaction was stopped by adding 1 ml 0.1 M HCl and absorbance was measured at 255 nm. The concentration of 5FU formed in the reaction was calculated using the molar extinction coefficient 5405 cm^{-1} M^{-1}) at 255 nm. One unit of enzyme activity was defined as 1µM 5FU formed per min at 37°C. Protein concentration was measured by Bradford method (1986) using BSA as standard.

2.2.5. Determination of K_m and V_{max}

Kinetic values of CD for cytosine were obtained by measuring the enzyme activity from the reaction solutions with cytosine concentrations of 0.2.0.3, 0.4, 0.5, 0.6, 0.7, 0.8 mM in PBS (pH7.3). The measurements were repeated 3 times using the same amount of enzyme for each cytosine concentration. K_m and V_{max} were determined by using the Line Weaver- Burk reciprocal plot (1934). Similarly, kinetic values of CD for 5FC were obtained from the reaction solutions containing 0.5, 1, 3, 5, 7, 9, 11 and 13 mM 5FC in PBS (pH 7.3).

2.2.6. Determination of pH and temperature optima and stability of cytosine deaminase

The optimum pH was determined by carrying out the enzyme reaction in pH range of 4 to 11 using at 50 mM of acetate buffer (pH4.0 and 5.0), phosphate buffer (pH 6.0, 7.0 and 8.0), Tris buffer (pH 9.0and 10.0), Glycine buffer (pH 11.0) 37 °C. The optimum temperature was determined by carrying out the enzyme reaction at 10, 20.30, 37, 40.50,60 and 70°C at (pH 7.3) using PBS. The stability was determined as the percent original activity remaining at the end of specified time intervals. The pH stability was studied by incubating the enzyme in a pH range of 4-10 using above mentioned buffers up to 72 hours at 4°C. Similarly the temperature stability was studied by incubating the enzyme sample at 37. 45, 55 and 65°C temperatures at pH 7.3 and then residual activity was measured by standard assay procedure at different time intervals

2.3. Results and discussions

2.3.1. Purification of cytosine deaminase

Cytosine deaminase was 50 fold purified using DEAE- cellulose anion exchange column chromatography. The purification steps and the degree of purification have been summarized in detail in Table 2.1. The specific activity was found 3.74 ±.0.53U/mg. A linear gradient 0-1 M NaCl was used to elute bound proteins from the DEAE cellulose column. Cytosine deaminsae was eluted at 0.6 M NaCl at flow rate of 1 ml/min (Fig.2.1). The active fractions of the enzyme were analyzed in Commassie blue stained SDS PAGE. Subunits of 35 and 46 kDa subunits of the enzyme were observed (Fig.2.2).

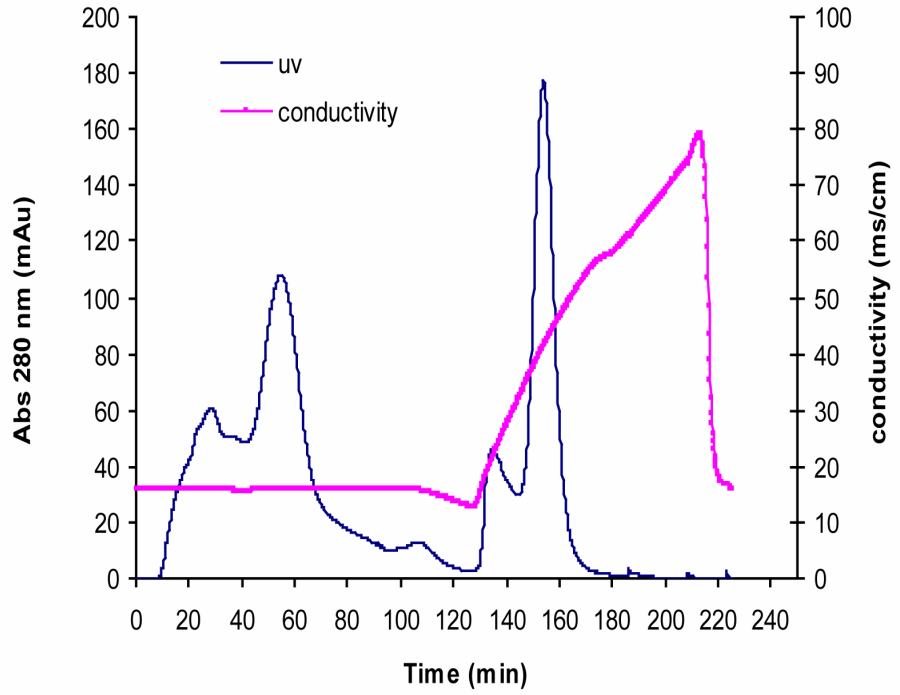

Figure.2.1. DEAE anion exchange chromatogram of cytosine deaminase. Ammonium sulphate (35 %) precipitated protein was loaded on to a pre equilibrated DEAE cellulose column at a flow rate of 0.5 ml/min. The bound protein was eluted with NaCl (0 to 1M) in a linear gradient at flow rate of 1ml/min.

Table.2.1. Purification profile of cytosine deaminase.

Purification steps[a]	Enzyme activity (U/ml)	Protein (mg/ml)	Specific activity (U/mg)	Purification fold
Crude lysate	0.314	4.3	0.073	1
$(NH_4)_2SO_4$ precipitated protein	5.3	3.5	1.057	14
DEAE cellulose	6.4	1.7	3.74	51

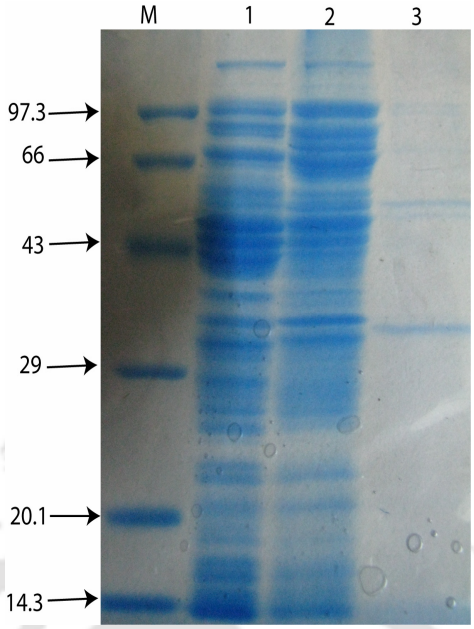

Figure.2.2. Coomassie Brilliant blue R250 stained SDS-PAGE analysis (12% gel) of cytosine deaminase at different purification steps. M, molecular weight markers (kDa); lane 1, cell free extract after lysis; Lane 2, 35% ammonium sulphate precipitated protein; lane 3, pooled active fractions of DEAE-cellulose column.

2.3.2. Effect of pH and Temperature

The enzyme was found to be stable up to 55°C. Around 11 % activity was retained after 24 hours of incubation at 65°C (Fig. 2.3a). Within temperature 4-37°C, the enzyme was almost stable for 48hr with slight reduction in the activity. The optimum reaction temperature was 50°C (Fig. 2.3b). The enzyme was stable at pH 7 to 10. Around 96% and 30% enzyme activity was retained after 48 hours incubation at pH 10 and 5, respectively (Fig. 2.3c).The enzyme was highly active at pH ranges 7 - 11. The optimum pH for the reaction was observed at pH 9 (Fig. 2.3d).

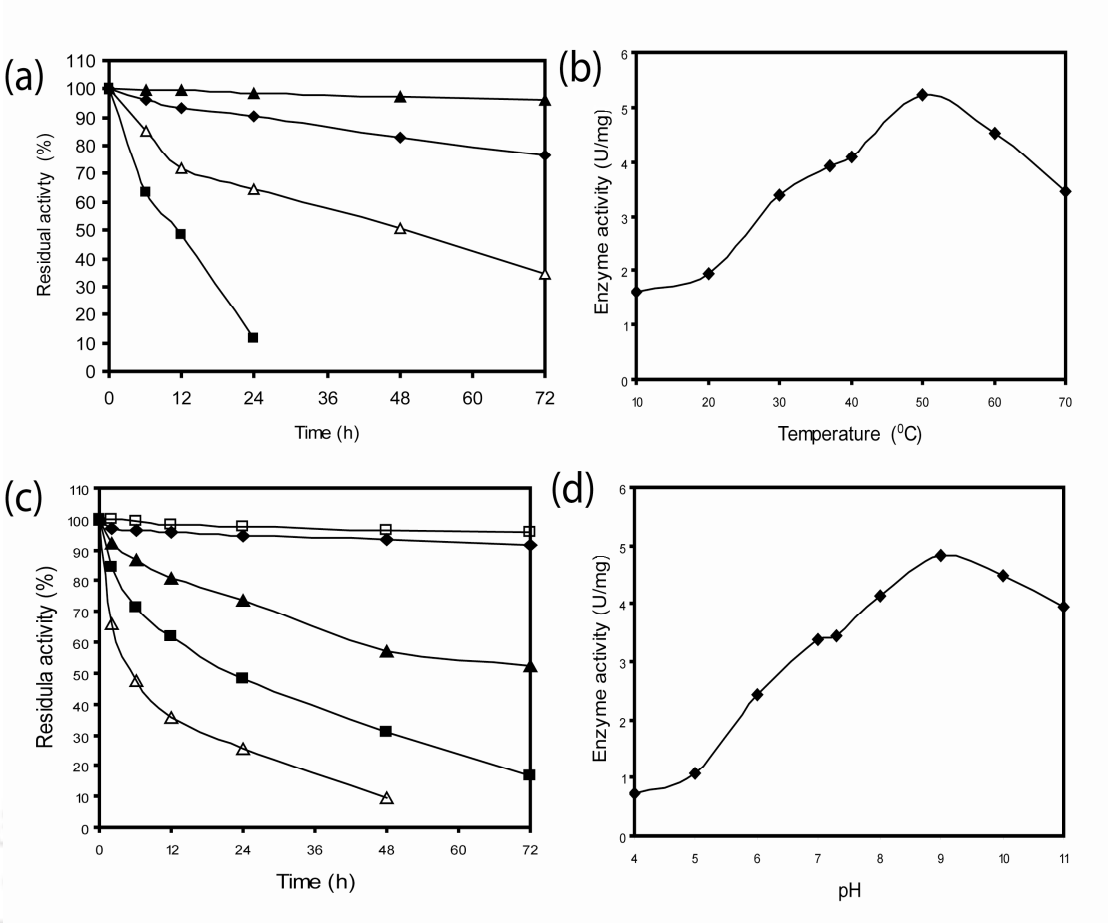

Figure.2.3. (a) Temperature stability at 37°C (*filled triangle*), 45°C (*filled diamond*), 55°C (*empty triangle*) and 65°C (*filled square*) (b) Temperature optima.The enzyme reactions were carried out between the temperatures 10 and 70°C at pH 7.3 (c) Stability at pH 10 (*empty square*), pH 7 (*filled diamond*), pH 6 (*filled triangle*), pH 5 (*filled square*) and pH 4 (*empty triangle*) (d) pH optima of cytosine deaminase. The enzyme reactions were carried out in pH range of 4 to 11 at 37°C using 50 mM of each acetate buffer (for pH 4 and 5), phosphate buffer (for pH 6, 7 and 8), tris buffer (for pH 9 and 10) and glycine buffer (for pH 11.0). The stability was determined as the percent original activity remaining at the end of specified time intervals (enzyme activity at 100% was 3.9 U/mg).

2.3.3. Kinetic analysis and substrate specificity

Cytosine deaminase showed 7 fold higher K_m and 2.6 fold lower V_{max} value for 5FC than cytosine (Table.2.2). The V_{max}/K_m ratio confirms that cytosine is a better substrate than 5FC for CD.

Table.2.2. Characterization profile of cytosine deaminase from *E.coli* K-12.

Substrate	K_m (mM)	V_{max} (nM/min/µg)
Cytosine	0.26	3.8
5-Fluorocytosine	1.82	1.4

2.4. Summary

In conclusion, cytosine deaminase has been purified from *E.coli* k- 12 by modifying the existing methods. Purity of the enzyme was confirmed in SDS-PAGE. Cytosine showed lower K_m and higher V max than 5FC, which indicates cytosine deaminase has higher affinity for cytosine than 5FC.

Chapter 3

Purification and *in silico* characterization of *E. coli* uracil phosphoribosyltransferase

3.1. Overview

E. coli uracil phosphoribosyltransferase (UPRT, EC 2.4.2.9) is a key enzyme involved in the pyrimidine salvage pathway for nucleotide biosynthesis, which catalyzes uracil and α D-5-phosphoribosyl-1-R-diphosphate (PRPP) to uridine monophosphate (UMP) (Neuhard 1983). This non-mammalian enzyme expressing gene showed successful applications in suicide gene therapy for targeted killing of human cancer cells. Suicide gene therapy strives to deliver genes to the cancer cells, which eliminate cancer cells by local production of toxic agents. The most intensely studied suicide genes are herpes simplex virus thymidine kinase (HSV-tk), *E.coli* cytosine deaminase (CD) and bifunctional *E.coli* cytosine deaminase - uracil phosphoribosyltransferase (CD-UPRT). With these strategies, the prodrug is converted to the toxic agent only in cancer cells, thereby allowing a maximal therapeutic effect while limiting toxicity in non- cancer cells. HSV-tk has its limitations due to the requirement of cell-to-cell contact for active transport of prodrug, ganciclovir metabolites to neighbouring cells to exert bystander-killing effect (Portsmouth et al. 2007). On contrary, CD converts the prodrug antifungal agent 5-fluorocytosine (5-FC) into antitumor agent 5-fluorouracil (5-FU), and UPRT further converts 5FU into toxic metabolites, which diffuses across the cell membrane that kills adjacent neighbouring cells by inhibiting DNA and RNA synthesis. Therefore,

application of UPRT along with CD has strong therapeutic potential in suicide gene therapy for anti cancer activity (Gopinath and Ghosh 2009). *E.coli* UPRT enzyme inhibition by 5FU and its activity towards the conversion of 5FU to 5 fluorouracil monophospahte (5FUMP) has already been reported (Rasmussen et al, 1986; Jensen and Mygind 1996). Kinetic studies have shown that *E. coli* UPRT is inhibited by 5FU with an inhibition constant (K_i) value lower than *T. gondii* UPRT (Carter et al. 1997; Rasmussen et al. 1986). Moreover, expression of *E.coli* UPRT gene in human cancer cell lines has been reported to increase cytotoxicity to anticancer drug 5FU compared to non – UPRT expressing cells (Kawamura et al. 2000). In addition, combination of *E. coli* CD and UPRT genes expression in cancer cells demonstrated enhanced 5-FC toxicity than CD alone (Gopinath and Ghosh 2009;Adachi et al. 2000). To improve CD-UPRT strategy, it is necessary to engineer the recombinant *E. coli* UPRT to increase its catalytic efficiency toward an existing substrate. An accurate determination of inhibition constant for protein-ligand complexes plays a critical role in describing binding interactions. The primary purpose of this study was to study the interaction of 5FU with *E.coli* UPRT by molecular dynamics (MD) simulations and subsequent docking studies.

As *E.coli* UPRT is promising for salutary applications, the inhibition and docking studies of the UPRT is considered to be an expectant approach to improve the efficiency of suicide gene therapy. In biological system, we know that enzymes can shift structural orientation among several conformations in cellular environment. Therefore, it is necessary to consider the protein flexibility during the docking process to improve the reliability and engender new insights. Protein flexibility plays a vital role in accepting ligands with different sizes, shapes and in finding the best ligand enzyme complex conformations (Carlson 2002). In order to incorporate a more practical representation of the receptor flexibility during docking experiments, we have considered 1250 of

receptor conformations, generated by MD simulation. Recent advances in MD simulation could generate an ensemble of UPRT conformations, which are used in subsequent docking experiments to evaluate the free energy of binding (FEB) changes of dockings with uracil and anticancer drug 5FU. In my docking experiments, the lowest energy structure obtained at different snapshots was considered as correctly docked structure. The significant conformational flexibility of UPRT may be essential for its catalytic action.

3.2. Experimental Approaches

3.2.1. Materials

Sepahcryl-300, 5FU, PRPP, guanosine triphosphate (GTP) and phosphate buffer saline (PBS) buffer (100 mM phosphate buffer containing 100 mM NaCl, pH 7.3)) were obtained from Sigma-Aldrich, USA. *E. coli* k-12 MTCC 1302 was procured from the Institute of Microbial Technology Chandigarh, India. Luria–Bertani medium was purchased from HiMedia, India for bacterial growth. All other materials and reagents were of the highest purity and commercially available.

3.2.2. Purification of UPRT

UPRT was purified from strain *E. coli* k-12 MTCC1302 with slight modifications of the method described previously (Natalini et al.1979). About 5L culture *E.coli* k-12 MTCC1302 was grown to log phase in Luria–Bertani media at 37 °C and then the cells were harvested by centrifugation at 8000 X g for 10 min. The cells were suspended in (PBS) buffer and lysed using CONSTANT CELL DISRUPTER at 15 kPsi. The crude lysate was collected by centrifugation at 1500 X g for 30 min and subjected to ammonium sulphate precipitation. The protein collected after centrifugation at 12000 x

g for 30 min was resuspended in PBS and dialyzed overnight at 4°C. The dialyzed protein sample was applied to a pre-equilibrated sephacryl -300 connected to FPLC ACTA system (GE Health care). Protein was eluted with PBS at a flow rate of 0.5 ml/min. Active fractions of the enzyme were analyzed in sodium dodecyl sulfate-polyacrylamide gel electrophoresis (SDS- PAGE) and visualized after silver staining. Finally, the fractions were lyophilized and stored at -20°C.

3.2.3. Enzyme assay and Determination of K_i

UPRT activity was measured spectrophotometrically based on the conversion of uracil to UMP at 280 nm (ε=2.5 $mmol^{-1}$ Lcm^{-1}) using established method (Fast and Skold 1917). One ml reaction mixture consists of 100 mM $MgCl_2$, 50 mM GTP, 50 mM PRPP, 10 mM uracil and enzyme sample in PBS buffer. After 1 h of incubation at 37°C, the reaction was stopped by heating at 100°C for 1 min. K_i value for 5FU was calculated from Lineweaver-Burk plots at 5, 20, 30 µM. One unit of UPRT activity is defined as 1 nmole of UMP formed per minute at 37°C.

3.2.4. MD simulation

The X- ray structure of UPRT (2EHJ) was taken from Protein Data Bank (PDB) and used as starting model for the MD simulation. Its explicit flexibility was obtained from a fully solvated MD simulation trajectory generated by the SANDER module of AMBER 8 using HP Proliant server with eight processors as previously described method (Kumar and Swaminathan 2010). During the MD simulation, instantaneous snapshots were recorded at every 0.002 pico seconds (ps) for 1000 ps. As consecutive snapshots have closely related conformations, we picked up snapshots separated by time intervals larger than 0.8 ps. A total of 1,250 snapshots were converted to PDB format

files by PTRAJ, which is an AMBER utility that converts the trajectory of protein snapshots generated by MD simulation into the PDB file format. A computer program was developed to establish the communication between Shark and PTRAJ. The system was prepared by LEaP module of the AMBER program package (Pearlman et al. 1995; Case et al. 2005). The protein was solvated with TIP3P (Mahoney and Jorgensen 2000) waters and neutralized with the counter ions using the LEaP module. Atomic interactions were explained by The AMBER force field FF99SB (Hornak et al. 2006). Long range electrostatic interactions were treated by the Particle Mesh Ewald method (Essmann 1995). Constant temperature and pressure was maintained by Berendsen's thermostat and barostat (Berendsen et al. 1984). SHAKE algorithm was used to control the bonds involving the hydrogen atoms. The MD simulation was conducted with an 8.0 Å cut-off on real-space interactions.

3.2.5 Ligand preparation

PRODRG2 server (Schüttelkopf and van Aalten 2004) was used to generate 3D coordinates of uracil and 5FU. UCSF (University of California, San Francisco) Chimera (Pettersen et al. 2004) was used to construct the molecular files for both the ligands. Nonpolar hydrogen atoms were added to the ligands and the charges were assigned to individual atoms using Gasteiger-Huckel rule.

3.2.6. Protein preparation

The 1250 PDB files of snapshots of UPRT obtained from MD simulation were written into separate PDB files without water molecules or cofactors or metal ions. Non polar hydrogen atoms were added to all of the receptors by using UCSF chimera

(Schüttelkopf and van Aalten 2004). Protein atomic charges were assigned using AMBER FF99SB (Hornak et al. 2006) force field.

3.2.7. Docking procedure

All docking runs were performed using UCSF DOCK version 5.2 (Kuntz and Moustakas 2005). The surface of protein was calculated with the Dms program (Ferrin et al. 1988) and spheres were generated by Sphgen module (Kuntz et al. 1982). A reference molecule (methane) was used to identify the exact position for docking on the protein. The grid program was used to generating the energy grid for docking (Meng et al. 1992). The box size, the grid space, energy cut off, max orientation and van der Waals repulsive exponent were set as 6 Å, 0.3 Å, 9999, 1500 and 8.0 Å respectively. All parameters used in docking were default except for the explained ones. The docking procedure was automated using Perl script for all 1250 snapshots. The resultant structure files were analyzed using UCSF chimera visualization programs (Pettersen et al. 2004).

3.3. Results and discussion

UPRT enzyme was purified 87 fold by ammonium sulphate fractionation followed by gel filtration chromatography, which conferred the final specific activity of 12 U/ml. The detail purification steps were shown in Table 3.1. We obtained a 23 kDa band corresponding to UPRT in SDS-PAGE (Fig.3.1A). 5FU inhibits competitively the binding of uracil to UPRT with an inhibition constant (K_i) of 13 µM (Fig.3.1B), indicating the formation of UPRT -5FU complex. The K_i value of 5FU obtained from our experiments agrees reasonably well with previous data available in the literature on the inhibition of UPRT (Rasmussen et al. 1986). The inhibition results established

efficient interaction between 5FU and *E.coli* UPRT. In previous report, computational studies were performed to elucidate the interactions of uracil and 5FU with *T. gondii* UPRT (Schumacher et al. 1998). Even though both the ligands bound in the same active site, it is an intriguing question whether uracil and 5FU would interact with the different residues of UPRT in realistic biological conditions. As *E. coli* UPRT has emerged as a key enzyme in suicide gene therapy (Gopinath and Ghosh 2009), therefore, I explored the binding interactions of anticancer drug 5FU with *E. coli* UPRT for designing the mutant enzyme for high selectivity towards the prodrug. Furthermore, molecular docking and inhibition studies strongly support and aid the design of novel, more potent inhibitors by edifying the mechanism of drug–protein interaction (Chung and Wong 2008). In order to elucidate the interactions, I have performed the simulation of UPRT and 1250 snapshots were taken for docking studies.

Table.3.1. Purification profile of UPRT. All experiments were performed in triplicate. Mean values and standard deviations are indicated

Purification step	Enzyme activity (U/ml)	Protein (mg/ml)	Specific activity (U/mg)	Purification fold
Crude lysate	0.52 ±0.05	3.6 ± 0.3	0.14± 0.2	1
Ammonium sulphate precipitated protein (50-60% saturation)	7.05 ± 0.5	1.3± 0. 4	5.21 ± 0.5	37
S-300 gel chromatography	11.37±0.4	0.9±0.6	12.22 ±0.5	87

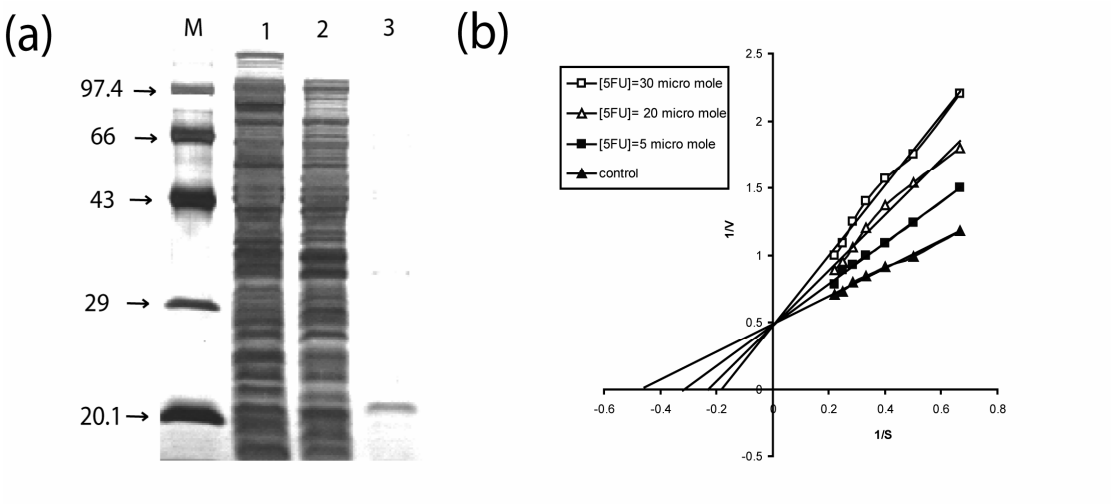

Figure.3.1. (A) Silver stained SDS-PAGE of UPRT. M, molecular weight markers (kDa); lane 1, cell free extract after lysis; Lane 2, Ammonium sulphate precipitated protein; lanes 3, purified UPRT (B) Lineweaver–Burk plot of the UPRT inhibition at different concentrations of 5FU

The crystal structure of the *E. coli* UPRT reveals the presence of four chains A, B, C, D (monomers) that include two tight dimers. The structure comprises 208 residues in each subunit. Four chains are found to be 100% similar (Fig.3.2) by using multiple sequence alignment tool CLUSTALW (Thompson et al., 1994). The 2ehj PDB structure was analyzed on the basis of the values of the Ramachandran plot (Fig .3.3) produced with Procheck program (Laskowski et al. 1993). The Procheck summary of Ramachandran Plot statistics showed that 85% of the residues were in the most favoured regions, 14.4% of the residues were in additional allowed region, 0 % in the generously allowed region, and only 0.6% in the disallowed region. In a previous study, four conserved regions among the UPRTases of *T. gondii, S. cerevisiae, B. subtilis, B. caldolyticus, L.lactis, E.coli, M.genitalium, N.tabacum* were demonstrated (Schumacher et al. 1998).

In *E. coli* four conserved regions are as follows: 1. residues 76-80 (sulphate binding site) 2. residues 103 -110 (flexible loop) 3. residues 130-139 (PRPP binding site) 4. Residues 192-208 (pyrimidine binding site)

Figure.3.2. Sequence alignment of four chains (A,B,C,D) of UPRT using CLUATALW

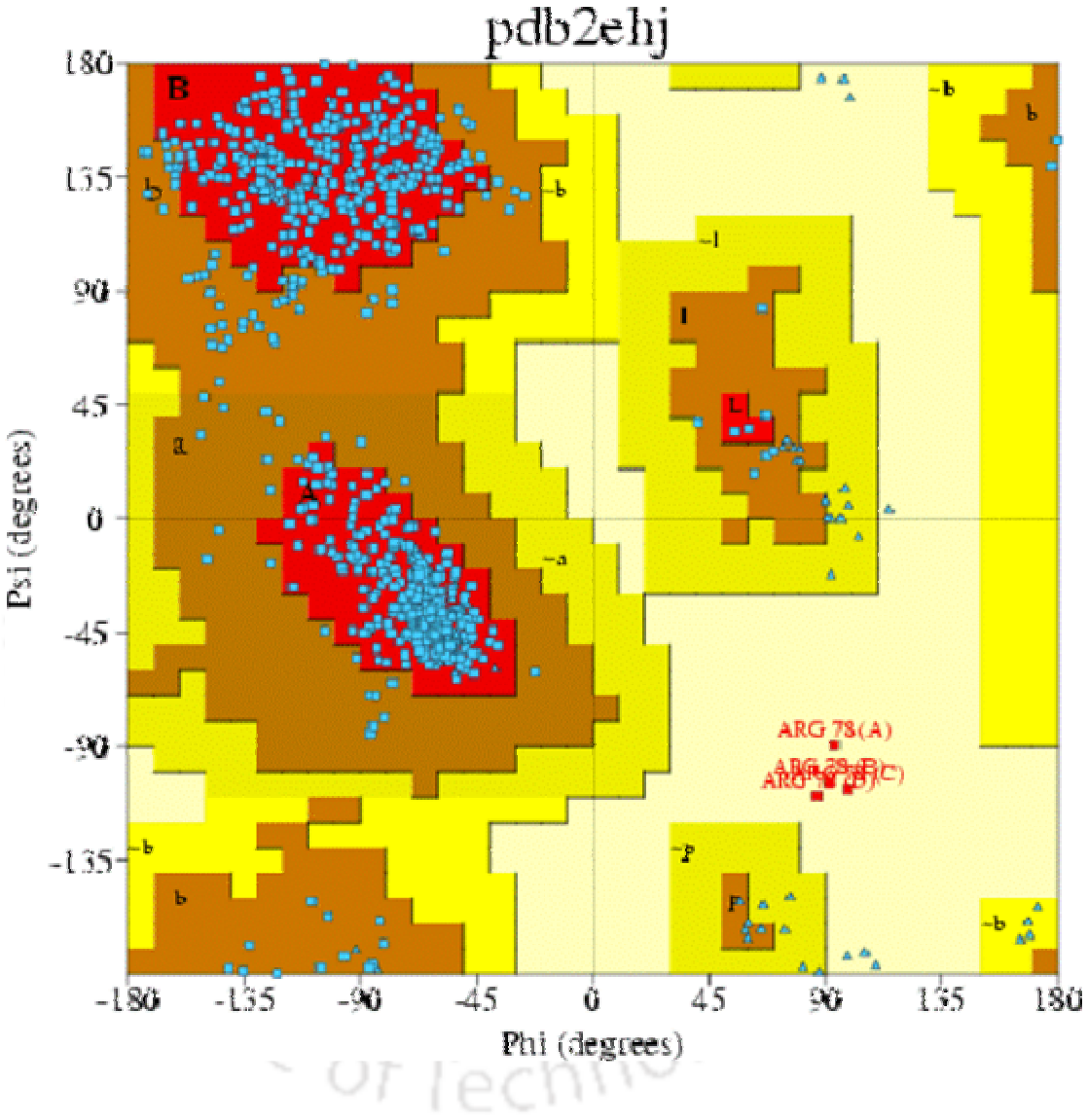

Figure.3.3. Ramachandran map of *E.coli* UPRT protein. The Plot calculation was done with PROCHECK program. (Most favoured regions - A, B, L; Additional allowed regions - a,b,l,p; Generously allowed region -~a,~b,~l,~p; Disallowed regions – in white).

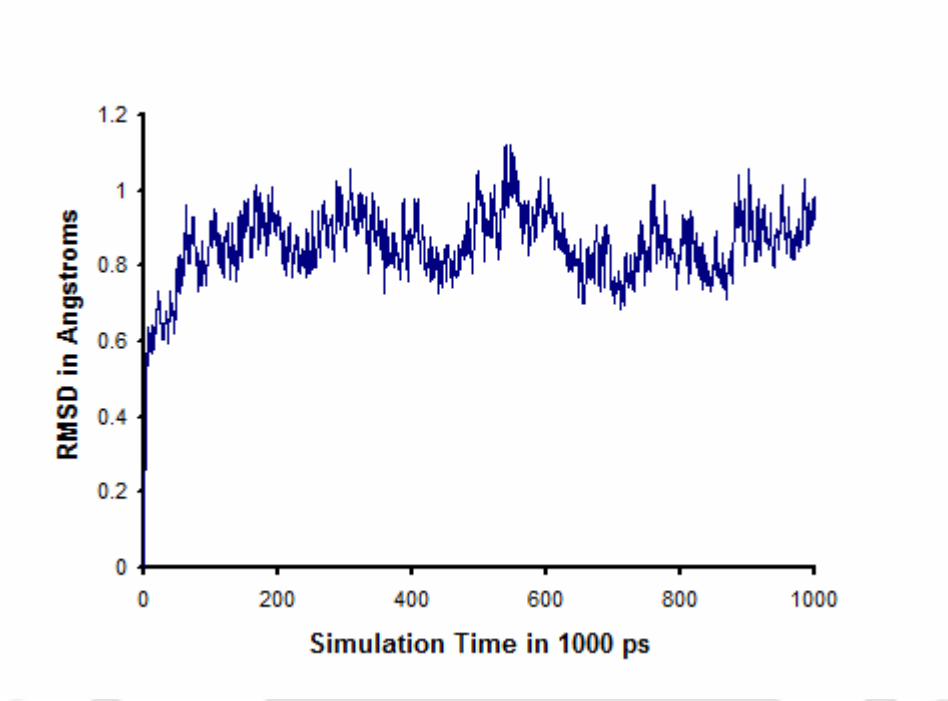

Figure.3.4. RMSD evaluation of *E.coli.* UPRT during MD simulation.

The stability of UPRT structure was analyzed by observing the Root Mean Square Deviations (RMSD) of the molecule and monitoring secondary structure of residues throughout the simulation period. The changes in structural conformation of UPRT were monitored in terms of RMSD of C_α atom (Fig.3.4). The enzyme was stabilized between RMSD values of 0.6 and 1.1 Å during 1000 ps of MD simulation indicated that the structure remained stable. Secondary structure analysis from figure 3.5 indicated that the protein retained the secondary structure for most of the residues, but noticeable changes observed in certain residues. Maximum flexibility observed in 104 to 110 residues, particularly 104 and 109 changed to irregular structure to anti parallel beta sheet where as 108 changed to irregular structure to turn. Another flexible region was in between residues 75 to 90. Particularly, 79 and 80 changed to turn to 3_{10} helix and alpha

helix, 81, 82, 83 changed to 3_{10} helix to alpha helix and 89, 90 changed to alpha helix to turn. Remaining residues have shown stable secondary structure with slight modifications throughout the simulation period.

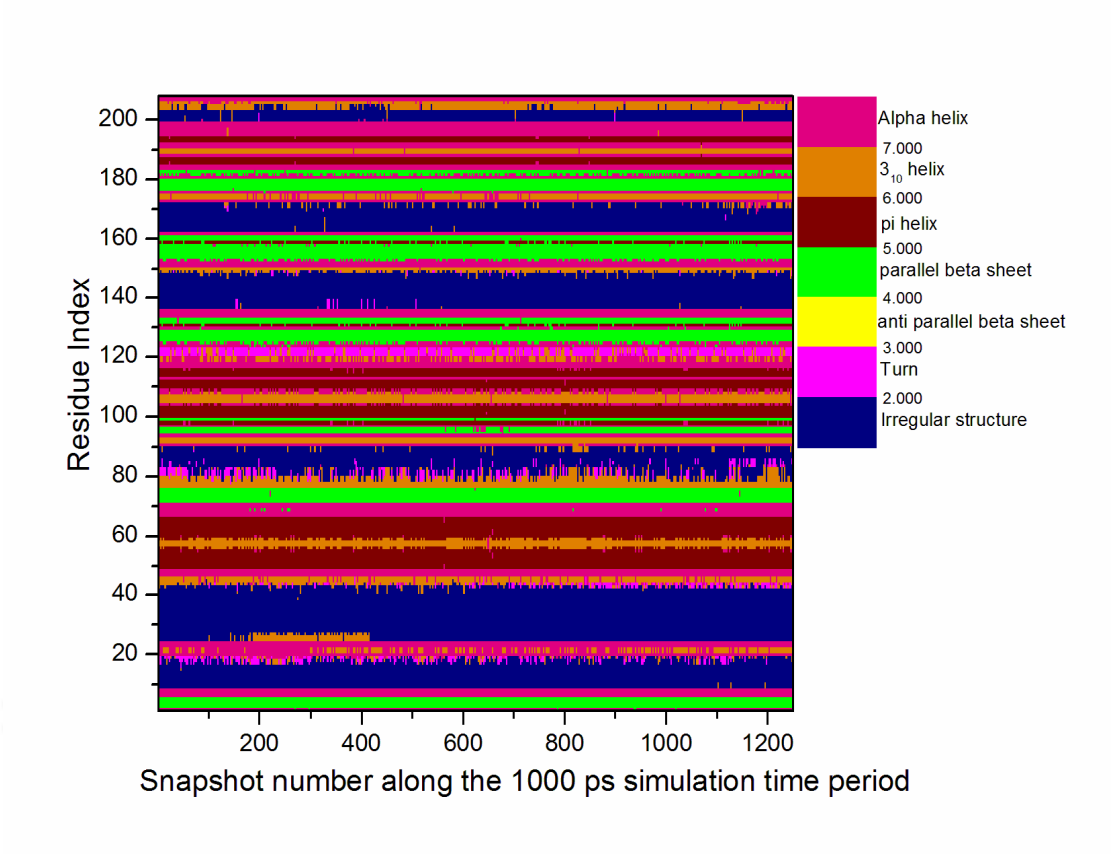

Figure.3.5. Stability of the secondary structures of UPRT during MD simulation.

MD simulation of UPRT resulted in 1250 PDB files, which represents different snapshots of UPRT in 1000 ps. Appropriate snapshot of the receptor for the ligand binding is important to describe binding interaction of the target molecules. Perfect elucidation of new modes of molecular recognition is possible by using protein flexibity in docking experiments as divergent to the typical application of docking to single pose of protein. 5FU and Uracil were successfully docked in pyrimidine binding site and out put showed that there was a distinct difference in the free energy binding between both

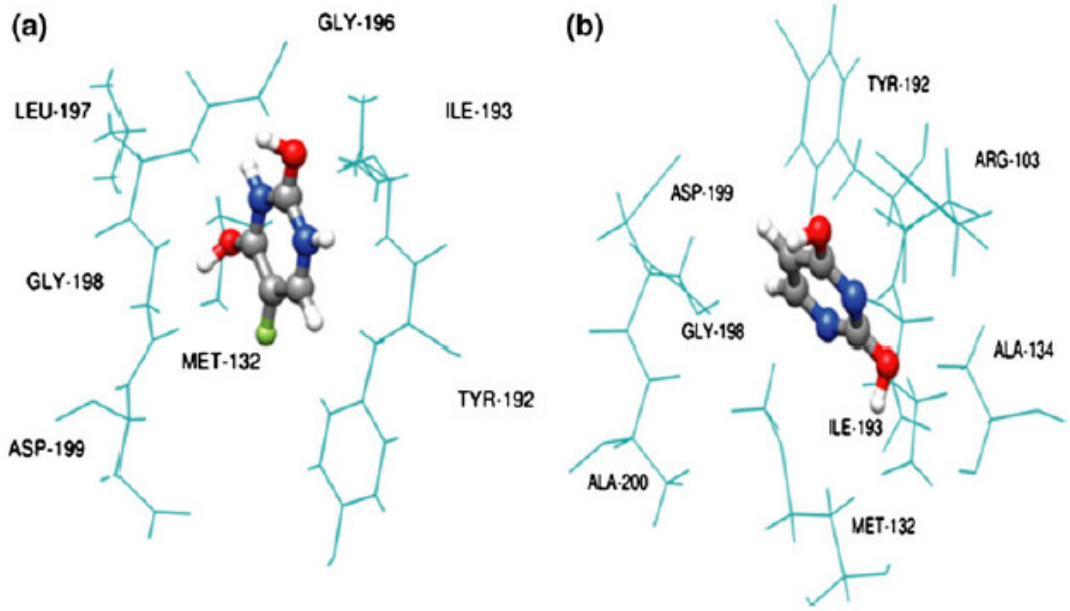

Figure.3.6. Best free energy binding dockings of (a) UPRT -5FU complex (b) UPRT - uracil complex.

the ligands. Total 1250 dockings were done for each ligand to the molecular dynamic snapshots of UPRT and resultant FEB changes were extracted. Among all the dockings 4 of 5FU and 5 of uracil out puts were exempted for analysis due to appearance of the ligand out side of defined grid box. Table 3.2 summarizes the result of the docking study presented as binding energies. 5FU has shown low average free energy binding with UPRT which indicates the stronger binding than its natural substrate uracil. 5FU and uracil were best docked to UPRT with FEB of - 37.8 k.cal/mol and - 28.4 k.cal/mol respectively. Both the ligands were binding in the same binding pocket (residue number 192-208) of UPRT in all favourable energy dockings, but interaction was varying among the residues within the binding pocket at different time points or receptor snapshots. Even though all favourable energy dockings of both the ligands were interacting with Tyr-192, Gly-196,Gly-198, and Met-132.we observed UPRT-uracil complexes form hydrogen bonds with Arg-103 (O-H),Ala-134 (O-H).Tyr-192(O-H)

Asp-199(O-H) and Met132 (N-H) residues of UPRT. Similarly, UPRT-5FU complexes form hydrogen bonds with the Tyr-192 (F-H), Gly-196(O-H), and Leu-197 (O-H) residues of UPRT. Among these, Met-132 (F-H,O-H) plays important role in pyrimidine base stacking in both the ligands. Figure 3.6a shows important interactions of 5FU with Tyr-192, Ile-193, Gly-196, Leu-197, Gly-198.Asp-199 and Met-132 residues of UPRT. Similarly, figure 3.6b shows major interactions of uracil with Arg-103, Ala-134.Tyr-192, Ile-193, Gly-198, Asp-199, Ala-200 and Met-132 residues of UPRT. In both figures interactions of residues and ligands within the 5 Å bond lengths was selected. Our results showed addition of fluorine to the 5^{th} position of pyrimidine ring resulted in change in binding energies due to change in the residue interactions. Majority of the favourable energy dockings involved same pattern of binding for both the ligands with in the same binding pocket. Calculated K_i values for 5FU are in agreement with experimental values for best docked complexes (data not shown) even though distinct variation is observed among the docking complexes through out the simulation period. This disparity indicates that proper orientation of UPRT is necessary for docking study to explain the interactions.

Table.3.2. Results of the automated molecular docking process with flexible UPRT protein- ligands

Ligand	Average FEB (-) (kcal/mol)	Total Number of FEB (-) (kcal/mol)	Total Number of FEB (+) (kcal/mol)	Deviations from docking energy score	Best Binding Free Energies (-) (kcal/mol)
5-fluorouracil	29.4	1229	17	4	37.8
uracil	25.1	1230	15	5	28.4

3.4. Summary

E.coli UPRT was purified to homogeneity and inhibition constant for 5FU was determined experimentally. As UPRT activity for uracil was found to be competitively inhibited by 5FU, the docking study for elucidating various interactions between the enzyme active site and the ligands (uracil and 5FU) have been carried out. MD simulation snapshots of UPRT were incorporated in docking to consider the enzyme flexibility to represent exact biological conditions. The docking results suggested that uracil and 5FU were attached to the different amino acid residues of the same binding site of UPRT throughout the 1000 ps simulation time and exhibited different energy scores for binding. Furthermore, docking results elucidated the key residues of UPRT involved in the binding of anticancer drug 5FU and its natural substrate uracil. The results are important for engineering the recombinant *E.coli* UPRT to alter specificity towards prodrug and also helpful in designing the potent prodrug for improving anticancer activity in suicide gene therapy.

Chapter 4

Development of chitosan nanocarrier using green fluorescent protein (GFP) as a model protein

4.1. Overview

Recently, polymer nanoparticles have been used extensively as carriers for protein delivery (George and Abraham 2006). Nanoparticles from biocompatible polymers have been reported as useful carriers for protein delivery, in which entrapped proteins maintain stability even after release (Lynch and Dawson 2008). Chitosan based nanoparticles have gained a lot of attention due to their properties such as biodegradability, biocompatibility, non-toxicity and membrane permeability both *in vitro* and *in vivo* (DeCampos et al. 2004). Furthermore, chitosan polymer is compatible with the stability of many bioactive molecules (Prabaharan and Mano 2005, Carrara and Rubiolo 1994) and this fact allows its exploitation as a nanocarrier for entrapping proteins, with numerous applications in biotechnology.

Therapeutic protein entrapment is quite a promising approach for sustained protein release, but little attention has been paid to the stability of the protein structure. The green fluorescent protein (GFP) of *Aequorea victoria* has been used extensively as a live marker and a unique tool to monitor localization and trafficking of proteins in living cells (Gerdes and Kaethe 1996).The major advantage of GFP to the cell biologist is its ability to exhibit intrinsic fluorescence without a cofactor or substrate, whereas most other fluorescent proteins require cofactors, substrates or any other proteins

(Zimmer 2002). In the present study, we have chosen GFP as a model protein for entrapment in chitosan nanocarrier and studied the structural stability and fluorescence properties of GFP after release from chitosan nanocarriers.

4.2. Experimental approaches

4.2.1 Materials

Chitosan was obtained from Sigma-Aldrich, USA. All other materials and reagents were of highest purity and commercially available.

4.2.2. Purification of GFP

GFP was purified in our laboratory according to a previously published method (Sanpui et al.2008). In brief, GFP was purified from overnight grown culture of recombinant GFP expressing *E. coli* DH5α. In brief, cells (4 x 10^9 cfu/ml) were centrifuged at 4000 x g for 10 min and the pellet was suspended in 15 ml 0.02 M Tris–HCl pH 8.0 buffer containing 0.15 M sodium chloride and 0.005 M EDTA. The cells were then disrupted in a Constant Cell Disrupter at 103 MPa. The disrupted cell suspension was centrifuged at 16000 xg for 15 min. The crude extract in 50 mM Tris–HCl pH 7.0 was saturated with 20% ammonium sulphate followed by the addition of tert-butanol (2 ml) 25 °C. The mixture was vortexed gently and allowed to stand for 1 h. After this, the mixture was centrifuged (2000 × g for 5 min) to form three phases. The middle interfacial precipitate containing GFP was collected and dissolved in 1ml of 50 mM Tris–HCl pH 7.0. After purification of GFP, excess salts from the protein sample were removed by gel filtration chromatography. The purified GFP was subsequently lyophilized and stored at −20 °C for further use.

4.2.3. Synthesis of chitosan nanocarriers

Chitosan nanocarriers were prepared in our laboratory by an ionic gelation method. Briefly, 200 mg of chitosan was dissolved in 20 ml of 0.1 M HCl. The clear solution was continuously purged with nitrogen gas for 15 minutes. The reaction mixture was agitated continuously using a mechanical stirrer (250 rpm) at 37°C. After 2 hours, 1 ml of Na_2HPO_4 solution (2 mg/ml) was added drop-wise to the reaction mixture. Finally, the product was passed through a 0.2 μm filter and the filtrate was lyophilized to obtain dried chitosan nanocarriers.

4.2.4. Loading of GFP in chitosan nanocarriers

The dried chitosan nanocarriers (30 mg) and lyophilized GFP (20 mg) were transferred in a 20 ml centrifuge tube containing 10 ml PBS (pH 7.4) buffer and incubated at 10°C for 24 hrs. GFP- loaded nanocarriers were separated by ultra-centrifugation at 20,000 X g and 10 °C for 30 min. In a control experiment, the same amount of GFP with out chitosan nanoparticles was used and the amount of GFP taken by the surface of the container was estimated by Bradford method. The unloaded amount of GFP was calculated by adding the amount of GFP taken by the surface of the container to the amount of GFP present in the supernatant. The GFP encapsulation efficiency (EE) was calculated by the following equation:

$$EE = \frac{\text{Total amount of GFP} - \text{Unloaded amount of GFP}}{\text{Total amount of GFP}} \times 100$$

The morphology and particle size measurements of the nanoparticles were performed by AFM (Picoscan™ 2500, Molecular imaging corporation-USA). XRD measurements

were obtained by a Bruker D8 ADVANCE X-ray powder diffractometer using Cu-Ka (k = 1.54 A °) source at room temperature.

4.2.5. *In vitro* release of GFP from chitosan nanocarriers

The GFP loaded chitosan nanocarriers separated from 10 ml PBS buffer were lyophilized and re-suspended in 5 ml PBS buffer (pH 7.4). The sealed tube was placed in a water bath at 37°C. At specified collection times, 100 µl samples were taken out from the tube and protein concentration was measured by Bradford method using BSA as standard.

Circular dichroism spectra of released GFP were obtained at room temperature using circular dichroism spectrophotometer (J-18, JASCO, UK) at GFP concentrations of 0.2 mg/ml. FTIR-spectra were measured using a FTIR spectrometer (Spectrum one, Perkin Elmer, USA). The fluorescence of GFP was measured by recording the fluorescence emission spectra of GFP using excitation at 395 nm with a fluorescence spectrophotometer (LS55, Perkin Elmer,USA).

4.3. Results and discussions

Herein, I have taken GFP as a model protein and loaded in to the chitosan nanocarriers by incubation method as described in methods section. In the present study, chitosan nanocarriers were produced as a result of ionic gelation between chitosan and Na_2HPO_4. GFP was isolated from recombinant GFP expressing *E. coli* by three-phase partitioning method. The molecular weight of the protein was found to be 27 kDa by SDS-PAGE (Fig.4.1) which was in accordance to the previous report (Jain et al. 2004).

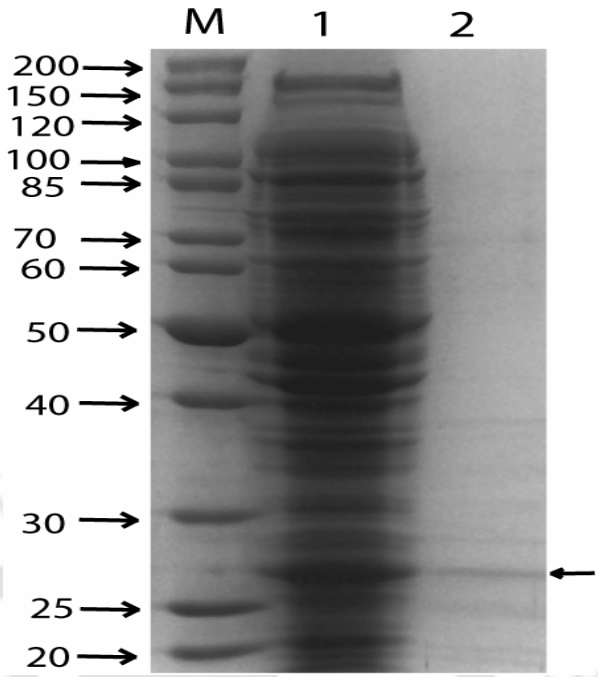

Figure.4.1. Purification of GFP from recombinant *E. coli* expressing GFP. *M:* molecular weight markers (kDa) *Lanes 1*: cell extract of recombinant *E. coli*, *lane 2*: purified GFP (shown with arrow head).

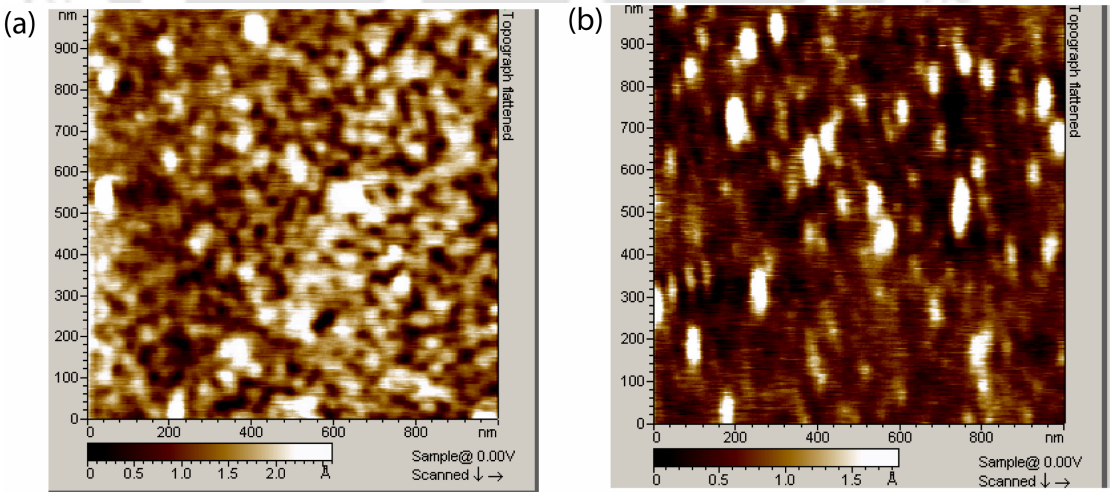

Figure.4.2. AFM images of (*a)* chitosan nanocarriers (*b)* GFP loaded chitosan nanocarriers.

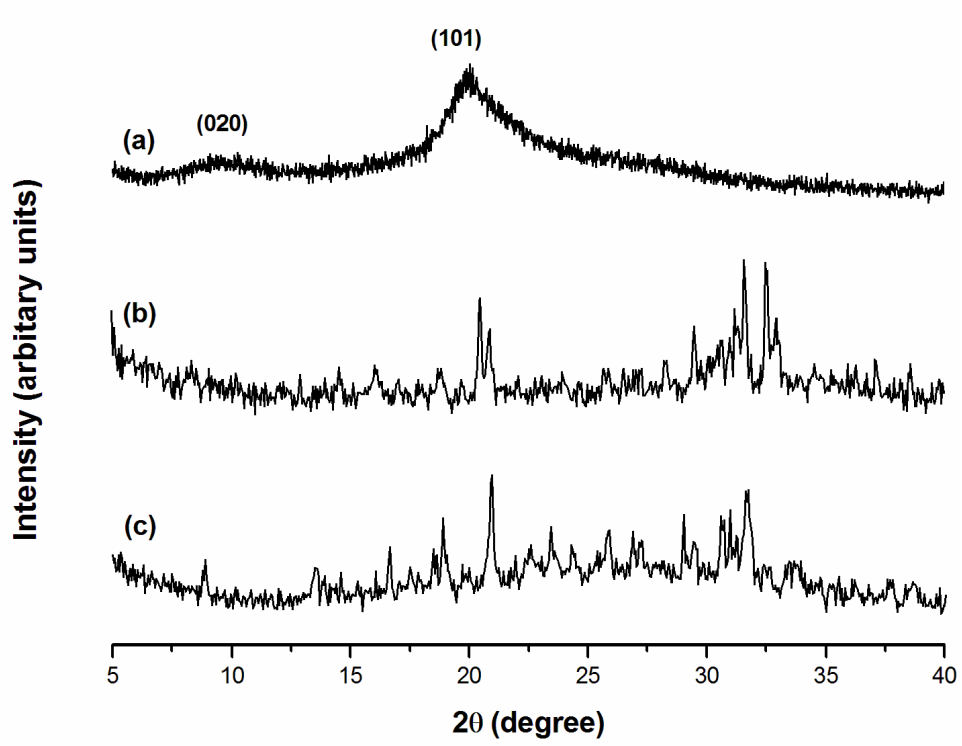

Figure.4.3. XRD patterns of (a) chitosan (b) CS nanonarriers (d) GFP loaded nanocarriers

The purified GFP was loaded by incubation method and EE was found to be 68 %.This high EE might be due to the entrapment of protein into the nanocarrier as well as adsorption of GFP on nanocarrier surface, which will settle at the bottom of tube during centrifugation. Low molecular weight of GFP could be one of the reasons for high encapsulation efficiency.Atomic force microscopy (AFM) measurement showed that the average particle diameter was 55 nm and 90 nm for chitosan nanocarriers and GFP loaded chitosan nanocarriers, respectively (Fig. 4.2). The GFP loaded chitosan nanocarriers were comparatively much larger than chitosan nanocarriers. X-ray diffraction pattern of chitosan, chitosan nanocarriers and GFP loaded chitosan nanocarriers revealed marked differences in their crystalline structure (Fig. 4.3 a,b). Sharp Peaks at 2θ = 9, 19° appeared while a peak at 32.5° disappeared in GFP loaded

chitosan nanocarriers when compared to the unloaded chitosan nanocarriers (Fig.4.3 b, c). The slight changes in XRD pattern indicated the presence of the GFP in chitosan nanocarriers.

Fig.4.4 shows cumulative GFP release profile from the chitosan nanocarriers over a period of 48 hrs. About 64 % of the loaded protein was released within 6 hrs followed by slow release up to 88 % over 48 hrs. In incubation method, protein loading in chitosan nanocarriers is mediated by adsorption of protein on the surface of the nanocarriers and partially through the ionic interaction between protein and nanocarriers (Bhattarai et al. 2006). The initial fast release of protein is associated with desorption of the protein located close to the nanocarrier surface, which then immediately diffuses out in the release buffer in the initial incubation time (Xu and Du 2003).

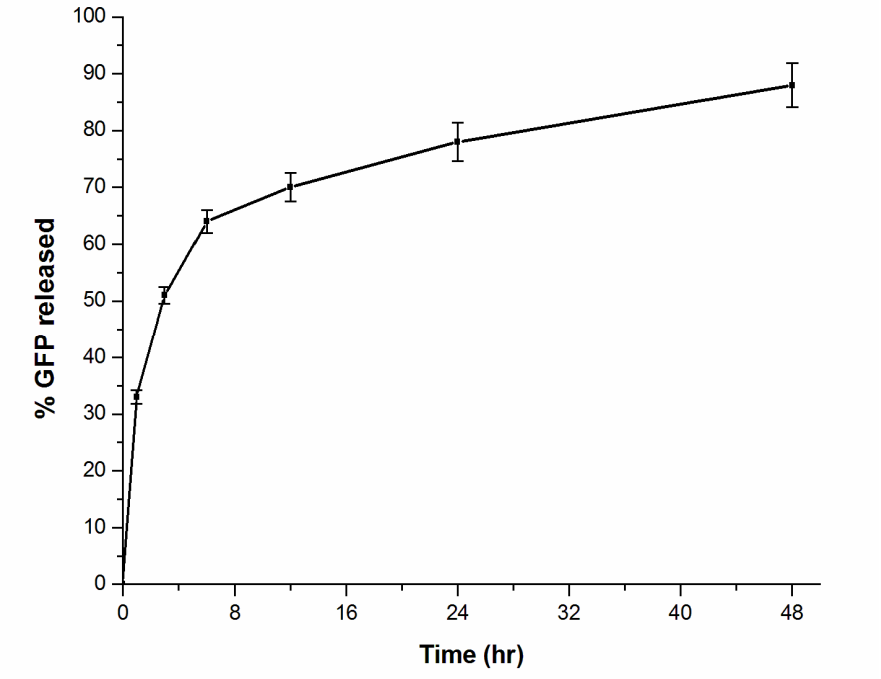

Figure.4.4. Release profile of GFP from chitosan nanocarriers. *Error bars* showed standard deviation among three observations.

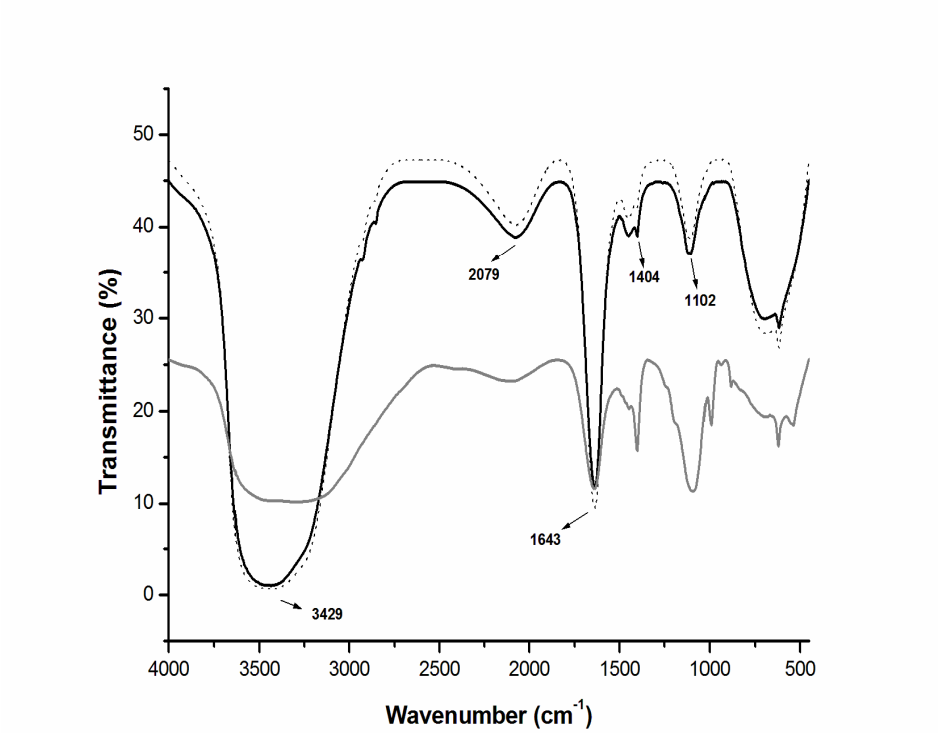

Figure.4.5. FTIR spectrum of native GFP (*straight line)* and released GFP (*dashed line*) from chitosan nanocarriers. Entrapped GFP (*gray line*) spectrum was shown by subtracting the chitosan nanocarriers spectra from GFP entrapped chitosan nanocarriers spectra.

The FTIR spectrum of GFP in water is presented in Fig. 4.5. For α-helical structures, the frequency band at 1640 cm^{-1} was primarily governed by the stretching vibrations of the C=O and C-N groups. This band frequency also corresponded to the amide I, which is the most intense absorption band in proteins. The band at 3429 cm^{-1} was due to the N-H stretching vibration which is very sensitive to hydrogen bonding. The band at 1404 cm^{-1} corresponded to the side chain vibrations in amide I and amide II region. The bands at 1640 and 1105 cm-1 appeared to be specific for GFP in aqueous phase (vanThor et al.1998).The results indicated that the GFP structure was slightly affected after entrapment in the chitosan nanocarriers. This may be due to the ionic interaction

between the chitosan polymer and GFP. However, after release, the secondary structure of GFP remained unchanged, which indicated that the protein secondary structure was not significantly altered.

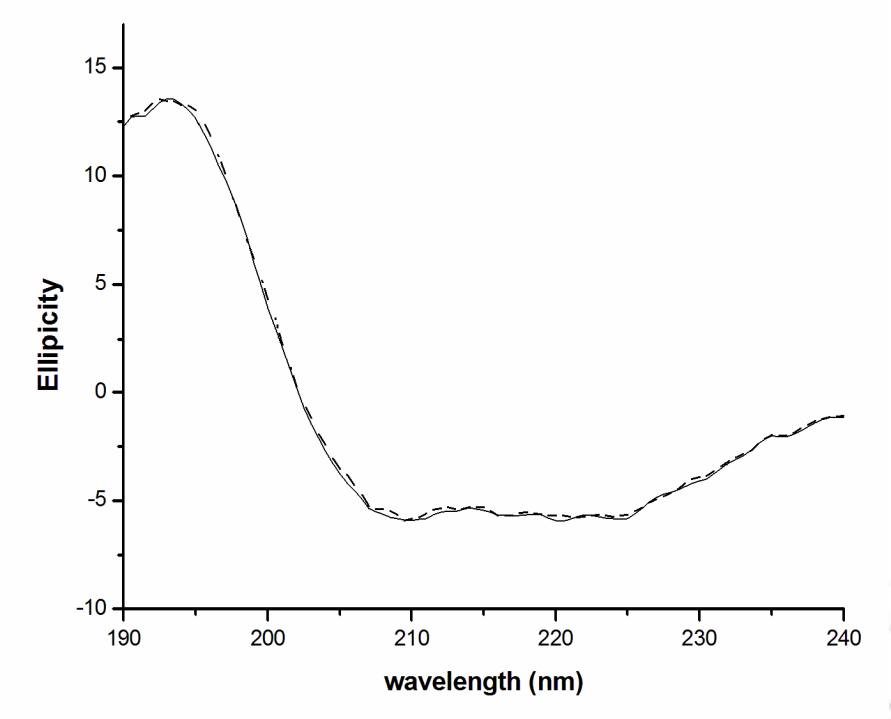

Figure.4.6. Far-ultraviolet circular dichroism analysis of native GFP (*straight line*) and released GFP (*dotted line*) from chitosan nanocarriers.

In addition, circular dichroism analysis was done to further investigate the structural changes between the released and native GFP (Fig.4.6). The circular dichroism spectrum of GFP standard solution in water showed marked negative bands at 220 and 208 nm and a positive band at 193 nm, which is typical of predominant α-helix structure of proteins (Visser et al. 2002, Pelton et al. 2000]. The circular dichroism spectra of released and native GFP were found to be almost similar. No substantial alterations were noted in circular dichroism spectral bands and similar conclusions were drawn as from the FTIR spectra.

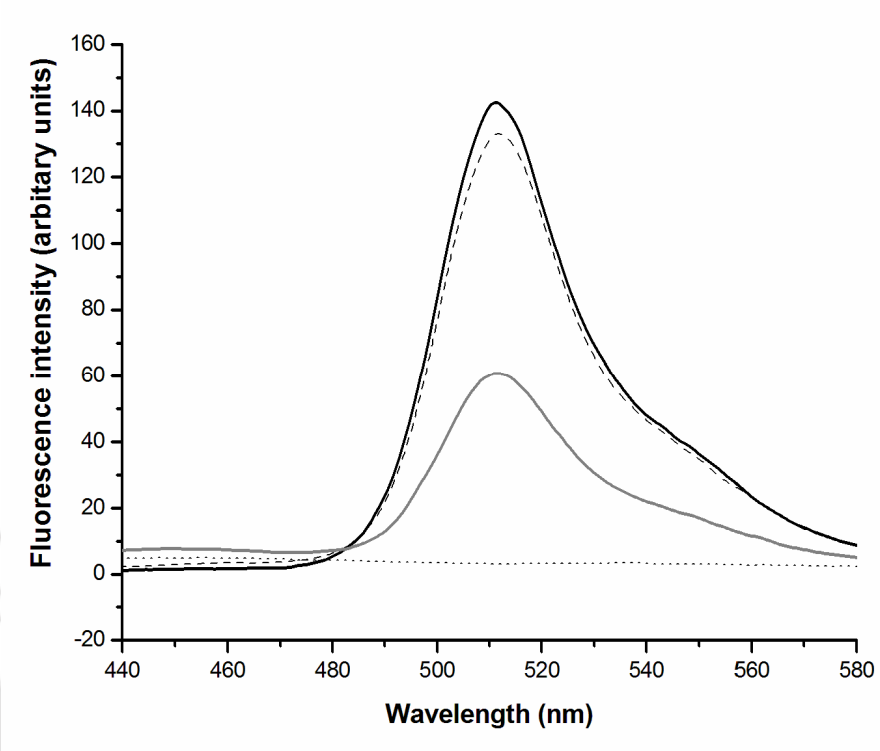

Figure.4.7. Fluorescence spectra of native GFP (*straight line*), released GFP (*dashed line*), entrapped GFP in chitosan nanocarriers (*gray line*) and chitosan nanocarriers (*dotted line*).

The fluorescence emission of GFP was found to be at 510 nm at excitation wavelength of 395 nm. This result is consistent with the previous report (Sanpui et al. 2008).The emission spectrum of released protein was similar to that of the native protein with respect to both the emission maximum and fluorescence intensity after normalization for the concentration (Fig.4.7). But there was a significant decrease in the fluorescence intensity of GFP entrapped in the chitosan nanocarriers due to the interference of polymer absorbance, whereas chitosan nanocarriers did not have any detectable fluorescence.

4.4. Summary

In conclusion, chitosan nanocarriers appeared to be a highly promising vehicle for delivery of GFP. Our investigations depicted quantitative recovery of GFP from chitosan nanocarriers where the structure and the fluorescence properties of GFP were preserved throughout the process. The circular dichroism and FTIR spectra of released GFP almost overlapped with native GFP spectra indicating that entrapment did not affect secondary structure to any significant extent. The present study also indicated the feasibility of using chitosan nanocarriers to deliver therapeutic proteins *in vitro* and *in vivo,* where the natural structure of the proteins entrapped in the nanocarriers may be maintained.

Chapter 5

Development of cytosine deaminase-chitosan nanocarrier

5.1. Overview

Recent advances in suicide gene therapy opened up new therapeutic avenues to combat a wide range of malignant tumors (Portsmouth et al. 2007). Cytosine deaminase, a microbial pyrimidine salvage pathway enzyme, which catalyzes hydrolytic deamination of cytosine to uracil, has been found to be efficient for prodrug mediated suicide gene therapy. It converts prodrug 5 fluorocytosine (5FC) to toxic 5 fluorouracil (5FU), which inhibits DNA synthesis (Springer and Duvaz 1996). In our present study, bacterial cytosine deaminase is chosen as suicide enzyme due to its higher enzymatic stability compared to the yeast analogue (Kievit et al. 1999). The enzyme was purified using DEAE-cellulose ion exchange column by fast performance liquid chromatography (FPLC). Enzyme activity was measured by spectrophotometrically using 5FC as a substrate.

The effect of cytosine deaminase suicide gene therapy is often inadequate due to either inefficient gene delivery or poor expression of the gene at therapeutic levels (Yazawa et al. 2002). Immobilization of heat labile yeast cytosine deaminase on biopolymers has been reported to increase the enzyme stability with its improved half life (Katsuragi et al. 1989). Hence a chitosan based nanocomposites has been developed, because chitosan is a well known biocompatible and biodegradable material for delivering bio molecules and drugs (Prabaharan and Mano 2005). Cytosine deaminase was

encapsulated within chitosan to develop chitosan cytosine deaminase (CSCD) nanocarrier. Microscopic techniques, such as atomic force microscopy (AFM) and transmission electron microscopy (TEM) were used to study the morphology of the nanocomposites. Fourier transform infrared spectroscopy (FTIR) analysis depicted the chemical composition, whereas X-ray diffraction measurements (XRD) confirmed structural integrity in terms of crystallinity of the composite compared to chitosan nanocarriers (CSNCs) or chitosan alone. *In vitro* time dependent studies showed prolong release of cytosine deaminase. This is the first unique experimental approach of the generation of a chitosan entrapped cytosine deaminase nanocarrier and its subsequent sustained delivery for potential application in prodrug enzyme therapy.

5.2. Experimental Approaches

5.2.1. Synthesis of CSCD nanocarrier

About 200 mg of chitosan was dissolved in 20 ml of 0.1 M HCl. The clear solution was continuously purged with nitrogen gas for 15 minutes. The pH was adjusted to 6 with sodium phosphate dibasic hydrate (Na_2HPO_4) solution (2 mg/ml) to synthesis CSCD nanocarrier; however, this step was not required for the synthesis of CSNCs. Purified cytosine deaminase enzyme was added to the CSCD solution and the mixture was agitated continuously using a mechanical stirrer (250 rpm) at 37 °C. After 2 h, 1 ml of Na_2HPO_4 solution (2 mg/ml) was added drop wise to the CSCD nanocarrier reaction mixture. Finally, the product was passed through a 0.2 µm filter and the filtrate was lyophilized to obtain dried CSCD nanocarrier. Similarly, CSNCs were prepared with out adding cytosine deaminase.

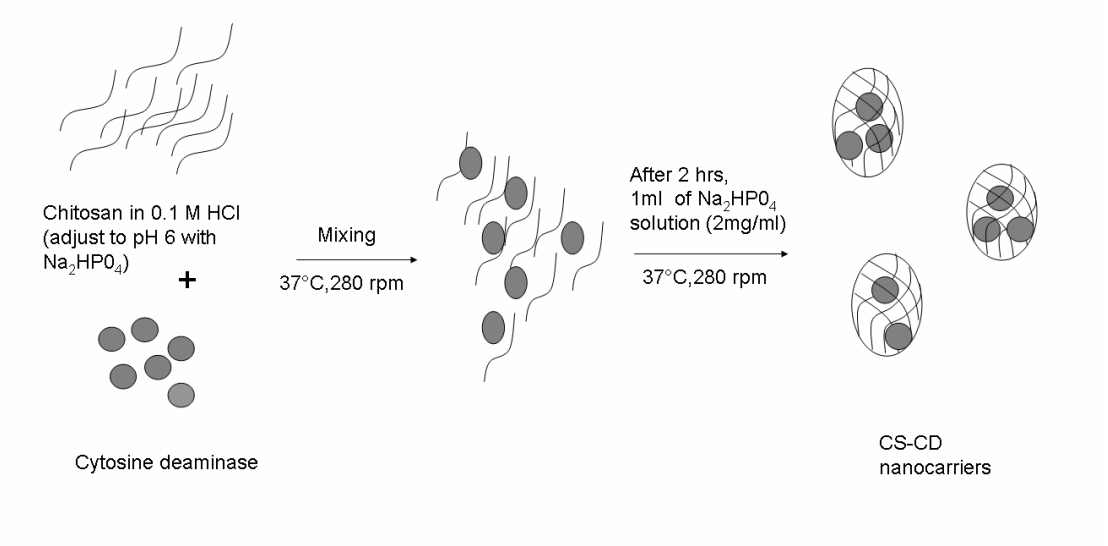

Figure.5.1. Schematic representation of synthesis of CS-CD nanocarriers

5.2.2. Characterization of CSCD nanocarrier

The morphology and particle size measurements of the nanoparticles were performed by TEM and AFM. 5 µL of liquid samples were drop cast on carbon coated copper TEM grids and air dried at room temperature. The grids were then analyzed by a JEOL 2100 UHR-TEM operating at an accelerating voltage of 200 KeV. The AFM sample was prepared by depositing nanocarrier solution on freshly cleaved mica surface and dried by nitrogen. Images were acquired in non contact mode using silicon nitrite cantilever with frequency of 150 KHz for XRD measurements, the nanocarrier was lyophilized and subsequent diffraction patterns of the powder samples were obtained by a Bruker D8 ADVANCE. X-ray powder diffractometer using Cu-Kα (λ=1.54 Å) source at room temperature. FTIR spectra of the lyophilized nanocarriers were recorded in KBr pellets using a Perkin-Elmer spectrum one spectrophotometer.

5.2.3. *In vitro* release studies of cytosine deaminase from CSCD nano carrier

The CSCD nanocomposite suspension (20 ml) was lyophilized and then resuspended in 5 ml of PBS buffer and incubated in a shaking (20 rpm) water bath at 37°C. At regular time intervals of 12, 24, 48, 96 and 168 h, the suspension was centrifuged at 19,000 rpm for 15 min. The release of cytosine deaminase in the supernatant from the composite was measured at the above time intervals and the pellet was resuspended in fresh 5 ml of PBS buffer. The concentration of cytosine deaminase was quantified by Bradford method (1976) using BSA as standard. The supernatant was lyophilized and dissolved in 0.3 ml of PBS for enzyme activity assay.

5.3. Results

5.3.1 Characterization of CSCD nanocarrier

TEM (Fig.5.2) and AFM analysis (Fig.5.3) was performed to study the shape, size and surface appearance of the CSCD nanocarrier. The average particle diameters were55 nm and 80 nm for CSNCs and CSCD nanocrarrier, respectively. CSNCs were found to be spherical, where as CSCD nanocarrier appeared as elongated spheres and their surface was more ‘fluffy’ than CSNCs.

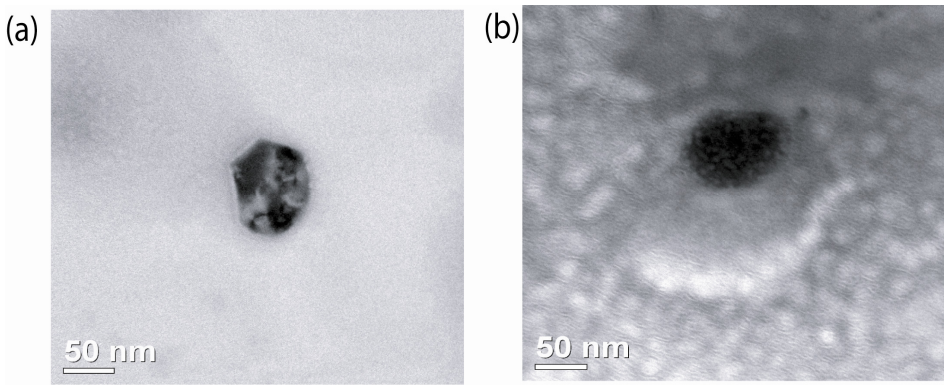

Figure.5.2. TEM images of (a) single CS nanocarrier (b) single CSCD nanocarrier.

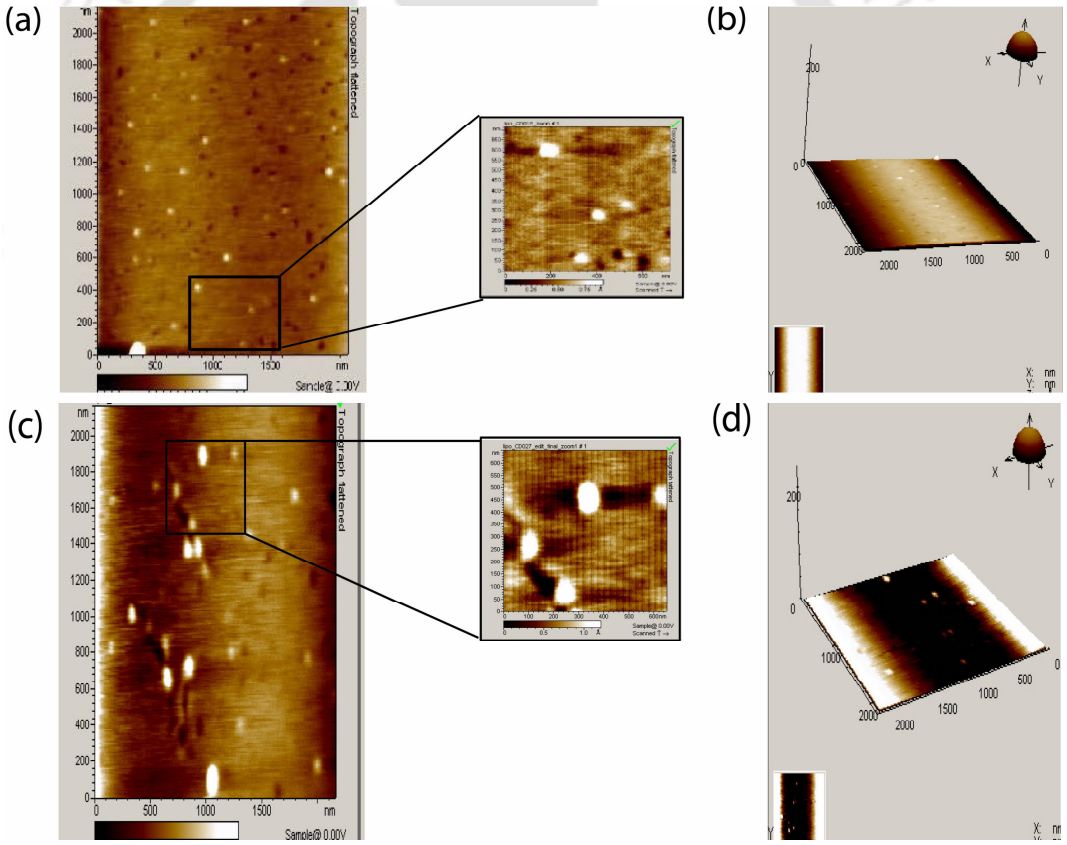

Figure.5.3. Non contact mode AFM images of CSNCs (a) topograph b) 3D view; and CSCD Nanocarrier (c) topograph (d) 3D view; inset shows AFM image zoom.

FTIR analysis (fig.5.4) of chitosan and chitosan nanocarrier showed characteristic absorption peaks for chitosan at 1649 cm^{-1}(amide I), 1554 cm^{-1}(amide II) and 1385 cm^{-1} (amide III). In chitosan nanocarriers, the peak was shifted from 3543 cm^{-1} to 3441 cm^{-1} and 3447 cm^{-1} and the peaks became wider, indicating the enhanced hydrogen bonding in the nanocarriers. The peaks of 1554 cm^{-1} and 1385 cm^{-1} disappeared while a sharp peak at 1645$cm^{-1}$was observed, which indicated the polymerization of chitosan. Characteristic peaks at 3139 cm^{-1} and 1400 cm^{-1} that corresponded to the $–NH_2$ stretch and 1630 cm^{-1} that corresponded to the C=O stretch, suggested the presence of a peptide bond. The bands at 1114 cm^{-1} and 616 cm^{-1} attributed to a combination of N-H bending and C-N stretching.

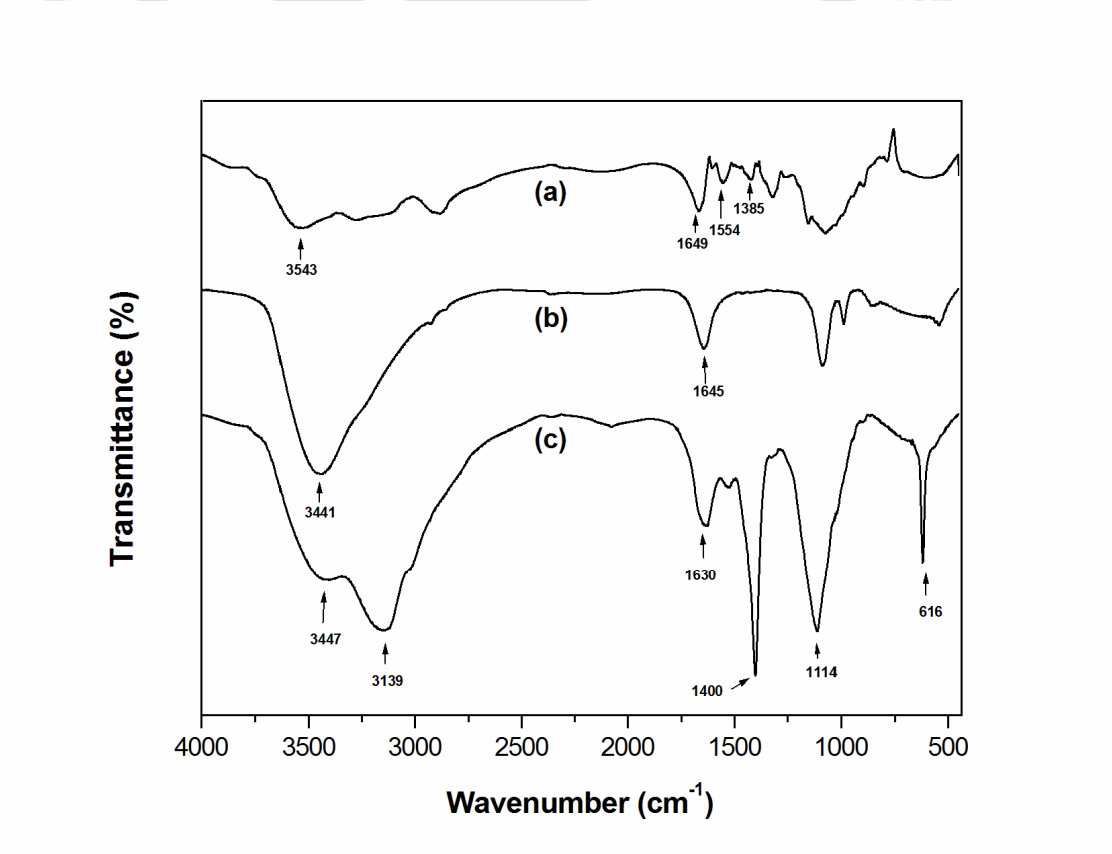

Figure.5.4. FTIR spectra of (a) chitosan (b) CSNCs (c) CSCD nanocarriers

X-ray diffraction pattern of chitosan, salt Na_2HPO_4 salt, chitosan nanoparticle alone and CSCD nano carrier revealed marked differences in their crystalline structure (Fig. 5.5). Diffractogram of chitosan depicted two distinct Bragg diffraction peaks from the (020) and (101) planes at 2θ values 9.9 and 20°, respectively (Remant et al. 2009). In CSCD nanocarrier, three highly intense peaks were found at 2θ values 32.8, 20.8 and 18.8°. A peak at the 2θ value of 20.8° was observed, where as the two other peaks at 2θ values of 32.8 and 18.8° was possibly be due to the salts.

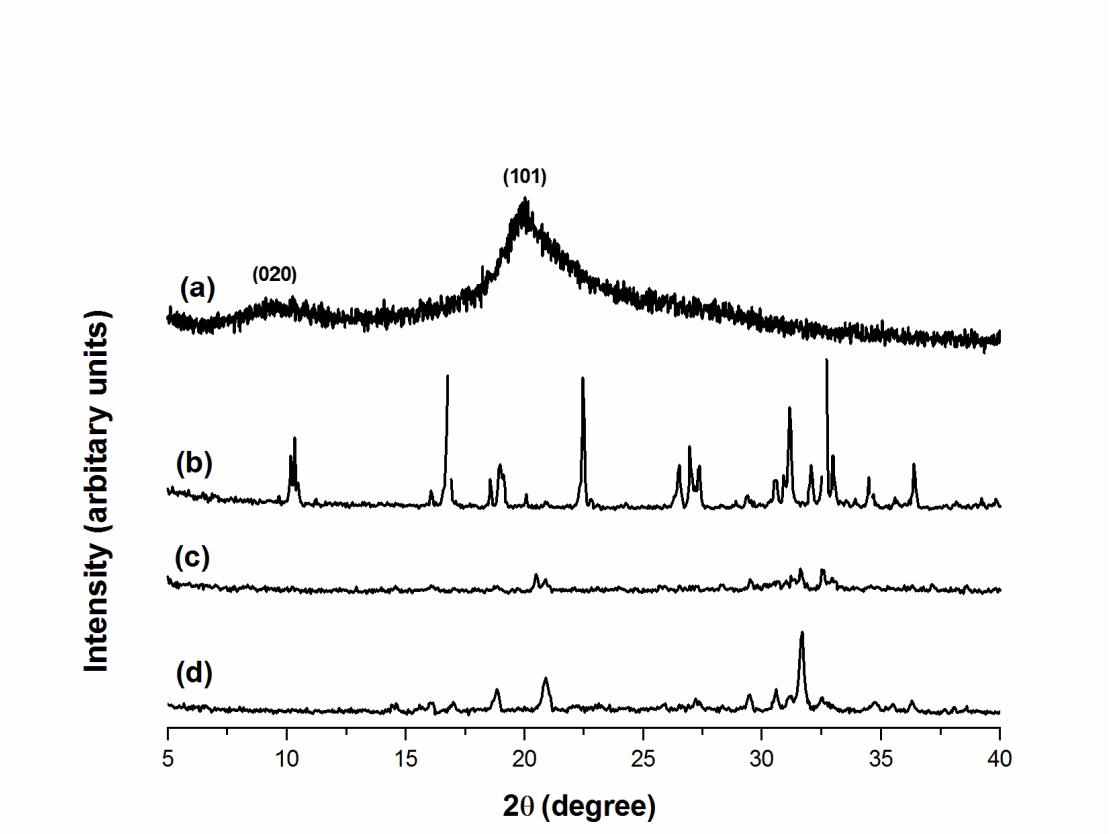

Figure.5.5. XRD patterns of (a) chitosan (b) salt (Na_2HPO_4) (c) CSNCs (d) CSCD nano carriers

5.3.2. *In vitro* release of cytosine deaminase

As shown in Fig.5.6, an initial 9% burst release of cytosine deaminase within the first 12 h was followed by a sustained release up to 168 h. About 9, 12, 19, 22 and 27% of cytosine deaminase was released at 12, 24, 48, 96 and 168 h respectively. After release, the cytosine deaminase retained 92, 91, 89, 86 and 71 % activity at the above mentioned time intervals, respectively.

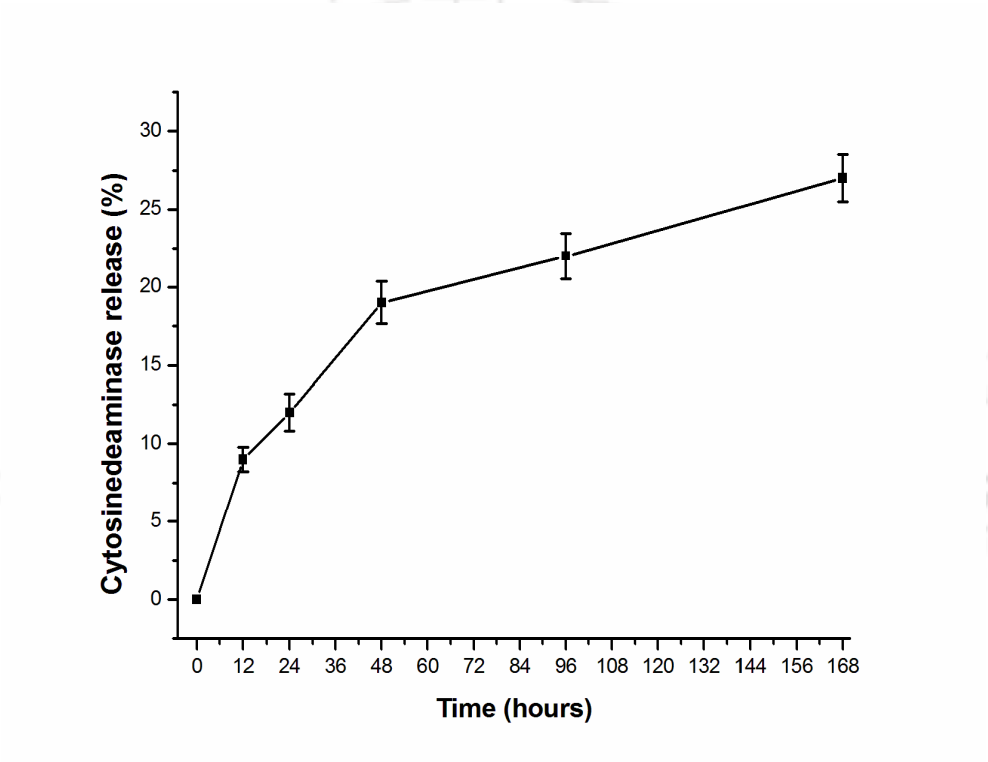

Figure.5.6. Release profile of cytosine deaminase from CSCD nanocarrier. Error bars show standard deviation among three observations.

5.4. Discussion

Herein, a CSCD nanocarrier has been developed for potential application in enzyme based therapy. In the experimental method, gel formation of the nanocarrier was started above pH 6. Therefore, chitosan initially dissolved in acidic pH solution was brought to pH 6 and then cytosine deaminase was added to form the nanocarrier at alkaline pH.

FTIR results of chitosan and its nanocarrier were in agreement with the previous reports for gel formation (Li et al. 2008c; Xu and Du 2002). TEM analysis showed morphological changes after entrapment of cytosine deaminase in the nano carrier. Furthermore, the average 55 nm diameter of the CSNCs, as obtained from AFM measurement was less than earlier reports (149 nm,116 nm diameter) though the spherical morphology remained unchanged (Chaleawlert-umpon and Pimpha 2009; Li et al. 2009). XRD pattern of CSCD nanocarrier indicated the entrapment of cytosine deaminase in CSCD nanocarriers. Hence, AFM, TEM, FTIR and XRD results suggested the incorporation of cytosine deaminase in chitosan nanocarriers. The initial burst was possibly due to the enzyme that was located near the nanosphere surface, which could easily diffuse out at initial incubation time. Such events of initial burst release of protein from delivery systems has been reported previously (Zhang and Chu 2002; Patil et al.1996). Cytosine deaminase released from CSCD nano carrier with in 168h was capable of converting 5 FC to 5 FU.

5.5. Summary

In conclusion, purified cytosine deaminase from *E.coli* K-12 MTCC 1302 strain was encapsulated in biofriendly chitosan polymer to synthesize a novel CSCD nano carrier. The nanocomposite was uniform in size and shape, and cytosine deaminase retained its activity after entrapment. Sustained release of active cytosine deaminase from the nanocarrier has potential application in prodrug enzyme based cancer therapy.

Chapter 6

Development of folic acid conjugated targeted delivery system

6.1. Overview

The arena of tumour specific targeting is being developed in order to reduce harmful side effects of anticancerous agents, which are often associated with highly unacceptable toxicity to normal tissues and their virtually low selectivity to the cancer cells (Jaracz et al. 2005). Nanoparticles are currently under consideration for delivery of therapeutic agnets due to the accumulation of nanoparticles at the tumor site and results in the localisation of a greater amount of the therapeutic agnet load at the tumour site (Brannon-Peppas et al. 2004; Peer et al. 2007). Moreover, it is evident from previous reports that the receptor-mediated delivery via folic acid conjugated nanoparticles such as , metal (Sonvico et al. 2005; Tsai et al. 2008) ,magnetic (Lin et al. 2009) lipid (Hattori et al. 2005) and polymer (Yang et al. 2010; Lin et al. 2009) based nanoparticles further accumulate in human cancer cells that highly overexpress the folate receptor (FR) by increasing cellular uptake. FR is a glycosylphosphatidylinositol anchored protein, over expressed on epithelial malignancies, such as ovarian, colorectal and breast cancer cells (Parker et al, 2005; Ross et al. 1994).Concentration of FR increases with the increasing age of tumour and its presence is highly restricted in normal tissues and in accessible to the circulation whereas FR in tumors is accessible via circulation (Elnakat et al. 2004). The folic acid (FA) , a member of vitamin B , which plays a crucial role in cell growth and biosysnthesis of nucleic and amino acid shows a great deal of promise as a tumor-homing agent. From the previous reports, it is evident that

folic acid is a high affinity ligand (K_D = 10^{-10} M) for the FRs, which will help in internalization of the FA (Kamen et al. 1986) , FA-drug conjugates (Low et al. 2004) and FA functionalized nanoparticles (Chatterjee et al. 2007) in to the cancer cells.The polymeric nano particle based delivery systems have considerable potential for targeted delivery of the proteins (Pridgen et al. 2007). Among the various 'smart polymers' Poly (*N*-isopropylacrylamide) (PNIPAM) and chitosan (CS) have gained much importance due to the biocompatibility and the tuneable thermo responsive properties (Ganta et al. 2008). Presence of high number of hydroxyl and reactive amino groups on chitosan provides possibilities for its use in controlled release (Kas et al. 1997). Moreover, thermal properties were improved for PNIPAM when it was polymerized with co-polymers like acrylic acid and chiotosan (Khan 2007).

Herein, a FA conjugated CS/PNIPAM nanocarrier was developed for delivery of suicide enzyme to the FR positive cancer cell lines. Cytosine deaminase (CD) is proved as a successful suicide enzyme for prodrug enzyme cancer therapy for the last three decades. Previous studies suggest that, CD mediated intratumoral conversion of prodrug 5-fluorocytosine (5FC) to anticancer drug 5-flurouracil (5FU) leads to the appotoic mediated cell death in variety of cancer cells (Gopinath and Ghosh 2007,2008a). The main difficulty associated with CD mediated prodrug enzyme therapy is the inefficient delivery of enzyme or gene to the tumor cells. To overcome this problem, there is a necessity to develop the efficient delivery system which can release the enzymes at therapeutic levels for longer periods with in the cancer cells. In my previous study (chapter 5), I have encapsulated CD enzyme with in the chitosan nanocarrier and its ability to convert the prodrug 5FC to 5FU was evaluated after sustained release for 7 days. In the present study, CD was delivered through FA conjugated nanocarriers to the 5FC treated HT-29 cancer cell lines, which showed high levels of FR expression. The

capacity of FA conjugated nanocarrier as an enzyme delivery system was demonstrated *in vitro* tests. The solid state properties of the nanocarriers were characterized to analyze the morphology, composition and thermal properties.

6.2. Experimental approaches

6.2.1. Materials

N-isopropylacrylamide (NIPAM),Chitosan, N,N-methylene-bisacrylamide (MBA), folicacid (FA), 1-(3-dimethylaminopropyl)-3-ethylcarbodiimide hydrochloride (EDC) , 2,3-bis[2- Methoxy-4-nitro-5-sulfophenyl]-2H-tetrazolium-5-carboxyanilide inner salt (XTT), Tri reagent and M-MLV Reverse Transcriptase, Dulbecco's Modified Eagle's medium (DMEM), fetal bovine serum (FBS) were obtained from Sigma–Aldrich Chemical Corporation Ltd. Ammonium persulfate (APS) and Dimethyl sulfoxide (DMSO) were purchased from Merck India. All other materials and reagents were of the highest purity commercially available.

6.2.2. Synthesis of CS/PNIPAM nanocarriers

For a total volume of 50 ml, 0.1 gm of Chitosan was first dissolved in 2 % v/v of glacial acetic acid. A mixture of 0.5 gm NIPAM and MBA (0.05 g/mL) was added to the reaction mixture in a 100 ml three necked round bottom flask with mechanical stirring at 250 rpm for 30 minutes. Then the solution was purged with nitrogen gas to remove the oxygen which can interrupt the polymerization. The temperature was raised to 80^0 C in an oil bath and the reaction was allowed to for 6hours after adding 20 mg of APS to the reaction mixture. Dry CS/PNIPAM nanocarriers were obtained by lyophilisation.

6.2.3. Folic acid conjugation of CS/PNIPAM nanocarriers

A solution of EDC and FA in anhydrous DMSO was prepared and stirred at room temperature until FA was well dissolved (1 h). It was added to the aqueous dispersion of CS/PNIPAM nanocarrier (10 mg/mL) which was maintained under stirring for 1 h. The resulting mixture was stirred at room temperature in the dark for 16 h. it was dialyzed against water for 3 days. The FA-conjugated CS/PNIPAM nanocarriers (FANCs) were isolated by lyophilisation. Schematic diagram of synthesis of CS/PNIPAM nanocarriers and its conjugation with FA was shown in Fig 6.1.

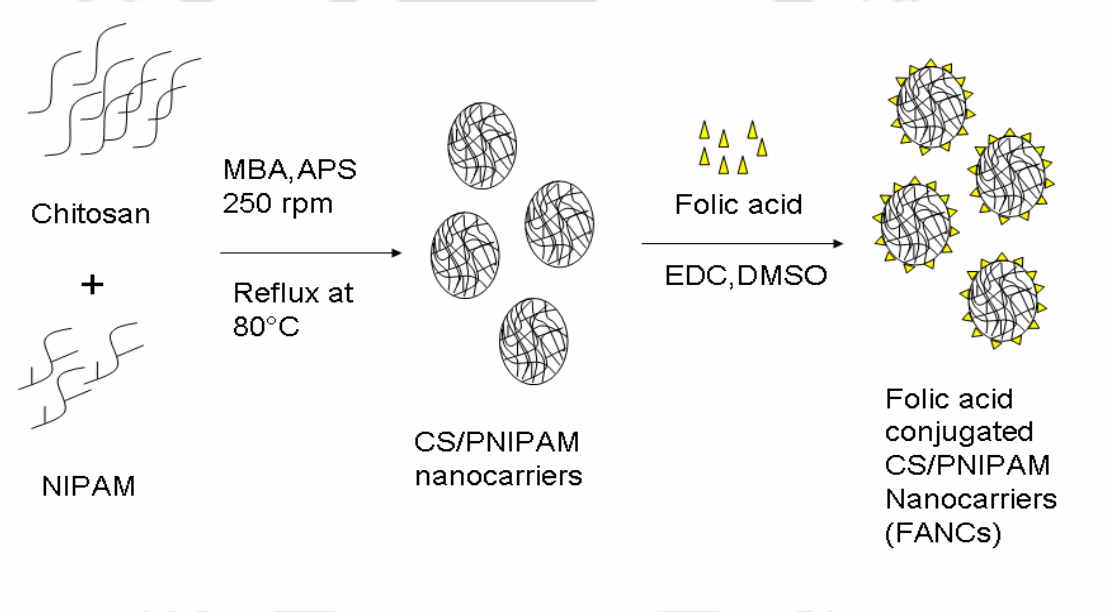

Figure .6.1. Synthesis of folic acid conjugated nanocarriers

6.2.4. FTIR spectroscopy

FTIR spectra of the lyophilized nanoparticles were recorded at room temperature using a Perkin-Elmer spectrum-one spectrophotometer,MA,USA The samples were ground with KBr crystals and the mixture was then pressed into a pellet for IR measurement.

6.2.5. Simultaneous TG-DSC analysis

The thermal analysis were performed in a simultaneous thermogravimetric/differential scanning calorimetery (TG-DSC) equipment, model STA449F3 Jupiter (NETZSCH-Gerätebau GmbH), with a 10 K min^{-1} constant heating rate from 25 to 650°C. About 1 mg of sample was used in platinum pans in each analysis. An empty alumina crucible was used as the reference for the DSC measurements.

6.2.6. Loading of CD in FANCs and *in vitro* release

The procedure for CD purification was described in chapter 2. The dried nanocomosites were swollen in PBS solvent at 10°C for one day,then transferred to PBS solution of cytosine deansae (25 µg/ml) to load at 10°C for one day then dried in lyophilizer. Then loaded and unloaded noncomposites were observed under AFM for comparison AFM (Picoscan™ 2500, Molecular imaging corporation-USA). The sample was prepared by depositing nanoparticle solution on freshly cleaved mica surface and dried by nitrogen gas stream. Images were acquired in non contact mode using silicon nitrite cantilever with frequency of 150 KHz. The protein loaded FANCs (obtained from 20 ml suspension) were resuspended in 5 ml PBS (pH 7.3). The suspended solution was kept at shaking water bath at 37° C with 10 rpm. At different time intervals, supernatant was collected by centrifugation at 19,000 rpm for 15 minutes and the nanocomposites were resuspended in fresh buffer. CD protein released into the supernatant was quantified by Bradford method (1976) using BSA as standard.

6.2.7. Cell culture

HT-29 cells were grown and maintained in Dulbecco's Modified Eagle'e Medium (DMEM) supplemented with 10% FBS and 5% penicillin-streptomycin in a humidified atmosphere with 5% CO2 at 37°C.

6.2.8. Semi-quantitative reverse transcriptase-polymerase chain reaction (RT-PCR)

Total RNA was isolated form HT-29 cells using Tri reagent and the cDNA was generated by reverse transcription of 3 µg of total denatured RNA using M-MLV Reverse Transcriptase at 37^{o}C for 50 min in a total mixture of 20 µl. Finally, RT-PCR was performed with random hexamer primers for folate receptor. Initial denaturation at 94^{o}C for 3 min was followed by a PCR cycle of denaturation at 94^{o}C for 35 s, annealing at 50,55.5,59.7^{o}C for 30 s, extension at 72^{o}C for 45s for 28 cycles and final extension at 72^{o}C for 7 min. The PCR products were separated on a 1.2% agarose gel and stained with ethidium bromide.

The following primer sequences were used for Folic acid receptor:

Fwd- 5' GATTGCATGGGCCAGGACTGAGC 3'

Rev- 5' TGCCAGTTGCTCTTGCAGGTGTAGG 3'

The β-actin gene expression was used as internal control and The following primer sequences were used for b-actin:

Fwd-5' CTGTCTGGCGGCACCACCAT 3',

Rev-5' GCAACTAAGTCATAGTCCGC 3'

6.2.9. Cell viability studies

6.2.9.1. *XTT assay*

HT-29 cells were seeded in a 96-well plate at a density of $1x10^4$ cells/well in DMEM containing 10% FBS at 37°C and 5% CO_2. Confluent cells were treated with CD loaded FANCs (0.2 mg/ml) and 5FC (0.5) mM for 24 hours. In experimental control, the cells were treated with same concentrations of FANCs (with out cytosine deaminase) and 5FC. After incubation, the medium was removed and the cells were washed three times with PBS. Cell viability was determined using XTTsystem according to the manufacturer's instructions (Sigma). The XTT assay is based on the mitochondrial activity and therefore provides an indicator of overall functional cell viability (Scudiero et al. 1988, Roehm et al.1991).

6.2.9.2. Acridine orange (AO)/ ethidium bromide (EB) staining

Cell samples for microscopic evaluation were stained with acridine orange (AO)/ethidium bromide (EB) (100 lg/ml in PBS) (Ribble et al. 2005). The AO stained live cells shown green fluorescence under confocal microscope at 488 nm excitation with a band pass filter ranging between 505 and 530 nm. On the other hand, dead cells become permeable to red dye EB and fluorescence was observed at 585 nm long pass filter. Represented images were generated by superimposition of both green and red fluorescence to find live and apoptotic cell.

6.3. Results and discussion

FANCs formed by polymerization method were examined interms of ther size, shape and thermoresponsiveness.The nanocarriers described in this study were smaller than 120 nm , being suitable size for mammalian cells uptake.

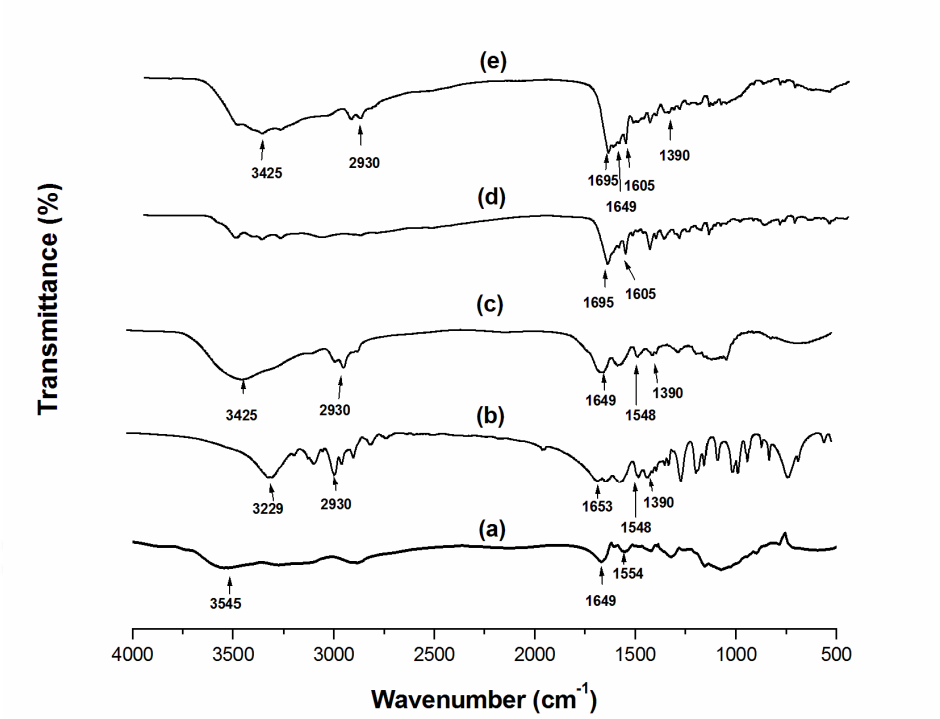

Figure.6.2. FTIR spectra of (a) chitosan, (b) n-isopropyl acrylamide (c) CS-NIPAM nanocarrier, (d) folic acid (e) folic acid conjugated CS-NIPAM nanocarreirs

The chemical composition of synthesized FANCs was confirmed by FTIR. Figure 6.2 (a) and (b) shown characteristic absorption peaks of chitosan and NIPAM, respectively. FTIR spectra of FANCs (Figure 6.2 (c)) has shown absorption peaks at 1649 cm^{-1}, which denotes incorporation of CS and remining peaks at, 1548, 1390 and 2930 cm^{-1} denotes incorporation of PNIPAM in the nanocarrier (Khan 2007). FTIR spectra of pure folic acid shown (figure 6.2 (d)) characteristic absorption peaks at 1695 and 1605 cm^{-1}.

Finally, FANCs spectra figure 6.2 (e) shown peaks at 1390, 2930, 1695 and 1605 cm^{-1}, which indicates the incorporation of CS, NIPAM and folic acid in the nanocarrier.

Fig. 6.3 presents the thermogravimetric analysis (TGA) curve with two samples. The weight-loss stage below 100 °C is a result of the evaporation of physically adsorbed water (Cansell et al. 1997)**.** CS/PNIPAM nanocarrier exhibit rapid weight-loss stage below approximately 20 wt. % in the region 420– 650°C and totally 94 wt. % was decreased in 650 °C. On the contrary, FANCs measures a weight-loss, 70 wt.% was decreases in 650° C. Total reduction in weight percent of the FANCs is less than the CS/ PNIPAM nanocarrier and it is indicated that the FANCs have a large amount of folic acid at the surfaces .

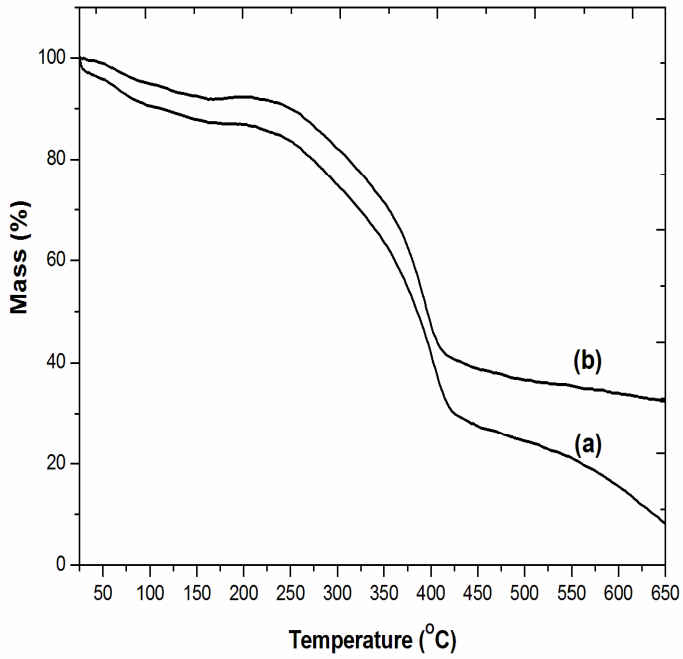

Figure.6.3. TGA thermogram of (a) CS-PNIPAM nanocarriers (b) folic acid conjugated CS-PNIPAM nanocarriers

Thermal analysis using Differential Scanning Calorimetry (DSC) has been employed to examine the solid samples (Fig.6.4) .The thermogram of CS/ PNIPAM nanocarrier exhibits four discernable peaks of which three are endothermic and one exothermic. The first endothermic peak was around 115°C and is typical of free water (Cansell et al. 1997). The third peak in Figure 3 was endothermic and occurred at 318°C. On contrary, FANCs exhibits two endothermic and two exothermic peaks. Where as endothermic peak at 318°C was missing, which indicates the increased stability of folic acid functionalised nanocarrier.

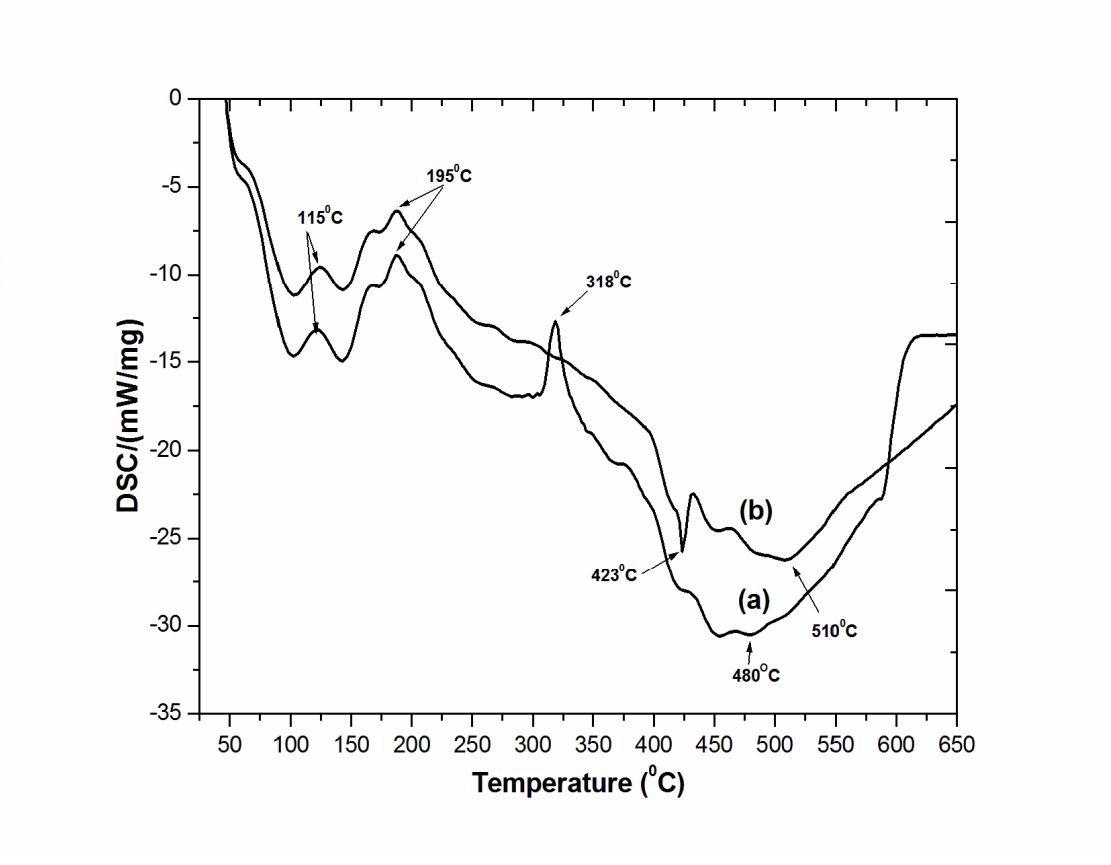

Figure.6.4. DSC thermogram of (a) CS-PNIPAM nanocarrier (b) folic acid conjugated CS-PNIPAM nanocarrier

AFM image analysis (Fig.6.5) was performed to study the shape, size and surface appearance of the FANCs. The average particle diameter was found about 105 nm for unloaded nanocarrier and 120 nm for protein loaded nanocarriers. Unloaded nanocarriers were found to be in spherical shape, core-shell structure is clearly visible, where as in loaded nanocarrier core-shell structure was not observed and these were appeared like elongated sphere shape with fluffy surface, which confirmed protein entrapment in the FANCs.

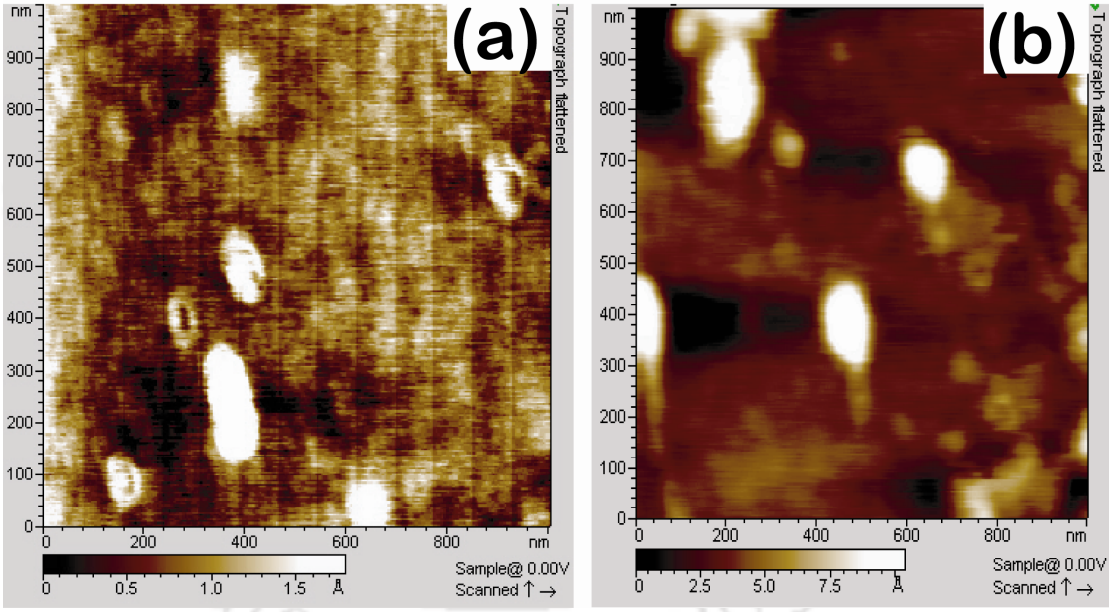

Figure.6.5. Non contact mode AFM images of (a) unloaded FANCs (b) FANCs entrapped with purified CD and the sample was prepared by depositing nanoparticle solution on freshly cleaved mica surface and dried by nitrogen. Images were acquired in non contact mode using silicon nitrite cantilever with frequency of 150 KHz

Protein delivery profile (Fig.6.6) exhibited triphasic release and thermoresponsive release behaviour. From release data, it was observed that all tests exhibited triphasic release, with an initial burst release (with in first two hour) and a sustained burst release from 1-10 hours) followed by plateau release (up to 96 hours). Most of the protein was released within the first 10 hours of the study. The release profiles at 37°C are the same as those at 22°C, but the amounts of the cumulative release at the end of the study period (4 days) were lower than those at 22°C. This may be due to the change in hydrophobic protein–gel interactions at different temperatures. In addition, we observed that the encapsulated proteins were not completely released from FANCs after a certain period of time due to the presence of interactions between the proteins and the gel matrix.

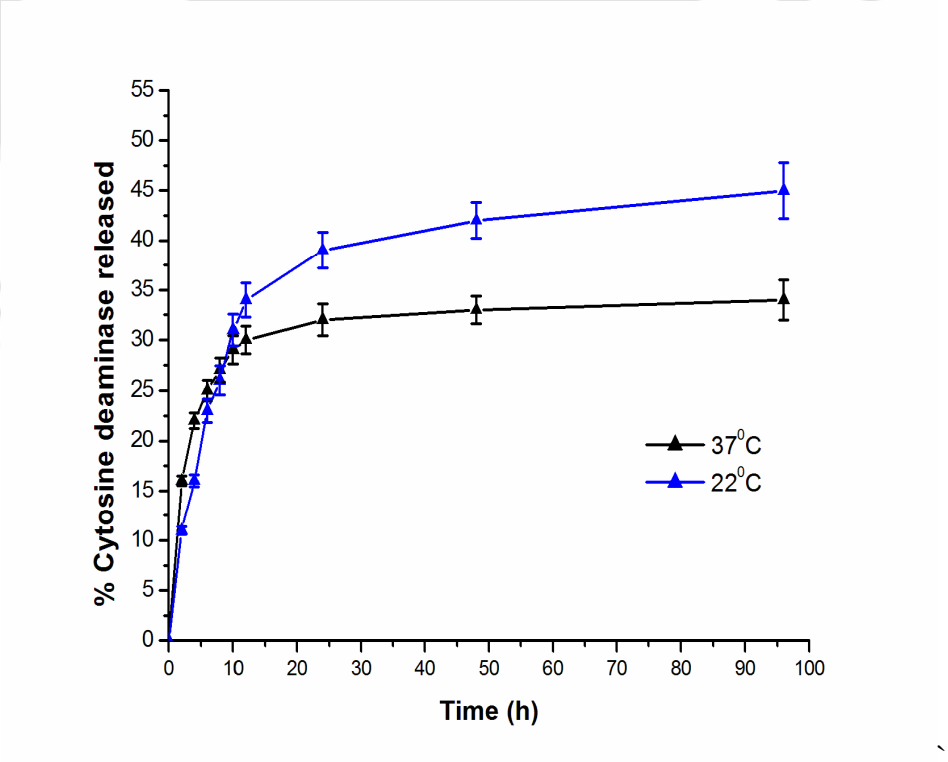

Figure.6.6. cumulative amounts of CD protein released from the folic acid conjugated CS-NIPAM nanocarriers at different temperatures (22°C and 37°C)

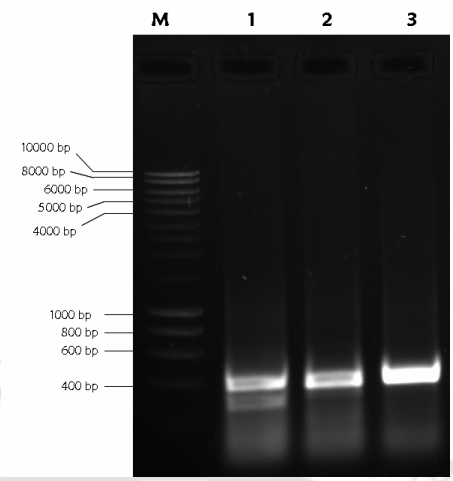

Figure.6.7. M; marker, PCR products of FRs at different annealing temperature conditions; lane 1:;50 °C , lane 2: 55.5 °C, lane 3: 59.7 °C

Semi-quantitative PCR results (Fig.6.7) demonstrated that, HT-29 cells restrain high level of expression of folate receptors which can bind with the folic acid functionalized nanoparticles for internalization. FANCs were successfully employed to transfer cytosine deaminase enzyme to the HT-29cells. CD loaded FANCs showed significant cytotoxicity on 5FC treated HT-29 cell lines (Fig.6.8). On the other hand, dual staining of 5FC/CD-FANCs treated HT-29 cells (Fig.6.9) confirming our earlier findings that 5FC/CD induced apoptosis is mediated for cell death (Gopinath and Ghosh 2007).Cytotoxic analyses showed that CD-FANCs could be targeted and endocytosed into HT-29 cells by a fast folate receptor-mediated endocytosis process. Upon uptake, the CD loaded FANCs would be released in the cell and convert the 5FC to toxic 5FU, and thereby inhibit cancer cell growth. Particularly, *in vitro* studies, there are chances of conversion of 5FC present in the media or on the surfeace of the cells which can also leads to the cell death (Fig .6.10). Therefore *in vivo* evaluation of FANCs will be required for demonstrating targeted delivery.

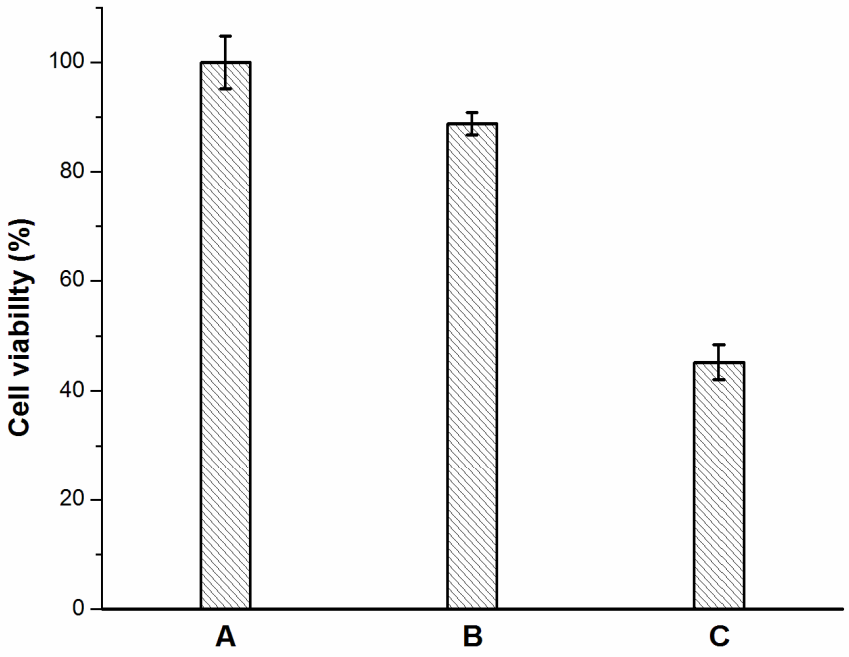

Figure.6.8. Cell viability of HT- 29 cells after 24 h incubation. A.Control cells B. Cells treated with 5FC and CS/PNIPAM nanocarriers C. Cells treated with 5FC and CD loaded FANCs

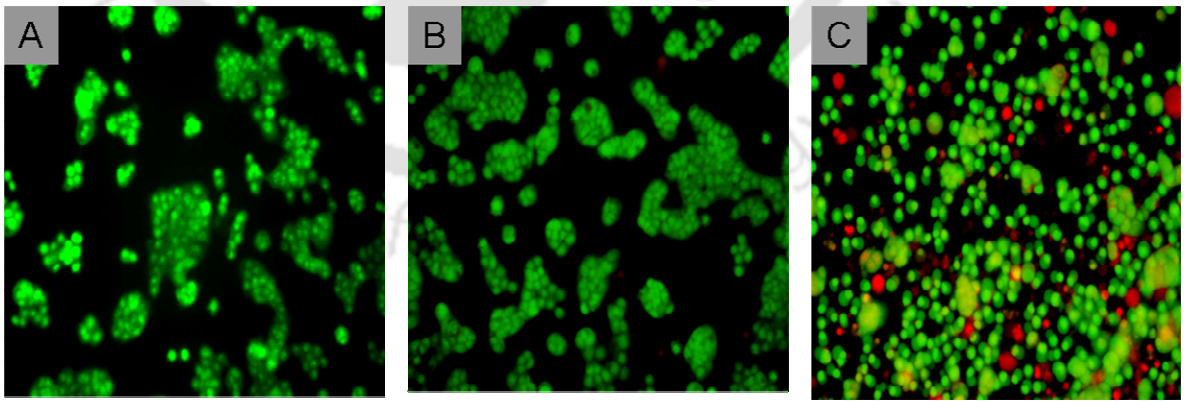

Figure.6.9 AO/EB staining of HT-29 cells after 24 h incubation. A.Control cells B. Cells treated with 5FC and CS/PNIPAM nanocarriers C. Cells treated with 5FC and CD loaded FANCs

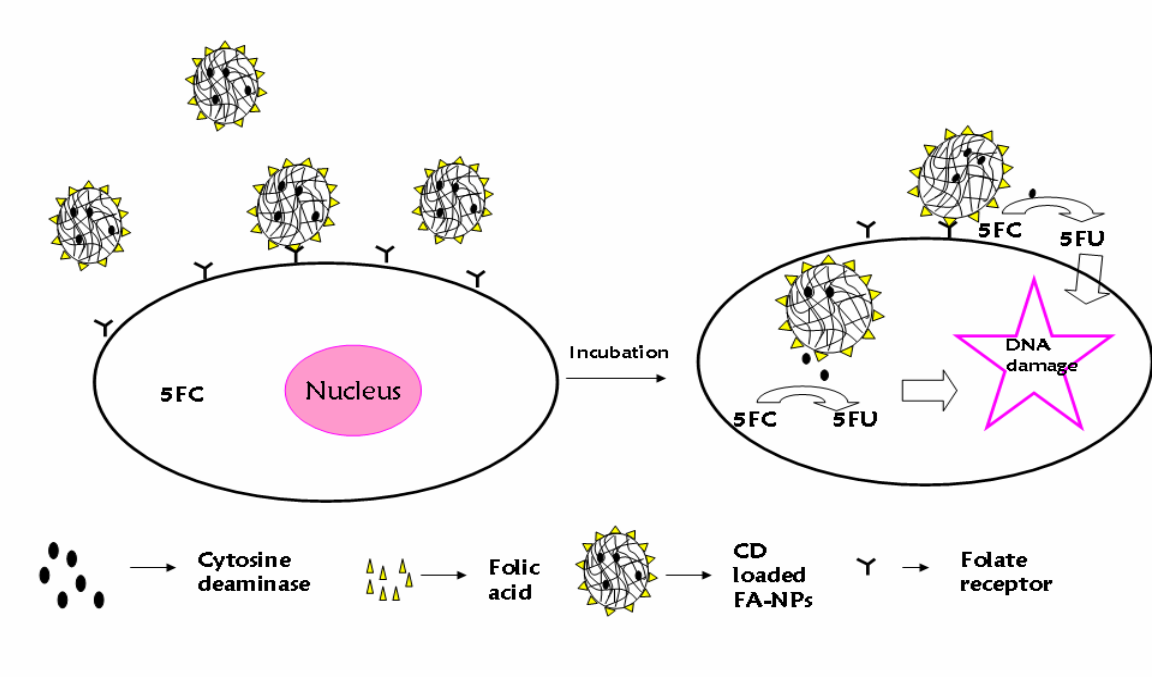

Figure.6.10. Proposed mechanism for targeted delivery of CD loaded FANCs to the cancer cells

6.4. Summary

CS/NIPAM nanocarriers were successfully conjugated with folic acid, and endorsed by FTIR. On the base of the respective decomposition onset temperatures obtained from respective TG and DSC curves, FANCs presents the highest thermal stability than unconjugated nanocarriers. The use of CD loaded NCs with folate conjugation appears to be the most appropriate way for nanoprticle deposition in tumors and binding of NCs to FR on tumor cells. Present results implicate folate targeting as a toll for prodrug/enzyme therapy.

Chapter 7

Conclusions and scope for future work

I have purified cytosine deaminase from *E.coli* K- 12 by ion-exchange column chromatography. Two subunits of 35 kDa and 46 kDa of cytosine deaminase were confirmed by SDS-PAGE. A lower K_m and higher V_{max} values for cytosine than 5FC confirmed that cytosine deaminase has higher affinity for cytosine than 5FC. This limitation has more recently led to the use of combination approach of CD/5FC along with UPRT enzyme for effective synergy of two. In this regard, I have also purified *E .coli* UPRT and determined the inhibition constant for 5FU. As UPRT activity for uracil was found to be competitively inhibited by 5FU, the docking study for elucidating various interactions between the UPRT active site with uracil and 5FU were performed. MD simulation snapshots of UPRT were done to consider the enzyme flexibility to represent exact biological conditions during docking. The docking results suggested that uracil and 5FU were attached to the different amino acid residues of the same binding site of UPRT throughout the 1,000 ps simulation time and exhibited different energy scores for binding. Furthermore, docking results elucidated the key residues of UPRT involved in the binding of anticancer drug 5FU and its natural substrate uracil. It opens up new avenue for engineering the recombinant *E. coli* UPRT to alter specificity towards prodrug and also helpful in designing the potent prodrug for improving anticancer activity in suicide gene therapy.

The polymer nanocarriers are being used to deliver therapeutic peptides proteins, antigens, oligonucleotides and genes by intravenous, oral, and mucosal administration. Herein, I have investigated the structural integrity of GFP upon entrapment in chitosan nanocarriers produced by ionotropic gelation method. Experimental results depicted

quantitative recovery of GFP from chitosan nanocarriers, where the structure and the fluorescence property of GFP could be preserved. The spectral data analysis of released GFP as well as native GFP indicated that the secondary structure was not affected during entrapment Chitosan nanocarriers appeared to be very effective vehicle for delivery of GFP. Furthermore, I have also developed a chitosan-entrapped cytosine deaminase nanocarrier. Atomic force microscopy and transmission electron microscopy image analysis showed elongated sphere shape nanocarriers with average size of 80 nm diameter. Fourier transform infrared spectroscopy and X-ray diffraction results confirmed gel formation and entrapment of cytosine deaminase within the nanocarriers. Sustained release of cytosine deaminase from the nanocarriers was indicated the feasibility of using chitosan nanocariers to deliver therapeutic proteins *in vitro* and *in vivo,* where the natural structures of the proteins entrapped in the carrier would be maintained

One of the best-characterized ligand for targeting tumor cells is the folic acid (FA). Folate conjugates are reported to be taken up by folate receptor-mediated endocytosis in many cancer cells. Therefore, I have synthesized and characterized folic acid conjugated CS/NIPAM nanocarriers. Thermal decomposition studies (TG and DSC) showed high thermal stability of folic acid conjugated nanocarriers. The cytosine deaminase loaded folic acid-conjugated NPs showed significant cytotoxicity on 5FC treated HT-29 cells after 24 h incubation.

A targeted delivery system for suicide enzymes appears to be elegant strategy for selective anti-cancer therapy. Although future experiments are required to substantiate this view, but this current thesis work may lead to more selective and powerful therapeutics which could be translated into practical clinical applications.

Bibliography

Adachi Y, Tamiya T, Ichikawa T, Terada K, Ono Y, Matsumoto K, Furuta T, Hamada H,Ohmoto T (2000) Experimental gene therapy for brain tumors using adenovirus-mediated transfer of cytosine deaminase gene and uracil phosphoribosyltransferase gene with 5-fluorocytosine. Hum Gene Ther 11 (1):77–89

Aghi M, Kramm CM, Chou TC, Breakefield XO, Chiocca EA (1998) Synergistic anticancer effects of ganciclovir/thymidine kinase and 5-fluorocytosine/cytosine deaminase gene therapies. J Natl Cancer Inst 90(5):370-380

Alloush HM, Kerridge D (1994) Characterisation of a partially purified uracil phosphoribosyltransferase from the opportunistic pathogen *Candida albicans*. Mycopathol 125:129–141

Anderson PH, Smith JM, Mygind B (1992) Characterization of the upp gene encoding uracil phosphoribosyltransferase of *Escherichia coli* K12. Eur J Biochem 204:51–56

Anderson WF (ed.) (2002) NIH report: assessment of adenoviral vector safety and toxicity: report of the national institutes of health recombinant DNA advisory committee. Cancer Gene Ther 13:3–13

Antony AC (1996) Folate receptors. Annu Rev Nutr 16:501–21

Asai T, Lee CS, Chandler A, O'Sullivan WJ (1990) Purification and characterization of uracil phosphoribosyltransferase from *Crithidia luciliae*. Comp Biochem Physiol B 95:159–163

Bibliography

Brannon-Peppas L, Blanchette JO (2004) Nanoparticle and targeted systems for cancer therapy. Adv Drug Deliv Rev 56(11):1649-59

Bhattarai N, Ramay HR, Chou SH, Zhang M (2006) Chitosan and lactic acid-grafted chitosan nanoparticles as carriers for prolonged drug delivery. Inter J Nanomed 1(2): 181–187

Bradford MM (1976) A rapid and sensitive method for the quantification of microgram quantities of protein utilizing the principle of protein dye binding. Anal Biochem 72: 248–254

Berendsen HJC, Postma JPM, van Gunsteren WF, DiNola A, Haak JR (1984) Molecular dynamics with coupling to an external bath. J Chem Phys 81:3684–3690

Carlson HA (2002) Protein flexibility and drug design: how to hit a moving target. Curr Opin Chem Biol 6: 447–452

Cansell F , Grabielle-Madelmont C , Ollivon M (1991) Characterization of the aqueous phase and the water-polymer interface in latex suspensions by differential scanning calorimetry. J Colloid Interface Sci 144:1: 1-17

Carrara CR, Rubiolo AC (1994) Immobilization of β-galactosidase on chitosan. Biotechnol Prog 10 (2): 220–224

Carter D, Donald RG, Roos D, Ullman B (1997) Expression, purification, and characterization of uracil phosphoribosyltransferase from *Toxoplasma gondii*. Mol Biochem Parasitol 87:137–144

Case DA, Cheatham III TE, Darden T, Gohlke H, Luo R, Merz Jr KM, Onufriev A, Simmerling C, Wang B, Woods RJ (2005) The amber biomolecular simulation programs. J Comput Chem 26: 1668– 1688

Bibliography

Chabner BA, Jr Roberts TG (2005) Timeline: chemotherapy and the war on cancer. Nat Rev Cancer 5 (1): 65–72

Chaleawlert-umpon S, Pimpha N (2009) Morphology study of super paramagnetic iron oxide-chitosan nanoparticles. J Microsc Soc Thail 23:1: 62-65

Chatterjee DK, Zhang Y (2007) Multi-functional nanoparticles for cancer therapy.Sci Technol Adv Mater 8: 131–133

Chung F, Wong (2008) Flexible ligand–flexible protein docking in protein kinase systems. Biochim Biophys Acta 1784: 244–251

Colombo BM, Benedetti S, Ottolenghi S, Mora M, Pollo B, Poli G,Finocchiaro G (1995) The "bystander effect": association of U-87 cell death with ganciclovirmediated apoptosis of nearby cells and lack of effect in athymic mice. Hum Gene Ther 6:763-772

Corban-Wilhelm H, Hull WE, Becker G, Bauder-Wüst U, Greulich D, Debus J (2002) Cytosine deaminase and thymidine kinase gene therapy in a dunning rat prostate tumour model: absence of bystander effects and characterisation of 5-fluorocytosine metabolism with 19F-NMR spectroscopy. Gene Ther 9(23):1564-75

Dai YP, Lee CS, O'Sullivan WJ (1995) Properties of uracil phosphoribosyltransferase from *Giardia intestinalis*. Int J Parasitol 25:207–214

De Campos AM, Diebold Y, Carvalho EL, Sánchez A, Alonso MJ (2004) Chitosan nanoparticles as new ocular drug delivery systems: *in vitro* stability, *in vivo* fate, and cellular toxicity. Pharm Res 21(5): 803-810

Dhara D,Chatterji PR (2000) Phase transition in linear and cross-linked PNIPAAm in water: effect of various types of additives. J Macromol Sci Part C: Polym Rev 40 (1): 51-68

Bibliography

Dilber MS, Abedi MR, Christensson B, Bjorkstrand B, Kidder GM, Naus CC, Gahrton G, Smith CI (1997) Gap junctions promote the bystander effect of herpes simplex virus thymidine kinase *in vivo*. Cancer Res 57 (8):1523–1528

Elnakat H and Ratnam M (2004) Distribution, functionality and gene regulation of folate receptor isoforms: implications in targeted therapy. Adv Drug Deliv Rev 56 (8):1067-1084

Erbs P, Regulier E, Kintz J, Leroy P, Poitevin Y, Exinger F, Jund R, Mehtali M (2000) *In vivo* cancer gene therapy by adenovirus-mediated transfer of a bifunctional yeast cytosine deaminase/uracil phosphoribosyltransferase fusion gene. Cancer Res 60(14):3813-3822

Essmann U, Perera L, Berkowitz ML, Darden T, Lee H, Pedersen LG (1995) A smooth particle mesh ewald method. J Chem Phys 103: 8577–8593

Fast R, Skold O (1917) Biochemical mechanism of uracil uptake regulation in *Escherichia coli* B allosteric effects on uracil phosphoribosyltransferase under stringent conditions . J Biol Chem 252 (21): 7620-1624

Ferrin TE, Huang CC, Jarvis LE, Langridge R (1988) The MIDAS display system . J Mol Graph 6: 13–27

Fuchita M, Ardiani A, Zhao L, Serve K, Stoddard BL, Black ME (2009) Bacterial cytosine deaminase mutants created by molecular engineering show improved 5-fluorocytosine-mediated cell killing *in vitro* and *in vivo*. Cancer Res 69(11):4791-4799

Gantaa S, Devalapallya H, Shahiwalaa A, Amiji M (2008) A review of stimuli-responsive nanocarriers for drug and gene delivery. J Control Release 126:187-204

Bibliography

George M and Abraham TE (2006) Polyionic hydrocolloids for the intestinal delivery of protein drugs:alginate and chitosan — a review. J Control Release 114: 1–14

Gerdes HH,Kaethe C (1996) Green fluorescent protein: applications in cell biology. FEBS Lett 389: 44-47

Giffard PM, Rathsam C, Kwan E, Kwan DW, Bunny KL, Koo SP, Jacques NA (1993) The ftf gene encoding the cell-bound fructosyl transferase of *Streptococcus salivarius* ATCC 25975 is preceded by an insertion sequence and followed by FUR1 and clpP homologues. J Gen Microbiol 139:913–920

Gopinath P, Ghosh SS (2008a) Apoptotic induction with bifunctional *E .coli* cytosine deaminase-uracil phosphoribosyltransferase mediated suicide gene therapy is synergized by curcumin treatment *in vitro*. Mol Biotechnol 39(1):39-48

Gopinath P, Ghosh SS (2007) Monitoring green fluorescent protein for functional delivery of *E. coli* cytosine deaminase suicide gene and the effect of curcumin *in vitro*. Gene Ther Mol Biol 11: 219-228

Gopinath P, Ghosh SS (2008 b) Implication of functional activity for determining therapeutic efficacy of suicide genes *in vitro.* Biotechnol Lett 30(11):1913-1921

Gopinath P, Ghosh SS (2009) Understanding apoptotic signaling pathways in cytosine deaminase-uracil phosphoribosyl transferase-mediated suicide gene therapy *in vitro*. Mol Cell Biochem 324(1-2):21-29

Gopinath P, Gogoi SK, Chattopadhyay A,Ghosh SS (2008c) Implications of silver nanoparticle induced cell apoptosis for *in vitro* gene therapy. Nanotechnol 19 :7

Gottesman MM (2003) Cancer gene therapy: an awkward adolescence. Cancer Gene Ther 10(7):501-508

Harris BE, Manning BW, Federle TW, Diasio RB (1986) Conversion of 5-fluorocytosine to 5-fluorouracil by human intestinal microflora. Antimicrob Agents Chemother 29(1):44-48

Hattori Y, Maitani Y (2005) Folate-linked lipid-based nanoparticle for targeted gene delivery. Curr Drug Deliv 2(3):243-52

Hejazi R, Amiji M (2003) Chitosan-based gastrointestinal delivery systems. J Control Release 89:1–165

Hornak V, Abel R, Okur A, Strockbine B, Roitberg A, Simmerling C (2006) Comparison of multiple amber force fields and development of improved protein backbone parameters. Proteins 65: 712–725

Ieva E, Trapani A, Cioffi N, Ditaranto N, Monopoli A, Sabbatini L (2009) Analytical characterization of chitosan nanoparticles for peptide drug delivery applications. Anal Bioanal Chem 393:207–215

Ipata PL, Marmocchi F, Magni G, Felicioli R, Polidoro G (1971) Baker's yeast cytosine deaminase: Some enzymic properties and allosteric inhibition by nucleosides and nucleotides. Biochem 10(23):4270-4276

Ireton GC, Black ME, Stoddard BL (2003) The 1.14 Å crystal structure of yeast cytosine deaminase: evolution of nucleotide salvage enzymes and implications for genetic chemotherapy. Struct 11(8):961-972

Ireton GC, McDermott G, Black ME, Stoddard BL (2002) The structure of *Escherichia coli* cytosine deaminase. J Mol Biol 315(4):687-697

Ireton GC, Stoddard BL (2004) Microseed matrix screening to improve crystals of yeast cytosine deaminase. Acta Crystallogr D Biol Crystallogr 60:601-605

Islam MR , Kim H ,Kang SW , Kim JS ,JeongYM, Hwang HJ, Lee SY Woo JC , Kim SG (2007) Functional characterization of a gene encoding a dual domain for

uridine kinase and uracil phosphoribosyltransferase in *Arabidopsis thaliana*. Plant Mol Biol 63:465–477

Jain S, Singh R, Gupta MN (2004) Purification of recombinant green fluorescent protein by three-phase partitioning. J Chromatography A 1035: 83–86

Janes KA, Calvo P, Alonso MJ (2001) Polysaccharide colloidal particles as delivery systems for macromolecules. Adv Drug Deliv Rev 47: 83-9

Jaracz S, Chen J, Kuznetsova LV, Ojima I (2005) Recent advances in tumor-targeting anticancer drug conjugates. Bioorg Med Chem 13(17):5043-54

Jensen KF, Arent S, Larsen S, Schack L (2005) Allosteric properties of the GTP activated and CTP inhibited uracil phosphoribosyltransferase from the thermoacidophilic archaeon *Sulfolobus solfataricus*. FEBS J 272:1440–1453

Jensen KF, Mygind B (1996) Different oligomeric states investigated are involved in the allosteric behaviour of uracil phosphoribosyltransferase from *Escherichia coli* . Eur J Biochem 204: 637–64

Jung K, Yu TS (2004) Purification and properties of intracellular cytosine deaminase from *chromobacterium violaceum YK 391*. J Microbiol Biotechnol 14(6):1182–1189

Kambara H, Tamiya T, Ono Y, Ohtsuka S, Terada K, Adachi Y, Ichikawa T, Hamada H, Ohmoto T (2002) Combined radiation and gene therapy for brain tumors with adenovirus-mediated transfer of cytosine deaminase and uracil phosphoribosyltransferase genes. Cancer Gene Ther 9(10):840-845

Kamen BA, Capdevila A (1986) Receptor-mediated folate accumulation is regulated by the cellular folate content. Proc Natl Acad Sci 83: 5983-5987

Kanai F, Kawakami T, Hamada H, Sadata A, Yoshida Y, Tanaka T, Ohashi M, Tateishi K, Shiratori Y, Omata M (1998) Adenovirus-mediated transduction of *Escherichia*

coli uracil phosphoribosyltransferase gene sensitizes cancer cells to low concentrations of 5-fluorouracil. Cancer Res 58(9):1946-1951

Kanyama H, Tomita N, Yamano T, Aihara T, Miyoshi Y, Ohue M, Sekimoto M, Sakita I, Tamaki Y, Kaneda Y, Senter PD, Monden M (2001) Usefulness of repeated direct intratumoral gene transfer using hemagglutinating virus of japan-liposome method for cytosine deaminase suicide gene therapy. Cancer Res 61(1):14-18

Kas HS (1997) Chitosan: properties, preparations and application to microparticulate systems. J Microencapsul 14(6) : 689-711

Katherine B, Kam WL (2006) Chitosan nanoparticles for oral drug and gene delivery. Int J Nanomed 1(2): 117–128

Katsuragi T, Shibata M, Sakai T, Tonomura, K (1989) Stabilization of cytosine deaminase from bakers' yeast by immobilization. Agric Biol Chem 53:1515-1523

Katsuragi T,Sakai T,Matsumoto K, Tonomura K (1986) Cytosine deaminase from *Escherichia coli*-production, purification, and some characteristics. Agric Biol Chem 50 (7):1721 -1730

Kawamura K, Tasaki K, Hamada H, Takenaga K, Sakiyama S, Tagawa M (2000) Expression of *Escherichia coli* uracil phosphoribosyltransferase gene in murine colon carcinoma cells augments the antitumoral effect of 5-fluorouracil and induces protective immunity. Cancer Gene Ther 7 (4): 637–643

Kern L, de Montigny J, Jund R, Lacroute F (1990) The FUR1 gene of *Saccharomyces cerevisiae:* cloning, structure and expression of wild-type and mutant alleles. Gene 88:149–157

Khan A (2007) Preparation and characterization of n-isopropylacrylamide/acrylic acid copolymer core–shell microgel particles. J Colloid Interface Sci 313: 697–704

Bibliography

Khil MS, Kim JH, Mullen CA, Kim SH, Freytag SO (1996) Radiosensitization by 5-fluorocytosine of human colorectal carcinoma cells in culture transduced with cytosine deaminase gene. Clin Cancer Res 2(1):53-57

Kievit E, Bershad E, Ng E, Sethna P, Dev I, Lawrence TS, Rehemtulla A (1999) Superiority of yeast over bacterial cytosine deaminase for enzyme/prodrug gene therapy in colon cancer xenografts. Cancer Res 59(7):1417-1421

Kievit E, Nyati MK, Ng E, Stegman LD, Parsels J, Ross BD, Rehemtulla A, Lawrence TS (2000) Yeast cytosine deaminase improves radiosensitization and bystander effect by 5-fluorocytosine of human colorectal cancer xenografts. Cancer Res 60(23):6649-6655

Kim J, Yu TS (2004) Purification and properties of intracellular cytosine deaminase from *Chromobacterium violaceum* YK 391. J Microbiol Biotechnol 14: 1182-1189

Ko TP, Lin JJ, Hu CY, Hsu YH, Wang AH, Liaw SH (2003) Crystal structure of yeast cytosine deaminase. Insights into enzyme mechanism and evolution. J Biol Chem 278(21):19111-19117

Koechlin BA, Rubio F, Palmer S, Gabriel T, Duschinsky R (1966) The metabolism of 5-fluorocytosine-2-14-C and of cytosine-14-C in the rat and the disposition of 5-fluorocytosine-2-14-C in man. Biochem Pharmacol 15(4):435-46

Korkegian A, Black ME, Baker D, Stoddard BL (2005) Computational thermostabilization of an enzyme. Sci 308(5723):857-860

Koyama F, SawadaH., HiraoT , Fujii H, Hamada H, Nakano H (2000) Combined suicide gene therapy for human colon cancer cells using adenovirus-mediated transfer of Escherichia coli cytosine deaminase gene and *Escherichia coli* uracil

phosphoribosyltransferase gene with 5-fluorocytosine.Cancer Gene Ther 7 (7): 1015–1022

Kumar MVS, Swaminathan R (2010) A novel approach to segregate and identify functional loop regions in protein structures using their ramachandran maps. Proteins 78: 900-916

Kuntz ID, Blaney JM, Oatley SJ, Langridge R, Ferrin TE (1982) A geometric approach to macromolecule–ligand interactions. J Mol Biol 161: 269–288

Kuntz ID, Moustakas DT, Paula Therese Lang (Ed.) (2005) DOCK Version 5.2 user manual. Department of pharmaceutical chemistry, university of california, san francisco

Kurozumi K, Tamiya T, Ono Y, Otsuka S, Kambara H, Adachi Y, Ichikawa T, Hamada H, Ohmoto T (2004) Apoptosis induction with 5-fluorocytosine/cytosine deaminase gene therapy for human malignant glioma cells mediated by adenovirus. J Neurooncol 66(1-2):117-127

Laskowski RA, Macarthur MW, Moss DS, Thornton JM (1993) "Procheck - a program to check the stereochemical quality of protein structures. J Appl Crystallogr 26 :283-291

Lawrence TS, Davis MA, Maybaum J (1994) Dependence of 5-fluorouracil-mediated radiosensitization on DNA-directed effects. Int J Radiat Oncol Biol Phys 29(3):519-523

Lawrence TS, Rehemtulla A, Ng EY, Wilson M, Trosko JE, Stetson PL (1998) Preferential cytotoxicity of cells transduced with cytosine deaminase compared to bystander cells after treatment with 5-flucytosine. Cancer Res 58 (12):2588-2593

Bibliography

Lee WF, Chen YJ (2001) Studies on Preparation and Swelling Properties of the N-isopropylacrylamide/Chitosan Semi IPN and IPN Hydrogels. J Appl Polym Sci 82: 2487-2496.

Li F, Li J, Wen X Zhou S, Tong X, Su P , Li H, Shi D (2009) Anti-tumor activity of paclitaxel-loaded chitosan nanoparticles: an *in vitro* study. Mater Sci Eng C 29 (8):2392-2397

Li C, Penet MF, Winnard P Jr, Artemov D, Bhujwalla ZM (2008 a) Image-guided enzyme/prodrug cancer therapy. Clin Cancer Res 14(2):515-522

Li C, Wildes F, Winnard P Jr, Artemov D, Penet MF, Bhujwalla ZM (2008 b) Conjugation of poly-L-lysine to bacterial cytosine deaminase improves the efficacy of enzyme/prodrug cancer therapy. J Med Chem 51(12):3572-3582

Li C, Winnard PT Jr, Takagi T, Artemov D, Bhujwalla ZM (2006) Multimodal image-guided enzyme/prodrug cancer therapy. J Am Chem Soc 128(47):15072-15073

Li P, Zhu AM, Liu QL, Zhang QG (2008c) Fe_3O_4/ (n-Isopropylacrylamide)/chitosan composite microspheres with multi responsive properties. Ind Eng Chem Res 47:7700-7706

Lin JJ, Chen JS, Huang SJ, Ko JH, Wang YM, Chen TL, Wang LF (2009) Folic acid-Pluronic F127 magnetic nanoparticle clusters for combined targeting, diagnosis, and therapy applications. Biomater 28:5114-24

Linde L, Jensen KF (1996) Uracil phosphoribosyltransferase from the extreme thermoacidophilic archaebacterium *sulfolobus shibatae* is an allosteric enzyme, activated by GTP and inhibited by CTP. Biochem Biophys Acta 1296:16–22

Lineweaver H, Burk D (1934) The determination of enzyme dissociation constants. J Am Chem Soc 5 6 (3): 658–666

Low PS, Antony AC (2004) Folate receptor-targeted drugs for cancer and inflammatory diseases. Adv Drug Deliv Rev 56:1057-1238

Lv SQ, Zhang KB, Zhang EE, Gao FY, Yin CL, Huang CJ, He JQ, Yang H (2009) Antitumor efficiency of the cytosine deaminase/5-fluorocytosine suicide gene therapy system on malignant gliomas: an *in vivo* study. Med Sci Monit 15(1):BR13-20

Lynch I and Dawson KA (2008) Protein-nanoparticle interactions. Nano today 3:1 (3):40-47

Mahan SD, Ireton GC, Knoeber C, Stoddard BL, Black ME (2004) Random mutagenesis and selection of *Escherichia coli* cytosine deaminase for cancer gene therapy. Protein Eng Des Sel 17(8):625-633

Mahoney MW, Jorgensen WL (2000) A five site model for liquid water and the reproduction of the density anomaly by rigid, non-polarizable potential functions. J Chem Phys112: 8910–8922

Marais R, Spooner RA. Light Y, Martin J, Springer CJ (1996) Gene-directed enzyme prodrug therapy with a mustard prodrug/carboxypeptidase G2 combination. Cancer Res 56 (20): 4735–4742

Marshall E (1999) Gene therapy death prompts review of adenovirus vector. Science 286(5448):2244-2245

Martinussen J, Glaser P, Andersen PS, Saxild HH (1995) Two genes encoding uracil phosphoribosyltransferase are present in *Bacillus subtilis*. J Bacteriol 177:271–274

Martinussen J, Hammer K (1994) Cloning and characterization of upp, a gene encoding uracil phosphoribosyltransferase from *Lactococcus lactis*. J Bacteriol 176:6457–6463

Bibliography

McIvor RS, Wohlhueter RM, Plagemann PG (1983) Uracil phosphoribosyltransferase from *Acholeplasma laidlawii*: partial purification and kinetic properties. J Bacteriol 156:192–197

Meng EC, Shoichet BK, Kuntz ID (1992) Automated docking with grid-based energy evaluation. J Comput Chem 13: 505–524

Mierzwa ML, Nyati MK, Morgan MA, Lawrence TS (2010) Recent advances in combined modality therapy. Oncologist 15(4):372-381

Miller CR, Williams CR, Buchsbaum DJ, Gillespie GY (2002) Intratumoral 5-fluorouracil produced by cytosine deaminase/5-fluorocytosine gene therapy is effective for experimental human glioblastomas. Cancer Res 62(3):773-780

Moolten FL (1986) Tumor chemosensitivity conferred by inserted herpes thymidine kinase genes: paradigm for a prospective cancer control strategy. Cancer Res 46 (10): 5276–5281

Mullen CA, Kilstrup M, Blaese RM (1992) Transfer of the bacterial gene for cytosine deaminase to mammalian cells confers lethal sensitivity to 5-fluorocytosine: a negative selection system. Proc Natl Acad Sci USA 89 (1): 33–37

Natalini P, Ruggieri S, Santarelli I, Vita A, Magni G (1979) Baker's yeast UMP:pyrophosphate phosphoribosyltransferase purification, enzymatic and kinetic properties. J Biol Chem 254 (5): 1558-1563

Neuhard J (1983) Metabolism of nucleotides, nucleosides and nucleobases in microorganisms, edited by A. Munch-Petersen, London: Academic Press 95-148

Niculescu-Duvaz I, Springer CJ (2005) Introduction to the background, principles, and state of the art in suicide gene therapy. Mol Biotechnol 30(1):71-88

Nishiyama T, Kawamura Y, Kawamoto K, Matsumura H, Yamamoto N, Ito T, Ohyama A, Katsuragi T, Sakai T (1985) Antineoplastic effects in rats of 5-fluorocytosine in combination with cytosine deaminase capsules. Cancer Res 45(4):1753-61

Parker N, Turk MJ, Westrick E, Lewis JD , Low PS and Leamon CP (2005) Folate receptor expression in carcinomas and normal tissues determined by a quantitative radioligand binding assay. Anal Biochem 338 (2): 284-293

Patil NS, Dordick JS, Rethwisch DG (1996) Macroporous poly (sucrose acrylate) hydrogel for controlled release of macromolecules. Biomater 17:2343–2350

Pearlman DA, Case DA, Caldwell JW, Ross WS, Cheatham III TE, DeBolt S, Ferguson D, Seibel G, Kollman P (1995) AMBER, a package of computer programs for applying molecular mechanics, normal mode analysis, molecular dynamics and free energy calculations to simulate the structural and energetic properties of molecules. Comp Phys Commun 91: 1–41

Pederson LC, Buchsbaum DJ, Vickers SM, Kancharla SR, Mayo MS, Curiel DT, Stackhouse MA (1997) Molecular chemotherapy combined with radiation therapy enhances killing of cholangiocarcinoma cells *in vitro* and *in vivo*. Cancer Res 57(19):4325-4332

Peer D, Karp JM, Hong S, Farokhzad OC, Margalit R, Langer R (2007) Nanocarriers as an emerging platform for cancer therapy. Nat Nanotechnol 2(12):751-60

Pelton JT, McLean LR (2000) Spectroscopic methods for analysis of protein secondary structure. Anal Biochem 277:167–176

Perez-Zuniga EJ, Gunther Sillero MA, Sillero A (2008) Bisphosphonates activate the 5-fluorouracil/uracil phosphoribosyltransferase activity present in *Saccharomyces cerevisiae* cell extracts Implications for tumor treatments. Bio chem pharmacol 7 6:825– 830

Pettersen EF, Goddard TD, Huang CC, Couch GS, Greenblatt DM, Meng EC, Ferrin TE (2004) UCSF Chimera - a visualization system for exploratory research and analysis. J Comput Chem 25: 1605–1612

Plank J, Andres PR, Krause I, Winter C (2008) Gram scale separation of casein proteins from whole casein on a Source 30Q anion-exchange resin column utilizing fast protein liquid chromatography (FPLC). Protein Expr Purif 60:2:176-181

Polak A , Scholer HJ (1975) Mode of action of 5-fluorocytosine and mechanisms of resistance. Chemotherapy 21:113-130

Portsmouth D, Hlavaty J, Renner (2007) Suicide genes for cancer therapy. Mol Asp Med 28: 4–41

Prabaharan M, Mano JF (2005) Chitosan-based particles as controlled drug delivery systems. Adv Drug Deliv Rev 12:41–57

Pridgen EM, Langer R, Farokhzad OC (2007) Biodegradable, polymeric nanoparticle delivery systems for cancer therapy. Nanomedicine (Lond) 2(5):669-80

Quan J, Chai YQ, Branford-White C J, Zhu LM (2009) The purification and characterization of deoxycytidine kinase from calf thymus. World J Microbiol Biotechnol 25:475–480

Rasmussen UB, Mygind B, Nygaard P (1986) Purification and some properties of uracil phosphoribosyitransferase from *Escherichia coli* K12. Biochim Biophys Acta 881: 268- 275

Ribble D, Goldstein NB, Norris DA, Shellman YG (2005) A simple technique for quantifying apoptosis in 96-well plates. BMC Biotechnol 5:12

Roehm NW, Rodgers GH, Hatfield SM, Glasebrook AL (1991) An improved colorimetric assay for cell proliferation and viability utilizing the tetrazolium salt XTT. J Immunol Methods 142(2):257-65

Bibliography

Rogulski KR, Zhang K, Kolozsvary A, Kim JH, Freytag SO (1997) Pronounced antitumor effects and tumor radiosensitization of double suicide gene therapy. Clin Cancer Res 3(11):2081-2088

Ross JF, Chaudhuri PK, Ratnam M (1994) Differential regulation of folate receptor isoforms in normal and malignant tissues in vivo and in established cell lines. Physiologic and clinical implications. Cancer 73(9):2432-43

Sakai T, Katsuragi T, Tonomura K ,Nishiyama T, Kawamura Y (1985) Implantable encapsulated cytosine deaminase having 5-fluorocytosine-deaminating activity. J Biotechnol 2: 13-21

Sanpui P, Pandey SB, Ghosh SS, Chattopadhyay A (2008) Green fluorescent protein for *in situ* synthesis of highly uniform Au nanoparticles and monitoring protein denaturation. J Colloid Interface Sci 326 :129–137

Schüttelkopf AW, van Aalten DM (2004) PRODRG: A tool for high-throughput crystallography of protein-ligand complexes. Acta Crystallogr D 60: 1355–1363

Schumacher MA, Bashor CJ, Song MH, Otsu K, Zhu S, Parry RJ, Ullman B, Brennan RG (2002) The structural mechanism of GTP stabilized oligomerization and catalytic activation of the Toxoplasma gondii uracil phosphoribosyltransferase. Proc Natl Acad Sci USA 99:78–83

Schumacher MA, Carter D , Scott DM, Roos DS, Ullman B,Brennan RG (1998) Crystal structures of *Toxoplasma gondii* uracil phosphoribosyltransferase reveal the atomic basis of pyrimidine discrimination and prodrug binding . The EMBO J 17 (12): 3219–3232

Scudiero DA, Shoemaker RH, Paull KD, Monks A, Tierney S, Nofziger TH, Currens MJ, Seniff D, Boyd MR (1988) Evaluation of a soluble tetrazolium/formazan

assay for cell growth and drug sensitivity in culture using human and other tumor cell lines. Cancer Res 48(17):4827-33

Senter PD, Su PC, Katsuragi T, Sakai T, Cosand WL, Hellström I, Hellström KE (1991) Generation of 5-fluorouracil from 5-fluorocytosine by monoclonal antibody-cytosine deaminase conjugates. Bioconjug Chem 2(6):447-451

Sonvico F, Mornet S, Vasseur S, Dubernet C, Jaillard D, Degrouard J, Hoebeke J, Duguet E, Colombo P, Couvreur P (2005) Folate-conjugated iron oxide nanoparticles for solid tumor targeting as potential specific magnetic hyperthermia mediators: synthesis, physicochemical characterization, and *in vitro* experiments. Bioconjug Chem 16(5):1181-8

Springer CJ**,** Niculescu-Duvaz I (1996) Gene-directed enzyme prodrug therapy (GDEPT): choice of prodrugs. Adv Drug Deliv Rev 22: 351–364

Stribbling SM, Friedlos F, Martin J, Davies L, Spooner RA, Marais R and Springer CJ (2000) Regressions of established breast carcinoma xenografts by carboxypeptidase G2 suicide gene therapy and the prodrug CMDA are due to a bystander effect. Hum. Gene Ther 11: 285-292

Tangvarasittichai S, Tangvarasittichai O , Jermnim N (2009) Comparison of fast protein liquid chromatography (FPLC) with HPLC, electrophoresis & microcolumn chromatography techniques for the diagnosis of beta-thalassaemia. Indian J Med Res 129:3:242-248

Thomas CE, Ehrhardt A, Kay MA (2003) Progress and problems with the use of viral vectors for gene therapy. Nat Rev Genet 4(5):346-358

Thompson JD, Higgins DG, Gibson TJ (1994) CLUSTAL W: improving the sensitivity of progressive multiple sequence alignment through sequence

weighting,position-specific gap penalties and weight matrix choice. Nucleic Acids Res 22(22): 4673-4680

Trinh QT, Austin EA, Murray DM, Knick VC, Huber BE (1995) Enzyme/prodrug gene therapy: comparison of cytosine deaminase/5-fluorocytosine versus thymidine kinase/ganciclovir enzyme/prodrug systems in a human colorectal carcinoma cell line. Cancer Res. 55: 4808-4812

Tsai SW, Liaw JW, Hsu FY, Chen YY, Lyu MJ ,Yeh MS (2008) Surface-modified gold nanoparticles with folic acid as optical probes for cellular imaging. Sensors 8: 6660-6673

VanThor JJ, Pierik AJ, Nugteren-Roodzant I, Xie A, Hellingwerf KJ (1998) Characterization of the photoconversion of green fluorescent protein with FTIR spectroscopy. Biochem 37:16915-16921

Visser NV, Hinka MA, Borsta JW, vander Krogt GNM, Visser AJWG (2002) Circular dichroism spectroscopy of fluorescent proteins. FEBS Lett 521: 31-35

Waldorf AR, Polak A (1983) Mechanisms of action of 5-fluorocytosine. Antimicrob Agents Chemother 23(1):79-85

Wallace PM, MacMaster JF, Smith VF, Kerr DE, Senter PD, Cosand WL (1994) Intratumoral generation of 5-fluorouracil mediated by an antibody-cytosine deaminase conjugate in combination with 5-fluorocytosine. Cancer Res 54(10):2719-2723

West TP, Shanley MS, O'Donovan GA (1982) Purification and some properties of cytosine deaminase from *Salmonella typhimurium*. Biochim Biophys Acta 719(2):251-258

Xu Y , Du Y (2003) Effect of molecular structure of chitosan on protein delivery properties of chitosan nanoparticles. Int J Pharm 250: 215-222

Yang SJ, Lin FH, Tsai KC, Wei MF, Tsai HM, Wong JM, Shieh MJ (2010) Folic acid-conjugated chitosan nanoparticles enhanced protoporphyrin IX accumulation in colorectal cancer cells. Bioconjug Chem 21(4):679-89

Yao L, Li Y, Wu Y, Liu A, Yan H (2005) Product release is rate-limiting in the activation of the prodrug 5-fluorocytosine by yeast cytosine deaminase. Biochem 44(15):5940-5947

Yazawa K, Fisher WE, Brunicardi FC (2002) Current progress in suicide gene therapy for cancer. World J Surg 26(7):783-789

Yu TS, Kim JK , Katsuragi T, SakaiT, Tonomura K (1991) Purification and properties of cytosine deaminase from *Aspergillus fumigatus*. J Ferment Bioeng 72(4):266-269

Yuan F, Dellian M, Fukumura D, Leuning M, Berk DD, Yorchilin VP and Jain RK (1995) Vascular permeability in a human tumor xenograft: molecular size dependence and cutoff size. Cancer Res 55:3752–3756

Zhang YL, Chu CC (2002) The effect of degradation of biodegradable hydrogel network on its release of albumin. J Mater Sci Mater Med 13:667–676

Zimmer M (2002) Green fluorescent protein (GFP): applications, structure, and related photophysical behavior. Chem Rev 102: 759-781

List of publications

Research Papers

1. **Yata VK** and Ghosh SS (2010) Synthesis and characterization of a novel chitosan based *E. coli* cytosine deaminase nanocomposite for potential application in prodrug enzyme therapy. **Biotechnology Letters** 33(1):153-7

2.**Yata VK**, Sen K, Kumar MVS and Ghosh SS (2011) Interaction studies of *E. coli* uracil phosphoribosyltransferase with 5-fluorouracil for potent anti cancer activity. **Medicinal Chemistry Research** DOI: 10.1007/s00044-011-9627-z

3. Yata VK and Ghosh SS (2011) Investigating structure and fluorescence properties of green fluorescent protein released from chitosan nanoparticles. **Materials Letters** ***(Minor revision submitted)***

4.**Yata VK**, Banerjee S and Ghosh SS. Folic acid functionalized chitosan/poly n-isopropylacrylamide (CS/PNIPAM) nanocomposite: Synthesis, characterization and applications in prodrug enzyme cancer therapy. ***(Manuscript under preparation)***

Review paper

5.**Yata VK**, Gopinath P and Ghosh SS. Emerging implications of non- mammalian cytosine deaminases on cancer therapeutics **Applied Biochemistry And Biotechnology** ***(communicated)***

Abstracts published in international conferences/workshops

6. **Yata VK** and Ghosh SS (2010) Evaluation of chitosan based nanocomposite-mediated enzyme and gene delivery systems to introduce prodrug activating enzymes into cancer cells**. 5th International Conference on Bioengineering and Nanotechnology (ICBN-2010),** 1-4 August, 2010, Biopolis, Singapore. Abstract No: P1-11

7. **Yata VK** and Ghosh SS (2009) Chitosan nanoparticles as gene and protein carriers**. International Conference on Advanced Nanomaterials and Nanotechnology (ICANN-2009)**,9-11 December,2009, Indian Institute of Technology Guwahati, Guwahati 781039, Assam, India. Abstract No: C-282

8. **Yata VK** and Ghosh SS (2009) Core–shell nanogels for therapeutic protein and suicide gene delivery.**INDO-US Workshop on Nanotechnology: Applications and Implications** 10-12 November, 2009, Hyderabad, India. Abstract No: PP-03

****